

Glucosamine Effect on Propranolol Bioavailability

by

Hanadi Adi Alshaker

A Thesis Submitted in Partial Fulfillment of the Requirements for the

Degree of

Master of Science

in Pharmaceutical Sciences

at

University of Petra

Amman-Jordan

June 2015

Glucosamine Effect on Propranolol Bioavailability

by

Hanadi Adi Alshaker

A Thesis Submitted in Partial Fulfillment of the Requirements for the

Degree of

Master of Science

in Pharmaceutical Sciences

at

University of Petra

Amman-Jordan

June 2015

Supervisor

1. Dr. Nidal Qinna

Examination committee

1. Dr. Nidal Qinna

2. Prof. Salim Hamadi

3. Dr. Wael Abu-Dayyih

4. Dr. Basil Arafat

Abstract

Propranolol (PRN) undergoes extensive first-pass metabolism by the liver resulting in a relatively low bioavailability (BA). Thus, multiple doses are required to achieve therapeutic effect, which causes increased side effects. Glucosamine (GlcN) is an amino monosaccharide that is used to treat osteoarthritis (OA) and rheumatoid arthritis (RA) in elderly patients due to its ability to maintain connective and cartilage tissues strength and flexibility. Therefore, this research aimed to study the effect of GlcN on PRN BA, as a possible event of drug-drug interaction that may occur in patients especially elderly patients receiving both drugs. As a result, this could help to recommend whether PRN dose adjustment should be necessary with GlcN administration. Initially, in order to investigate such drug interaction a validated HPLC method of PRN in rat serum and Krebs buffer was developed and validated. Later, *in vivo* experiments were carried out to determine the effect of GlcN on PRN. PRN area under curve (AUC) and maximum concentration (C_{max}) were significantly decreased by 43% ($p < 0.01$) and 34% ($p < 0.05$), respectively for the highest GlcN dose 200 mg/kg. On the other hand, 100 mg/kg of GlcN did not change PRN AUC and C_{max} ($p > 0.05$). Additionally, 200 mg/kg of GlcN decreased intestinal permeability (P_{eff}) and increased PRN clearance by 50%. Rifampin is an enzyme inducer which potently induces many CYP450, whereas cimetidine is an enzyme inhibitor that effectively reduces the metabolism of concomitant drugs. Therefore, it is used as a control in many of literature studies documenting its role in drug interactions. The results showed that rifampin, at 9 mg/kg did not change PRN AUC and C_{max} ($p > 0.05$), whereas 5 mg/kg of cimetidine increased PRN C_{max} significantly by 86% ($p < 0.01$) and AUC by 20% ($p > 0.05$). However, in

the *in situ* single pass intestinal perfusion (SPIP) experiments, GlcN increased PRN BA significantly ($p < 0.05$) by two-fold at 60 min as compared to cimetidine and rifampin. This was confirmed by everted gut experiment where GlcN enhanced the absorption of PRN at 20, 40, and 60 min. Finally, using isolated hepatocyte cell culture, GlcN at 200 mM decreased PRN metabolism and increased PRN concentration significantly ($p < 0.05$). On the other hand, 50 μM of rifampin increased PRN metabolism and decreased PRN concentration, whereas cimetidine at 5 μM increased PRN concentration as expected for such positive controls.

Overall, GlcN decreased PRN BA in a dose-dependent manner by decreasing its *in vivo* intestinal absorption and permeability but increased PRN concentration levels *in situ* and *in vitro*. This might be attributed to factors prior intestinal absorption such as the pH of the stomach, PRN and GlcN pK_a and the efflux transporter P-glycoprotein (P-gp). Furthermore, only the highest tested dose of GlcN (200 mM) was capable of affecting PRN levels when incubated with viable rat hepatocytes. Therefore, it might be necessary to prescribe PRN with GlcN with caution due to the current reported interactions. A dosage regimen adjustment of PRN might be required to achieve the desired therapeutic effect in patients receiving GlcN.

Acknowledgement

First and foremost, I am thankful to his Almighty ALLAH's help to complete my thesis. It is a genuine pleasure to express my deep thanks to those who contributed to my thesis. I would like to express my deepest reverence to my advisor Dr. Nidal Qinna for his enthusiasm, valuable advice, immense knowledge, support, directions, and suggestions he provided me with. My sincere thanks go to Prof. Nasir Idkaidek for his logical way of thinking, his input and perspective which were of great value for this thesis. My thanks also go to Dr. Adnan Badwan and to everybody working at the Jordanian Pharmaceutical Manufacturing Company (JPM). My thanks also go to the examination committee for their valuable suggestions. I also would like to thank Mr. Mujtaba Badr and Hamza Al-Hroub for their assistance and help. Special thanks are owed to Mohammad Albayed's fine technical assistance, his invaluable help, and cooperation at the animal house. I am also grateful to my friend Mrs. Nehal Jaber for her friendly helpful attitude, cheerful and constant support and to my friend Ala' Murrar for her nice words.

Lastly but not least, I would like to thank my family. I cannot find words to express my gratitude toward the most special woman in my heart now and forever, for my mother who made it possible for me by her support, prayers, and special care. I owe a special debt of gratitude to my sister Dr. Heba, my father who encouraged me through this thesis and to my brothers for their infinite encouragement. I thank them all because they have believed in my ability and supported me throughout my study.

Contents

Subject	Page No.
Chapter One	2
1. Introduction	
1.1 Pharmacokinetics	2
1.1.1 Absorption	3
1.1.1.1 Bioavailability	4
1.1.1.2 Factors affecting drug BA	4
1.1.2 Distribution	5
1.1.2.1 Factors affecting drug distribution	5
1.1.2.2 Volume of distribution	5
1.1.3 Excretion	6
1.1.3.1 Factors affecting drug excretion	6
1.1.4 Metabolism	6
1.1.4.1 Phase I metabolism	7
1.1.4.2 Phase II metabolism	9
1.2 Drug interactions	10
1.2.1 Classification of drug interactions	11
1.2.2 Mechanisms of pharmacokinetic interactions	12
1.2.2.1 Drug interactions affecting absorption	12
1.2.2.2 Drug interactions affecting distribution	12
1.2.2.3 Drug interactions affecting excretion	13
1.2.2.4 Drug interactions affecting metabolism	13
1.3 Propranolol (PRN)	15
1.3.1 Propranolol mechanism of action	16
1.3.2 Propranolol medical uses	17
1.3.3 Propranolol Pharmacokinetics	18
1.3.3.1 Absorption and bioavailability	18
1.3.3.2 Distribution	19

1.3.3.3 Excretions	20
1.3.3.4 Metabolism	20
1.3.4 Propranolol toxicity	23
1.3.5 Propranolol adverse effects	23
1.3.6 Propranolol contraindications	23
1.3.7 Propranolol drug interactions	24
1.3.7.1 Propranolol Pharmacokinetic interactions	24
1.3.7.1 Propranolol pharmacodynamic interactions	24
1.4 Glucosamine (GlcN)	25
1.4.1 Glucosamine in the treatment of osteoarthritis	26
1.4.2 Other Glucosamine effects	26
1.4.3 Glucosamine Pharmacokinetics	27
1.4.3.1 Orally administered GlcN	27
1.4.3.2 Intravenously administered GlcN	27
1.4.4 Biochemical pathways	28
1.4.4.1 Hexosamine biosynthetic pathway	29
1.4.5 Glucosamine safety and toxicity	31
1.4.5.1 Orally administered GlcN	31
1.4.5.2 Intravenously administered GlcN	31
1.4.5.3 Glucosamine safety on human	31
1.5 Cimetidine	33
1.5.1 Cimetidine drug interactions	33
1.6 Rifampin (Rifampicin)	34
1.6.1 Rifampin drug interactions	34
1.7 Bioanalytical HPLC method validation parameters definitions (EMEA)	35
1.7.1 Accuracy	35
1.7.2 Precision	36
1.7.3 Linearity	37
1.7.4 Stability	37

1.7.4.1 Freeze and thaw stability test	38
1.7.4.2 Sample stability after preparation at room temperature (bench-top stability)	38
1.7.4.3 Autosampler stability	38
1.7.5 Recovery	38
1.7.6 Range	39
1.7.7 Reproducibility	39
2.3.8 Selectivity	39
1.7.9 Sensitivity	40
1.7.10 Limit of detection	40
1.7.11 Lower limit of quantification	40
1.8 Aim and objectives of the study	41
Chapter Two	42
2. Materials and methods	
2.1 Materials	43
2.2 Methodology	44
2.2.1 Chromatographic conditions	44
2.2.2 HPLC analysis procedure	44
2.2.2.1 Preparation of mobile phase	44
2.2.2.2 Preparation of stock solutions	45
2.2.2.3 Preparation of working solutions	45
2.2.2.4 Method of extraction	47
2.2.2.5 Method development	47
2.2.3 Method Validation	48
2.2.3.1 Intra-day accuracy and precision	48
2.2.3.2 Inter-day accuracy and precision	48
2.2.3.3 Linearity	49
2.2.3.4 Stability	49
2.2.3.5 Recovery	51
2.2.4 Animal handling	51

2.2.5 <i>In vivo</i> Glucosamine, cimetidine and rifampin effect on propranolol bioavailability	52
2.2.5.1 Drugs preparation	52
2.2.5.2 Study protocol	52
2.2.5.3 Pharmacokinetics and statistical analysis	53
2.2.5.4 Data Analysis (Optimized Effective Intestinal Permeability)	54
2.2.6 Anaesthesia and surgical protocol	54
2.2.7 <i>In Situ</i> Single-Pass Intestinal Perfusion (SPIP)	56
2.2.7.1 Washing and perfusion solution preparation	56
2.2.7.2 Intestinal perfusion	56
2.2.8 GlcN effect on PRN absorption by Everted rat intestinal sac (ERIS)	57
2.2.9 Isolation and primary culture of rat hepatic cells	58
2.2.9.1 Preparation of buffers	58
2.2.9.2 Rat perfusion for liver isolation	59
2.2.9.3 Hepatocyte cell isolation	59
2.2.9.4 Hepatocyte culture	60
2.2.9.5 Treatment of the cultured cell	60
Chapter Three	61
3. Results	
3.1 Krebs buffer validation	63
3.1.1 Intra-day validation	63
3.1.1.1 Accuracy	63
3.1.1.2 Precision	64
3.1.2 Inter-day validation	69
3.1.2.1 Accuracy	69
3.1.2.2 Precision	69
3.1.3 Stability	71
3.1.3.1 Freeze- thaw stability	71

3.1.3.2 Sample stability after preparation at room temperature (Bench-Top stability)	72
3.1.3.3 Autosampler stability	73
3.1.4 Linearity	74
3.1.4.1 Calibration curve 1	76
3.1.4.2 Calibration curve 2	77
3.1.4.3 Calibration curve 3	78
3.1.4.4 Calibration curve 4	79
3.1.4.5 Calibration curve 5	80
3.1.4.6 Calibration curve 6	81
3.1.5 Recovery	84
3.1.5.1 Recovery in the mobile phase	84
3.1.5.2 Recovery in Krebs buffer	84
3.2 Serum validation	87
3.2.1 Intra-day validation	87
3.2.1.1 Accuracy	87
3.2.1.2 Precision	88
3.2.2 Inter-day validation	92
3.2.2.1 Accuracy	92
3.2.2.2 Precision	92
3.2.3 Stability	94
3.2.3.1 Freeze- thaw stability	94
3.2.3.2 Sample stability after preparation at room temperature (Bench-Top stability)	96
3.2.3.3 Autosampler stability	97
3.2.4 Linearity	98
3.2.4.1 Calibration curve 1	99
3.2.4.2 Calibration curve 2	100
3.2.4.3 Calibration curve 3	101
3.2.4.4 Calibration curve 4	102

3.2.4.5 Calibration curve 5	103
3.2.4.6 Calibration curve 6	104
3.2.5 Recovery	107
3.2.5.1 Recovery in mobile phase	107
3.2.5.2 Recovery in the serum	107
3.3 Representative HPLC chromatograms of analyzed Sprague-Dawley rat serum and Krebs buffer samples	110
3.4 <i>In vivo</i> experiments	112
3.4.1 Effect of GlcN on PRN BA	112
3.4.2 Effect of cimetidine and rifampin on PRN BA	113
3.4.3 Effect of GlcN on PRN effective intestinal permeability (P_{eff}) and clearance	115
3.5 Effect of GlcN on PRN <i>in situ</i> single-pass intestinal perfusion	117
3.6 Effect of GlcN on PRN absorption in everted rat intestine sac (ERIS)	119
3.7 Hepatocyte cell isolation and culture	120
3.7.1 Effect of GlcN on PRN metabolism	120
3.7.2 Effect of cimetidine and rifampin on PRN metabolism	121
Chapter Four	122
4. Discussion	
Chapter Five	130
5. Conclusion and future work	

List of figures

Figure legends	Page No.
Figure 1.1 Illustration of the pharmacokinetic processes (ADME).	2
Figure 1.2 Division of enzymes into phase I and phase II, Phase I enzymes are normally oxidative and phase II conjugative.	10
Figure 1.3 Propranolol chemical structure.	15
Figure 1.4 Propranolol major metabolic pathways	22
Figure 1.5 Chemical structure of glucosamine	25
Figure 1.6 Hexosamine biosynthetic pathway.	29
Figure 2.1 Anesthesia system linked to an oxygen concentrator and a peristaltic perfusion pump.	55
Figure 3.1 Intra-day one calibration curve of propranolol in Krebs buffer.	76
Figure 3.2 Intra-day two calibration curve of propranolol in Krebs buffer.	77
Figure 3.3 Intra-day three calibration curve of propranolol in Krebs buffer.	78
Figure 3.4 Freeze-thaw stability test calibration curve of propranolol in Krebs buffer.	79
Figure 3.5 Bench-top stability test calibration curve of propranolol in Krebs buffer.	80
Figure 3.6 Autosampler stability test calibration curve of propranolol in Krebs buffer.	81
Figure 3.7 Propranolol concentrations versus mean area ratios for each concentration of standard points.	83
Figure 3.8 Intra-day one calibration curve of propranolol in serum.	99
Figure 3.9 Intra-day two calibration curve of propranolol in serum.	100
Figure 3.10 Intra-day three calibration curve of propranolol in serum.	101
Figure 3.11 Freeze-thaw stability test calibration curve of propranolol in serum.	102

Figure 3.12 Bench-top stability test calibration curve of propranolol in serum.	103
Figure 3.13 Autosampler stability test calibration curve of propranolol in serum.	104
Figure 3.14 Propranolol concentrations versus mean area ratios for each concentration of standard points.	106
Figure 3.15 A processed blank serum sample.	110
Figure 3.16 A processed zero serum sample spiked with sildenafil; the internal standard of propranolol analysis.	110
Figure 3.17 A processed lower limit of quantification (50 ng/ml) for serum sample spiked with sildenafil; the internal standard of propranolol analysis.	111
Figure 3.18 A processed upper limit of quantification (3000 ng/ml) for serum sample spiked with sildenafil; the internal standard of propranolol analysis.	111
Figure 3.19 <i>In vivo</i> serum concentration versus time curves of propranolol in rats after a single oral dose of 20 mg/kg of propranolol, propranolol with 100 and 200 mg/kg of glucosamine. Each data point represents the mean \pm SEM (n=7).	112
Figure 3.20 <i>In vivo</i> serum concentration versus time curves of propranolol in rats after a single oral dose of 20 mg/kg of propranolol, propranolol with 5 and 9 mg/kg of cimetidine and rifampin, respectively. Each data point represents the mean \pm SEM (n=5).	113
Figure 3.21 Observed versus SimCYP-predicted propranolol plasma concentrations of 20 mg/kg propranolol, propranolol with 100 mg/kg glucosamine and propranolol with 200 mg/kg glucosamine.	116
Figure 3.22 Time dependence curves of propranolol serum concentration in rats using <i>in situ</i> single pass intestinal perfusion. Rats were administered propranolol alone 1 mg/ml, propranolol with glucosamine 10 mg/ml, propranolol with cimetidine 1 mg/ml, and	118

<p>propranolol with rifampin 2 mg/ml. The data are presented as mean \pm SEM (n=6). Significant effect was seen between propranolol only and propranolol with GlcN (p<0.05).</p>	
<p>Figure 3.23 Absorption of propranolol in the everted rat intestinal sac versus time. Rats were administered 0.1 mg/ml propranolol, propranolol with 1 mg/ml glucosamine and propranolol with 0.01 mg/ml sodium lauryl sulfate for 60 min. The data are presented as mean \pm SEM (n=6).</p>	119
<p>Figure 3.24 Propranolol concentration versus time profiles in hepatocyte cell isolation and culture. Cells were cultured with 20 μM of propranolol with 40 mM glucosamine, glucosamine high and low concentrations of 200 mM and 4 mM, respectively, for 120 min. The data are presented as mean \pm SEM (***, p<0.001).</p>	120
<p>Figure 3.25 Propranolol concentration versus time profiles in hepatocyte cell isolation and culture. Cells were cultured with 20 μM propranolol with 5 μM cimetidine and 50 μM rifampin for 120 min. The data are presented as mean \pm SEM (**, p<0.01).</p>	121

List of tables

Table captions	Page No.
Table 2.1 Spiked serum or Krebs buffer of PRN serial spiking samples.	46
Table 2.2 Spiked serum or Krebs buffer of PRN quality control samples.	46
Table 2.3 Quality control concentrations used for method validation	48
Table 3.1 Summary of chromatographic conditions applied.	62
Table 3.2 Intra-day accuracy & precision data for all QC samples LLOQ, QC low, QC mid, and QC high of propranolol based on the standard calibration curves of the first day of validation (n=6). Corresponding calibration curve used in the calculation of measured concentration of intra-day one is shown in table 3.13 .	65
Table 3.3 Intra-day accuracy & precision data for all QC samples LLOQ, QC low, QC mid, and QC high of propranolol based on the standard calibration curves of the second day of validation (n=6). Corresponding calibration curve used in the calculation of measured concentration of intra-day two is shown in table 3.14 .	66
Table 3.4 Intra-day accuracy & precision data for all QC samples LLOQ, QC low, QC mid, and QC high of propranolol based on the standard calibration curves of the third day of validation (n=6). Corresponding calibration curve used in the calculation of measured concentration of intra-day three is shown in table 3.15 .	67
Table 3.5 Inter-day accuracy & precision data for the three days of QC samples validation (LLOQ, QC low, QC mid, and QC high) of propranolol based on the standard calibration curves of the three days of validation (n=6).	70
Table 3.6 Propranolol QC low samples (150 ng/ml) results for freeze-thaw stability test (n=3).	71
Table 3.7 Propranolol QC high samples (2500 ng/ml) results for freeze-thaw stability test (n=3).	71

Table 3.8 Propranolol QC low samples (150 ng/ml) results for bench-top stability test (n=3).	72
Table 3.9 Propranolol QC high samples (2500 ng/ml) results for bench-top stability test (n=3).	72
Table 3.10 Propranolol QC low samples (150 ng/ml) results for autosampler stability test (n=3).	73
Table 3.11 Propranolol QC high samples (2500 ng/ml) results for autosampler stability test (n=3).	73
Table 3.12 Summary of all R ² , slope and intercept data of the six calibration curves.	74
Table 3.13 Calibration curve data of intra-day one of validation.	76
Table 3.14 Calibration curve data of intra-day two of validation.	77
Table 3.15 Calibration curve data of intra-day three of validation.	78
Table 3.16 Calibration curve data of freeze-thaw test of stability.	79
Table 3.17 Calibration curve data of bench-top test of stability.	80
Table 3.18 Calibration curve data of autosampler test of stability.	81
Table 3.19 Calculated Accuracy % based on measured concentration mean for each concentration of standard points.	82
Table 3.20 Calculated Accuracy % based on area ratios mean for each concentration of standard points	82
Table 3.21 CV% values of AUC mean of propranolol and sildenafil (internal standard) in mobile phase.	84
Table 3.22 CV% values of AUC mean of propranolol and sildenafil (internal standard) in Krebs buffer.	85
Table 3.23 Absolute recovery ratios of propranolol in Krebs buffer.	85
Table 3.24 Absolute recovery ratios of sildenafil citrate (internal standard) in Krebs buffer.	86
Table 3.25 Intra-day accuracy & precision data for all QC samples LLOQ, QC low, QC mid, and QC high of propranolol based on the standard calibration curves of the first day of validation (n=6). Corresponding	89

calibration curve used in the calculation of measured concentration of intra-day one is shown in table 3.36 .	
Table 3.26 Intra-day accuracy & precision data for all QC samples LLOQ, QC low, QC mid, and QC high of propranolol based on the standard calibration curves of the second day of validation (n=6). Corresponding calibration curve used in the calculation of measured concentration of intra-day two is shown in table 3.37 .	90
Table 3.27 Intra-day accuracy & precision data for all QC samples LLOQ, QC low, QC mid, and QC high of propranolol based on the standard calibration curves of the third day of validation (n=6). Corresponding calibration curve used in the calculation of measured concentration of intra-day three is shown in table 3.38 .	91
Table 3.28 Inter-day accuracy & precision data for the three days of QC samples validation (LLOQ, QC low, QC mid, and QC high) of propranolol based on the standard calibration curves for the three days of validation (n=6).	93
Table 3.29 Propranolol QC low samples (150 ng/ml) results for freeze-thaw stability test (n=3).	94
Table 3.30 Propranolol QC high samples (2500 ng/ml) results for freeze-thaw stability test (n=3).	95
Table 3.31 Propranolol QC low samples (150 ng/ml) results for bench-top stability test (n=3).	96
Table 3.32 Propranolol QC high samples (2500 ng/ml) results for bench-top stability test (n=3).	96
Table 3.33 Propranolol QC low samples (150 ng/ml) results for autosampler stability test (n=3).	97
Table 3.34 Propranolol QC high samples (2500 ng/ml) results for autosampler stability test (n=3).	97
Table 3.35 Summary of all R ² , slope and intercept data of the six calibration curves.	98

Table 3.36 Calibration curve data of intra-day one of validation.	99
Table 3.37 Calibration curve data of intra-day two of validation.	100
Table 3.38 Calibration curve data of intra-day three of validation.	101
Table 3.39 Calibration curve data of freeze-thaw test of stability.	102
Table 3.40 Calibration curve data of bench-top test of stability.	103
Table 3.41 Calibration curve data of autosampler test of stability.	104
Table 3.42 Calculated Accuracy % based on measured concentration mean for each concentration of standard points.	105
Table 3.43 Calculated Accuracy % based on area ratios mean for each concentration of standard points.	105
Table 3.44 CV% values of AUC mean of propranolol and sildenafil (internal standard) in mobile phase.	107
Table 3.45 CV% values of AUC mean of propranolol and sildenafil (internal standard) in serum blood.	108
Table 3.46 Absolute recovery ratios of propranolol in serum.	108
Table 3.47 Absolute recovery ratios of sildenafil citrate (internal standard) in serum.	109
Table 3.48 Glucosamine effect on propranolol AUC, C_{max} , and other pharmacokinetic parameters after an oral dose of 20 mg/kg PRN, PRN with GlcN 100 or PRN with GlcN 200 mg/kg in rats. The data are presented as mean \pm SEM (n=7).	114
Table 3.49 Cimetidine and rifampin effect on propranolol AUC, C_{max} , and other pharmacokinetic parameters after an oral dose of 20 mg/kg of propranolol, propranolol with 5 and 9 mg/kg of cimetidine and rifampin, respectively in rats. The data are presented as mean \pm SEM (n=5).	114
Table 3.50 P_{eff} , Clearance, and V_d results of propranolol 20 mg/kg, propranolol with 100 and 200 mg/kg GlcN estimated by the Nelder–Mead algorithm using the SimCYP program.	115

List of abbreviations

Abbreviations	Phrasing
ADME	Absorption, distribution, metabolism and excretion
AUC	Area under curve
AUMC	Area under moment curve
BA	Bioavailability
BCS	Biopharmaceutics Classification System
C _{max}	Maximum plasma concentration
C _p	Drug concentration in plasma
CV%	Coefficient of variation
EMA	European Medicines Evaluation Agency
ERIS	Everted rat intestinal sac
FAD	Flavin adenine dinucleotide
FMN	Flavin mononucleotide
FMO	Flavin monooxygenase reactions
GIT	Gastrointestinal tract
GlcN	Glucosamine
GST	Glutathione S-transferase
h	Hour
HBSS	Hank's Balanced Salt Solution
HPLC	High performance (pressure) liquid chromatography
I.V.	Intravenous
IS	Internal standard
IVC	Inferior vena cava
L	Liter
LLOQ	Lower limit of quantification
MAC	Minimum alveolar concentration
min	Minute
MRT	Mean residence time

NSAIDs	Nonsteroidal anti-inflammatory drug
OA	Osteoarthritis
P_{eff}	Effective intestinal permeability
P-gp	P-glycoprotein
PK	Pharmacokinetics
PKA	Protein kinase
PRN	Propranolol
QC	Quality control
R^2	Regression factor
RA	Rheumatoid arthritis
SLS	Sodium lauryl sulphate
SPIP	Single pass intestinal perfusion
SULTs	Sulfotransferases
$t_{0.5}$	Half-life
T_{max}	The time in which maximum plasma concentration is reached
UGTs	UDP-glucuronosyltransferases
ULOQ	Upper limit of quantification
V_d	Volume of distribution
α_1 -Agp	α_1 -acid glycoprotein

Chapter One

Introduction

Chapter One

1. Introduction

1.1 Pharmacokinetics

Pharmacokinetics (PK) provides a mathematical basis to study the rate of a drug or a dosage form and its concentration-time course within the body along with drug disposition to quantify the processes of absorption, distribution, metabolism and excretion. These pharmacokinetic processes, that are often referred to as ADME; determine drug concentration in the body when drugs are prescribed (Caldwell *et al.* 1995; Hedaya 2012; Kubinyi *et al.* 1993) (**Figure 1.1**).

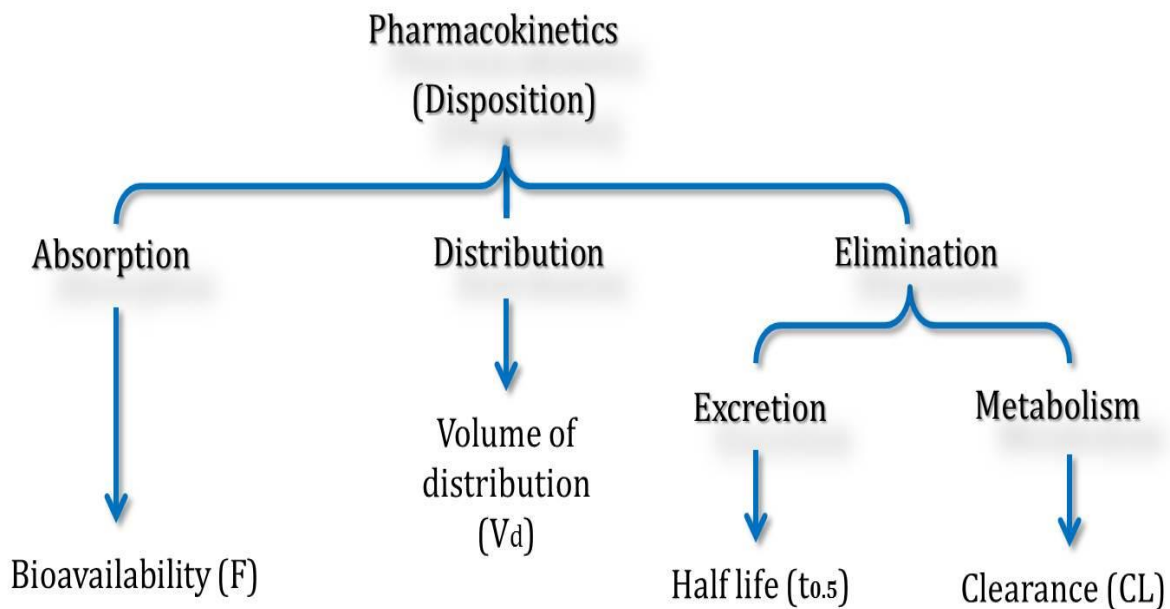


Figure 1.1 Illustration of the pharmacokinetic processes (ADME).

1.1.1 Absorption

Drug oral absorption is a complex transfer process across the intestinal lining which includes passive diffusion through the paracellular space or absorptive cells membranes, vesicular uptake (endocytosis/pinocytosis), and release at the basolateral space. Absorption depends initially on the dosage form dissolution in the aqueous contents of the gastrointestinal tract (GIT) to reach the blood (Le Ferrec *et al.* 2001a; Smith *et al.* 2012; Toutain and Bousquet-mélou 2004). Drug absorption from the GIT depends on various factors such as drug physicochemical properties (lipophilicity, size, molecular volume, stereochemistry, pK_a, solubility, chemical stability, partition and structure), gastric and intestinal motility, gastric emptying, physicochemical properties of small intestine environment, intestinal pH and the Surface area available for absorption (Dressman and Reppas 2010; Le Ferrec *et al.* 2001b). Drug absorption takes place at different sites of the GIT which include duodenum, jejunum and ileum. Many biological *in vitro* methods are used as an assessment for the permeability of the GI mucosa to predict *in vivo* drug absorption such as everted rat intestinal sacs (ERIS) and *in situ* single pass intestinal perfusion (*in situ* SPIP) (Dressman and Reppas 2010).

In situ SPIP technique is used for the assessment of permeability of drugs through intestines while keeping intact blood supply to the intestinal tract throughout the experiment, making it a reliable tool for simulating real *in vivo* conditions following oral drug administration (Amidon *et al.* 1995; Amidon *et al.* 1988; Varma *et al.* 2004; Varma and Panchagnula 2005). Everted rat intestinal sac model is used for measuring absorption and permeability at different sites in the small intestine via passive diffusion and/or

transporters in the small intestine. It is also a good model to realistically mimic the gut physiological conditions (Barthe *et al.* 1999; Chowhan and Amaro 1977; Lacombe *et al.* 2004; Lafforgue *et al.* 2008).

1.1.1.1 Bioavailability

Bioavailability (BA) is critically determined by the absorption. It is defined as the rate (T_{\max} and C_{\max}) and extent (AUC) of an active substance that is absorbed from its dosage form (pharmaceutical form) to reach the blood circulation at its site of action. C_{\max} represents maximum plasma concentration that is observed at that time T_{\max} following drug administration. BA is controlled by drug solubility, drug dissolution rate in the intestinal fluid, drug permeability across the intestinal membrane, pre-systemic metabolism and the efficiency of drug transporting system (Rescigno 2010; Toutain and Bousquet-mélou 2004; Zakeri-Milani *et al.* 2007).

1.1.1.2 Factors affecting drug BA

There are several factors affecting drug BA such as drug solubility, permeability, the rate of *in vivo* dissolution as well as patient attributes such as membrane transporters, GI and liver (presystemic) metabolism, the integrity of the GIT, physiological status, and extrinsic variables such as the effect of food or concomitant medication. Moreover, the potential impact of patient physiological status such as age, gender, and lifestyle also play a crucial role in drug BA (Dressman and Reppas 2010; Martinez and Amidon 2002).

1.1.2 Distribution

Once a drug enters the bloodstream, it distributes into different body cells and tissues by the influence of tissue hemodynamics and passive diffusion across lipid membranes. The drug binds to plasma proteins such as albumin forming drug-protein complexes. These complexes significantly influence the magnitude or the duration of drug's effect with no effect on the drug's therapeutic activity (Bauer 2001; Caldwell *et al.* 1995; Raffa 2010).

1.1.2.1 Factors affecting drug distribution

Many factors affect drug distribution such as the characteristics of the targeted compartment (bone, fat and muscles) and drug physicochemical properties (Dobesh 2004). Many proteins are involved in drug binding such as albumin, lipoproteins, and acid glycoprotein. Other intracellular proteins including myosin and actin in muscular tissue, melanin in pigmented tissue (particularly the eye) and ligandin that is present in liver, kidney and intestine can also influence drug distribution (Smith *et al.* 2012).

1.1.2.2 Volume of distribution

Volume of distribution (V_d) or the apparent volume of distribution is a theoretical PK parameter. V_d usually relates drug plasma concentrations to the total amount of the drug that is dissolved in the body (Bauer 2001; Dhillon and Gill 2006; Smith *et al.* 2012). The body is not a homogeneous unit, so the concentration of the drug in plasma is not necessarily the same in the liver, kidneys or other tissues. Therefore, V_d relates the total

amount of drug in the body at any time to the corresponding plasma concentration (Dhillon and Gill 2006).

1.1.3 Excretion

Both metabolism and excretion are the major processes responsible for elimination of the parent drug and its metabolite(s) from the body (Craig and Stitzel 2004). Excretion is the termination of the biological effect of exogenous substances by combined processes of redistribution, metabolism, and excretion. Each of these processes governs plasma drug concentrations at any time (Dhillon and Gill 2006; Leucuta and Vlase 2006; Raffa 2010).

1.1.3.1 Factors affecting drug excretion

Several factors influence the rate and extent of elimination. Accumulation occurs if the rate of absorption and distribution of a drug or a nutrient exceeds the rate of elimination (Raffa 2010). In humans, the kidneys are the major route of elimination for many drugs due to the fact that the kidneys receive about 20–25% of the cardiac output. Other sites of elimination include the feces and to a lesser extent sweat, saliva, gastric fluid, breast milk, and semen. However, some medications are eliminated unchanged in the bile (Bauer 2001; Raffa 2010).

1.1.4 Metabolism

Metabolism terminates the action of many drugs by forming a more water soluble metabolites which can be easily excreted by the kidney. Metabolism also changes the chemical structure of the drugs producing metabolites which are less pharmacologically active than the parent drug (Corrie and Hardman 2011; Craig and Stitzel 2004). However,

active metabolites can be formed from an inactive parent drug (prodrug). In general, all tissues can metabolize drugs, but the liver, GIT and lungs are the major sites for drug metabolism in humans. The strategic location of the liver relative to the portal circulation and the high level of enzymes capable of metabolizing foreign substances regarded the liver as one of the major sites responsible for drug metabolism (Raffa 2010). Drug metabolism is divided into two phases; phase I and phase II metabolism. Primary hepatocyte culture is used to study the expression and function of enzymes responsible on drug metabolism including cytochromes P450, drug-drug interactions, and the mechanisms of cytotoxicity and genotoxicity (Bu and Mashek 2010; Gomez-Lechon *et al.* 2004; Gonçalves *et al.* 2007; Saito *et al.* 2010; Schmidt *et al.* 2005).

1.1.4.1 Phase I metabolism

Phase I reactions take place in the cytoplasm, mitochondria, and the microsomes, which are a subcellular component containing membrane-associated enzymes on the smooth endoplasmic reticulum (Raffa 2010). Phase I reactions (oxidation, hydrolysis and rarely, reduction) are concerned with the addition or unmasking of polar groups, which is mediated by a large family of cytochrome P450 enzymes (Leucuta and Vlase 2006). These reactions result in small changes making a drug more hydrophilic and also provide a functional group that is used to complete phase II reactions. However, some drugs do not necessarily undergo phase I metabolism prior to phase II metabolism (Leucuta and Vlase 2006; Smith *et al.* 2012).

Phase I metabolism occurs during drug absorption, mainly in the liver as well as in the gut wall before reaching systemic circulation. The presystemic metabolism determines

the fraction of the oral dose that reaches systemic circulation to be bioavailable (Leucuta and Vase 2006). Phase I reactions include the following:

Oxidation

Oxidation process involves the addition of oxygen or the removal of hydrogen from the parent molecule which is a common type of phase I reaction. There is an extensive system of enzymes that are capable of catalyzing oxidation reactions, such as cytochrome P-450 reductase. Examples of microsomal oxidation reactions are aromatic oxidations (e.g., PRN, warfarin), aliphatic oxidations (e.g., amobarbital, ibuprofen), O-dealkylations (e.g., codeine), N-dealkylations (e.g., morphine), S-dealkylations (e.g., 6-methylthiopurine), epoxidations (e.g., carbamazepine), S-oxidations (e.g., cimetidine); N-oxidations of primary amines (e.g., chlorphentermine), secondary amines (e.g., acetaminophen) and tertiary amines (e.g., nicotine); in addition to deaminations (e.g., diazepam).

Other non-P450 oxidations are: Alcohol- and aldehyde dehydrogenase, tyrosine hydroxylase, xanthine oxidase and monoamine oxidase reactions, such example is the formation of imine followed by hydrolysis, such as flavin monooxygenase reactions (FMO). P450 reductases also use flavin as flavin adenine dinucleotide (FAD), and flavin mononucleotide (FMN) (Leucuta and Vase 2006; Raffa 2010).

Reduction

Reduction reactions involve the addition of hydrogen or the removal of oxygen from the parent drug; it occurs in both microsomal and nonmicrosomal fractions of hepatocytes and other cells. Examples of such reactions include, aldehyde-, ketone-, nitro-, azo-, and quinone reduction (Raffa 2010).

Hydrolysis

Hydrolysis reactions can occur in many locations throughout the body, including the plasma. Examples of some nonmicrosomal hydrolases include esterases, peptidases, and amidases (Raffa 2010).

1.1.4.2 Phase II metabolism

Phase II metabolism represents the synthetic reactions occurring after phase I metabolism and is characterized by conjugation with endogenous substances. This conjugation results in a decrease in biological activity due to three dimensional shape alterations. Furthermore, conjugation results in an increase in water solubility of the substance, which decreases the amount that is reabsorbed through renal tubules and thereby enhances the fraction that is excreted in the urine. Groups of phase II isozymes consist of acetyltransferases, sulfotransferases (SULTs) for sulfation, methyltransferases for methylation, glutathione S-transferase (GST) for glutathione conjugation, and UDP-glucuronosyltransferases (UGTs) for glucuronidation (Kashuba and Bertino Jr 2001; Leucuta and Vlase 2006; Raffa 2010). **(Figure 1.2)** represents phase I and II enzymes.

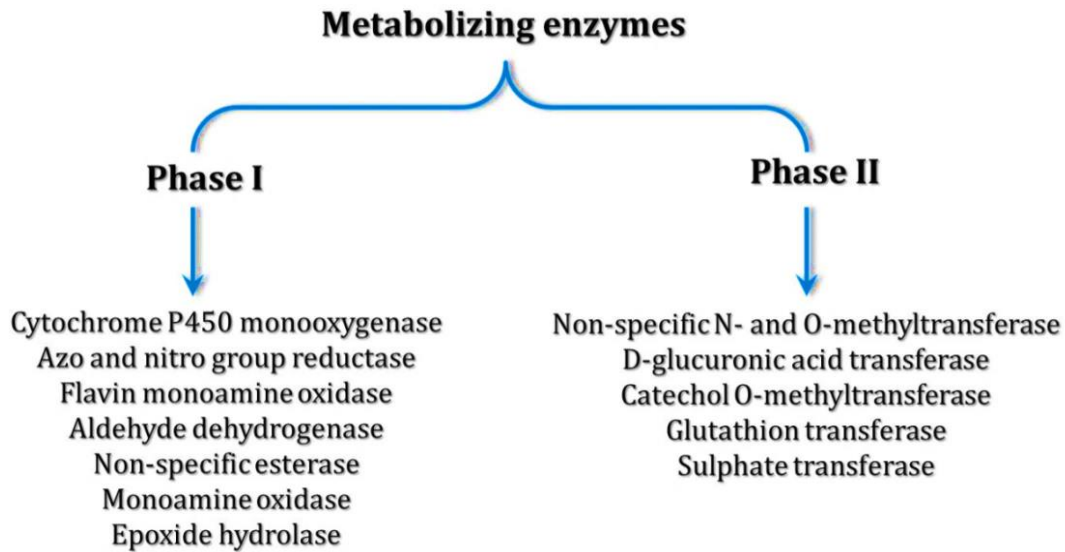


Figure 1.2 Division of enzymes into phase I and phase II, Phase I enzymes are normally oxidative and phase II conjugative. Adapted and modified from (Mannhold *et al.* 2000).

1.2 Drug interactions

Drug interactions occur when a combination of two drugs or more affect the activity of each other (Jonker *et al.* 2005). Interactions occur not only between drugs but also between drugs and other chemicals or food (Pleuvry 2005).

1.2.1 Classification of drug interactions

Drug interactions are classified as pharmacokinetic and pharmacodynamic interactions (Corrie and Hardman 2011; Ito *et al.* 1998; Kashuba and Bertino Jr 2001; Pleuvry 2005). Pharmacodynamic interactions occur due to the presence of two drugs at the same site of action, at an unspecified site of action or at different receptor sites to produce antagonistic, synergistic and additive interactions. Antagonistic interactions happens when two drugs interact at a specific receptor on the cell membrane, nucleus or cytoplasm such example is the competitive antagonism of benzodiazepines by flumazenil which is used as antidote for benzodiazepines overdose Synergistic interactions occur when the intensity of effect for the combined drugs is greater than would be of purely additive effect (Corrie and Hardman 2011; Jonker *et al.* 2005). Oral anticoagulants (e.g., warfarin) and heparin produce synergistic effect (Craig and Stitzel 2004). Additive effect is shown with nitrous oxide and volatile agent where fifty percent of the nitrous oxide minimum alveolar concentration (MAC) plus fifty percent of volatile agent MAC equal in anaesthetizing effect to that of 100% MAC of either agent alone (Corrie and Hardman 2011).

Pharmacokinetic interactions involve interactions due to absorption, distribution, metabolism, and excretion (Corrie and Hardman 2011; Ito *et al.* 1998; Pleuvry 2005).

1.2.2 Mechanisms of pharmacokinetic interactions

1.2.2.1 Drug interactions affecting absorption

Absorption mechanisms include active, facilitated, ion-pair transport and passive diffusion. In general, a drug interaction is considered clinically significant if the change in its extent of absorption is more than 20% (Kashuba and Bertino Jr 2001). Small intestine is the largest absorptive site in the GIT. Therefore, drugs that enhance gastric emptying such as metoclopramide accelerate drug absorption, whereas drugs that inhibit gastric emptying including muscarinic acetylcholine receptor antagonists slow absorption (Pleuvry 2005). Drug chelation results in the formation of insoluble compounds due to the formation of ring structure between a metal ion and an organic molecule, an example is the administration of magnesium and aluminum-containing antacids with quinolone antibiotics (Kashuba and Bertino Jr 2001).

1.2.2.2 Drug interactions affecting distribution

Drug interactions affecting distribution are drugs altering protein binding. Albumin is the major protein in the blood which binds acidic and basic drugs. However, acidic drugs are strongly bound to albumin more than basic drugs, whereas the latter binds to α_1 -acid glycoprotein (α_1 -A₁g_p) (Kashuba and Bertino Jr 2001). Warfarin displacement by erythromycin is an example of protein binding displacement leading to an increased plasma concentration and therapeutic activity of warfarin (Corrie and Hardman 2011; Rolan 1994).

1.2.2.3 Drug interactions affecting excretion

Drugs are excreted by different sites of the body. Lungs are responsible for the excretion of inhalational agents (Corrie and Hardman 2011; Pleuvry 2005). Kidney excretion can be altered by changes in protein binding (Kashuba and Bertino Jr 2001; Pleuvry 2005).

1.2.2.4 Drug interactions affecting metabolism

Liver is the major site responsible for drug metabolism in order to activate or terminate the action of many drugs (Corrie and Hardman 2011). Therefore, a change in drug metabolism is considered as one of the important causes of unexpected drug interactions. Metabolizing enzymes can be inhibited by many drugs resulting in reduced metabolism and prolongation of drug effect (Corrie and Hardman 2011; Craig and Stitzel 2004; Ito *et al.* 1998; Kashuba and Bertino Jr 2001; Snyder *et al.* 2012). On the contrary, numerous drugs and environmental pollutants can induce the P450 system increasing drug metabolism. Enzyme induction has been responsible for failure of therapy for many drugs (Pleuvry 2005).

Enzyme inhibition

Enzyme inhibition is the primary mechanism for drug–drug pharmacokinetic interactions. Enzyme inhibition occurs via four types; competitive, non-competitive, uncompetitive and mechanism based. All types of inhibition are affected by the characteristics of CYP isoform and the concentrations of drugs. However, several drugs are metabolized by multiple isozymes where they act as competitive with one CYP and non-competitive with another (Coleman 2010; Ito *et al.* 1998).

Enzyme induction

Drug interactions caused by induction of CYP450 are significantly less common than those caused by CYP450 inhibition and impact the efficacy and therapeutic goals rather than toxicity caused by CYP450 (Bjornsson *et al.* 2003; Kashuba and Bertino Jr 2001). Induction of drug-metabolizing activity can be due to either a decrease in the proteolytic degradation of the enzyme or due to synthesis of new enzyme protein. Synthesis of new enzyme protein is due to an increased messenger RNA (mRNA) production (transcription) or in the translation of mRNA into protein (Craig and Stitzel 2004). Barbiturates are the classical example for drugs that induce P450 enzyme system. Therefore, a susceptible drug will be metabolized more rapidly resulting in reduced BA, shorter half-life ($t_{0.5}$), and reduced efficacy (Corrie and Hardman 2011).

1.3 Propranolol (PRN)

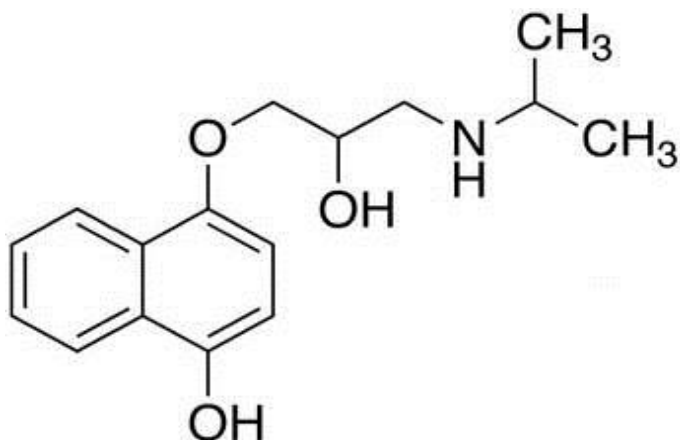


Figure 1.3 Propranolol chemical structure.

Propranolol (PRN) (**Figure 1.3**) is the prototype of all β -adrenergic receptor antagonists and is the first effective β -blocker interacting with both β_1 and β_2 receptors with equal affinity. It does not have α receptor or muscarinic receptor blocking activity but it may block some serotonin receptors in the brain (Brunton *et al.* 2006; Katzung *et al.* 2004; Wang *et al.* 2013). Additionally, PRN lacks intrinsic sympathomimetic activity (Brunton *et al.* 2006; Katzung *et al.* 2004; Wang *et al.* 2013), and is one of the essential drugs listed by World Health Organization's List of Essential Medicines as one of the drugs used for a basic health system (WHO 2011). It is present as a white crystalline powder and is soluble in both water and alcohol, its pK_a value is 9.4 (Salman *et al.* 2010).

1.3.1 Propranolol mechanism of action

Beta-receptor antagonists antagonize the effect of catecholamines at β adrenoceptors by occupying this receptor and competitively countering its binding by catecholamines and other β agonists, thus, preventing catecholamines action on cardiovascular tissues (Craig and Stitzel 2004; Katzung *et al.* 2004). β_1 receptors are located on the cardiac sarcolemma which belong to the G-protein coupled adenylyl cyclase system. When catecholamines stimulate the receptor, α subunit of G_s protein binds to and activates adenylyl cyclase and generates cAMP. Later, cAMP as a second messenger activates protein kinase A (PKA) which phosphorylates specific proteins and other membrane calcium channels leading to an increase in calcium entry into the cytoplasm. PKA also increases calcium release from the sarcoplasmic reticulum which leads to the positive inotropic effect. Additionally, PKA accelerated conduction across atrioventricular node and conduction tissues leads to a positive dromotropic effect (Mansoor and Kaul 2009). PRN also has a membrane-stabilizing action (local anesthetic effect or quinidine-like effect). As a result, it can be used for the treatment of cardiac arrhythmias due to this advantage (Craig and Stitzel 2004; Katzung *et al.* 2004).

1.3.2 Propranolol medical uses

PRN is used for the treatment of various cardiovascular diseases mainly essential hypertension because it decreases heart rate, myocardial contractility, and cardiac output (Brunton *et al.* 2006; Craig and Stitzel 2004; Wang *et al.* 2013). However, its action on blood pressure reduction is complex. After acute administration, PRN blocks vascular β_2 receptors leading to a reduction in the cardiac output so peripheral resistance increases in proportion that maintain blood pressure to normal, and compensatory reflexes resulting in activation of vascular α receptors which is not blocked by PRN. As a result, blood pressure is not altered significantly; on the other hand, chronic administration of PRN decreases blood pressure, and this is why PRN is used in essential hypertension but not for hypertensive crisis (Brunton *et al.* 2006; Craig and Stitzel 2004). PRN is also used for the treatment of patient with angina pectoris (Brunton *et al.* 2006; Craig and Stitzel 2004; Hebb *et al.* 1968), atrial fibrillation, congestive heart failure, myocardial infraction (ischemic heart disease), and is used in the treatment of supraventricular arrhythmias, supraventricular tachycardias as well as ventricular arrhythmias/tachycardias (Brunton *et al.* 2006; Chafin *et al.* 1999; Katzung *et al.* 2004; Wang *et al.* 2013). PRN is found to be effective in the treatment of neurologic diseases, such as headache, and is used in migraine prophylaxis because it reduces the frequency and intensity of migraine (Katzung *et al.* 2004; Shields and Goadsby 2005). Furthermore, PRN has anti-inflammatory, antioxidant properties, and lipid peroxidation inhibitory activity as well as some anti-cancer activities (Nkontchou *et al.* 2012). PRN is also used in the treatment of thyrotoxic crisis (Brunton *et al.* 2006). In addition to that, PRN and nadolol combination is used to decrease the

incidence of the first episode of bleeding from esophageal varices as well as bleeding in patients with cirrhosis (Katzung *et al.* 2004; Watson *et al.* 1987).

1.3.3 Propranolol Pharmacokinetics

1.3.3.1 Absorption and bioavailability

PRN is a highly lipophilic drug that is almost completely absorbed from the GIT following oral administration (Salman *et al.* 2010). PRN peak plasma concentrations occur after 1–3 hours (T_{max}) of ingestion (Ismail *et al.* 2004), and its oral BA is relatively low of 13-23% (Cid *et al.* 1986; Sastry *et al.* 1993). Thus, a major consequence is that oral administration of the drug leads to lower drug concentrations as compared to those achieved after I.V. injection of the same dose. However, its BA could be increased by the concomitant ingestion of food and throughout the long-term administration of the drug (Brunton *et al.* 2006; Katzung *et al.* 2004). PRN is concentrated mainly in the lungs and to a lesser extent in other organs such as the brain, liver, and kidneys. Moreover, it undergoes extensive hepatic metabolism, therefore, the proportion of PRN that reaches the systemic circulation increases as the PRN dose is increased due to saturation of hepatic extraction mechanisms (Craig and Stitzel 2004; Katzung *et al.* 2004). PRN plasma $t_{0.5}$ ranges from 3 to 6 hours (Castleden and George 1979; Ismail *et al.* 2004; Leahey *et al.* 1980). Concentrations of PRN after single oral doses have shown higher concentrations in elderly (2.3 times) than in the young as well as S (-)-PRN enantiomer concentrations are present in higher amounts than R (+)-PRN enantiomer (Walle *et al.* 1988). Moreover, in a study conducted by Johnson *et al.* they demonstrated that area under curve (AUC) for both R (+) and S (-)-PRN

enantiomer in white subjects has shown to be 292 ng.hr/ml versus 394 ng.hr/ml for black subjects (Johnson *et al.* 2000).

1.3.3.2 Distribution

Drug's V_d depends on its free concentration in the blood. As free drug concentration increases, its V_d will also increase because equilibrium is reached between the free drug and body tissues. PRN to plasma protein binding has been found to be 90 to 93.2% in man (Brunton *et al.* 2006; Evans *et al.* 1973; Ismail *et al.* 2004). α_1 -AGP and lipoproteins often bind lipophilic and basic drugs like PRN. On the contrary, acidic drugs are bound to albumin. The degree of drug binding to proteins will differ in pathophysiological states due to changes in plasma-protein concentrations (Brunton *et al.* 2006; Katzung *et al.* 2004; Walle *et al.* 1988). For example, α_1 -AGP is increased in acute inflammation, hence, total plasma concentration will be changed even though drug elimination is unchanged (Katzung *et al.* 2004). PRN-plasma binding has been found to be enantiomer-selective where R (+)-enantiomer binds to human serum albumin, whereas the opposite S (-)-enantiomer binds to α_1 -A₂g₂. Both enantiomers half-lives are identical. However, R (+)-enantiomer V_d is higher than S (-)-enantiomer which could be due to enantiomer selectivity in tissue binding or blood binding or both (Walle *et al.* 1988).

PRN is a lipophilic drug so; it can readily cross the blood-brain barrier. Furthermore, it is rapidly distributed and has large V_d of approximately 4 L/kg (Chidsey *et al.* 1975).

1.3.3.3 Excretion

The kidneys are the primary route of PRN excretion, whereas the liver is the primary route of metabolism (Craig and Stitzel 2004). PRN excretion maybe prolonged and its BA may increase in the presence of liver diseases (e.g., hepatic cirrhosis with portosystemic shunting), hepatic enzyme inhibition, decreased hepatic blood flow or administration of drugs that affect hepatic metabolism (Katzung *et al.* 2004). PRN clearance is enantiomer-selective with preferential removal of the R (+)-enantiomer from the blood. Clearance through naphthalene ring hydroxylation is 2.5 fold greater for the R (+)-enantiomer in comparison to the S (-)-enantiomer due to the differences in the catalytic activities of CYP450 isoenzymes. However, the clearance for both the (+)- and (-)-enantiomers through both glucuronidation and side chain oxidation is identical (Walle *et al.* 1988).

1.3.3.4 Metabolism

PRN is highly extracted by the liver, so it shows marked variations in its BA among patients due to differences in blood flow and hepatic function, and this explains the reason of different concentrations of PRN for patients given the same dose of drug (Ismail *et al.* 2004; Katzung *et al.* 2004). PRN is cleared from the blood at a rate of 16 ml/min per kg. Thus, the liver is able to remove the amount of PRN contained in 1120 ml blood of a 70 kg human in 1 minute (Brunton *et al.* 2006).

Propranolol metabolic pathways

PRN metabolism in man occurs via three primary metabolic pathways namely; naphthalene ring hydroxylation, side chain oxidation, and glucuronidation (Marathe *et al.*

1994) **(Figure 1.4)**. Ring hydroxylation that has the share of 42% (range, 27-59%) of PRN metabolism. It is considered as the “first choice” pathway, followed by side chain oxidation with 41% (range, 32-50%), and glucuronidation which accounts for the least percentage of the three pathways of 17% of the dose (range, 10-25%) (Walle *et al.* 1985). Ring hydroxylation process occurs in either position four, five or seven. 7-hydroxy propranolol present in a very small amount in human liver microsomes, whereas 4-hydroxy and 5-hydroxy propranolol are the primary metabolites (Masubuchi *et al.* 1994). However, both of 4-hydroxy and 5-hydroxy propranolol showing a preference for R (+)-PRN stereoselectivity (Marathe *et al.* 1994). The resulted hydroxypropranolol will be either sulphoconjugated favoring the R (+)-PRN enantiomer, whereas conjugation with glucuronic acid favors S (-)-enantiomer. Also, conjugation with glucuronic acid to forming PRN glucuronide, favors the S (-)-enantiomer (Walle *et al.* 1988). N-dealkylation process stereoselectivity is concentration dependent. Therefore, higher concentration accounts for S (-)-enantiomer and the R (+)-enantiomer for lower concentrations (Marathe *et al.* 1994) **(Figure 1.4)**.

As for cytochrome isoforms involved in PRN metabolism, N-desisopropylpropranolol of both S- and R- isomers are highly associated with naphthoflavone and phenacetin o-deethylase (selective inhibitors of CYP1A2), meaning that CYP1A2 is involved in the metabolism of this pathway. On the other hand, quinidine and debrisoquine-4-hydroxylase which are index reaction of CYP2D6 (both are selective inhibitors of CYP2D6) which inhibits both 4 and 5-hydroxypropranolol of both enantiomers (Masubuchi *et al.* 1994; Yoshimoto *et al.* 1995). Furthermore, CYP1A2 has some catalytic activity on 4-hydroxypropranolol because furaphylline, a selective CYP1A2

inhibitor, inhibits about 45% together with quinidine of about 55% (Johnson *et al.* 2000), meaning that CYP2D6 and CYP1A2 are involved in this metabolic pathway. However, CYP2C8/9, CYP2C19, CYP3A3/4 and CYP2E1 have weak inhibitory activities on PRN metabolism (Yoshimoto *et al.* 1995) (**Figure 1.4**).

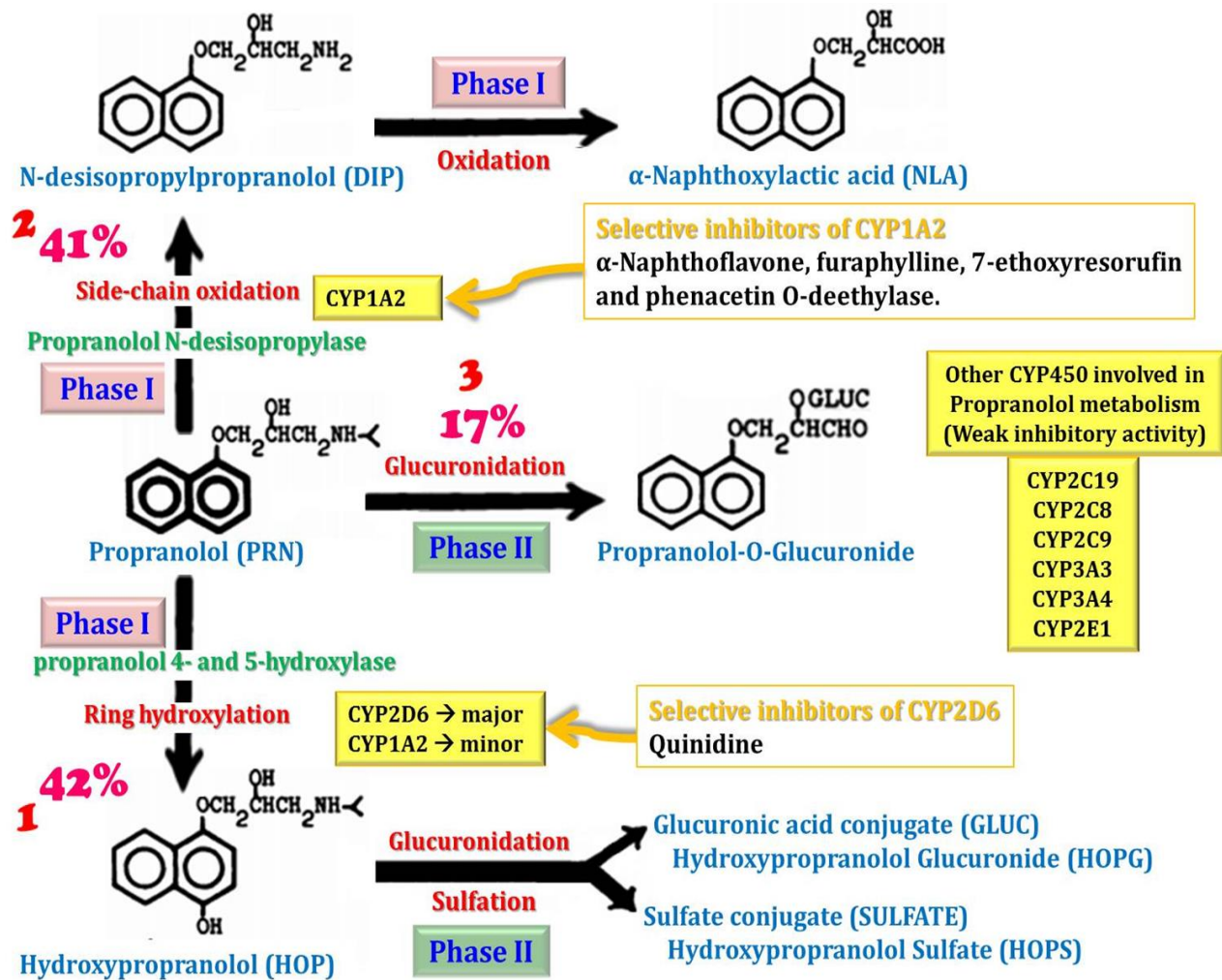


Figure 1.4 Propranolol major metabolic pathways. Adapted and modified from (Marathe *et al.* 1994; Walle *et al.* 1985).

1.3.4 Propranolol toxicity

PRN toxicity results from the blockage of bronchial, cardiac and vascular β receptors. Patients with peripheral vascular insufficiency, diabetes, asthma, bradycardia and cardiac conduction diseases may suffer from PRN toxicity. Many patients experience PRN withdrawal syndrome after abrupt discontinuation, such as tachycardia, nervousness, increase of blood pressure, increased angina intensity, and myocardial infarction due to supersensitivity or up-regulation of β adrenoceptors (Katzung *et al.* 2004).

1.3.5 Propranolol adverse effects

PRN is a lipophilic drug that enters blood-brain barrier causing central nervous system adverse effects, such as vivid dreams, mild sedation, and rarely, depression. Furthermore, patients administered PRN experience coolness of hand and feet in winter, in addition some patients may experience sexual deficiency and symptomatic arterial hypotension (Katzung *et al.* 2004; Nkontchou *et al.* 2012).

1.3.6 Propranolol contraindications

PRN is contraindicated in severe bradycardia, high grade atrioventricular blockage and ventricular asystole in the presence of digitalis toxicity. It is also contraindicated in cardiogenic shock and severe depression (Craig and Stitzel 2004; Mansoor and Kaul 2009). PRN is used in extreme caution in severe bronchospasms in chronic obstructive pulmonary disease patients as well as moderate to severe persistent asthmatic patients since it blocks β_2 receptors in bronchial smooth muscle (Brunton *et al.* 2006; Chafin *et al.* 1999; Craig and Stitzel 2004; Mansoor and Kaul 2009).

1.3.7 Propranolol drug interactions

1.3.7.1 Propranolol Pharmacokinetic interactions

Aluminum salts, colestipol, and cholestyramine decrease the absorption of PRN. PRN is extensively metabolized by the liver. Therefore, many drugs such as rifampin, phenytoin, and phenobarbital as well as smoking induce hepatic biotransformation enzymes resulting in decreased PRN plasma concentration. However, cimetidine and hydralazine increase PRN concentration and BA by affecting hepatic blood flow (Brunton *et al.* 2006).

1.3.7.1 Propranolol pharmacodynamic interactions

Indomethacin, a nonsteroidal anti-inflammatory drug (NSAIDs), can oppose the antihypertensive response of PRN and other β blockers. This effect may be related to inhibition of prostacyclin synthesis (Beckmann *et al.* 1988). Other PRN drug interactions include the additive effect of Ca^{2+} channel blockers and PRN on the cardiac conducting system, whereas PRN and other antihypertensive drugs have additive effect on blood pressure (Brunton *et al.* 2006).

1.4 Glucosamine (GlcN)

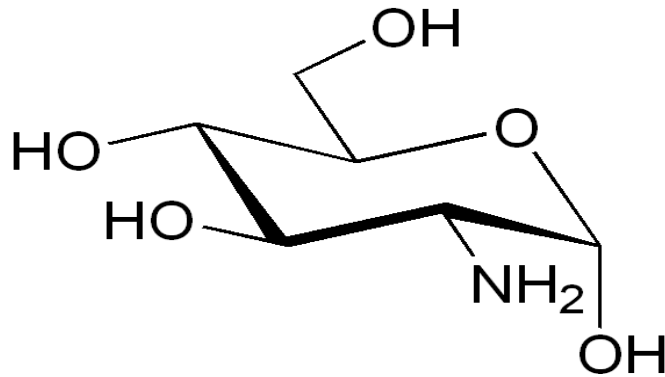


Figure 1.5 Chemical structure of glucosamine.

Glucosamine (GlcN) (2-amino-2-deoxy-d-glucose) is one of several 6-carbon amino sugars naturally occurring in the body which is water soluble and is generally nontoxic (**Figure 1.5**). GlcN is a monosaccharide compound generated by hydrolysis of chitosan or chitin. It is one type of amino sugars that are considered as an important building blocks for mucoproteins, mucopolysaccharides, and mucolipids such as heparin, hyaluronic acid and chondroitin (Al-Hamidi *et al.* 2010; Kirkham and Samarasinghe 2009; Xing *et al.* 2006). Chitosan is a polymer made from acetylglucosamine units and its structure is basically composed of D-glucosamine monomer units. It is the N-deacetylated derivative of chitin, which is present in the exoskeletons of crustaceans, fungi cell walls, and cuticles of insects (Guibal 2005; Liu *et al.* 2006).

GlcN is found in most of human tissues such as GIT mucosal membranes, higher concentrations are found in connective tissues (e.g., cartilage). GlcN can be found in many forms, including hydrochloride, chlorohydrate sulfate salt, N-acetyl-glucosamine, and as a

dextrorotatory isomer (Dahmer and Schiller 2008; Kirkham and Samarasinghe 2009; Xing *et al.* 2006).

1.4.1 Glucosamine in the treatment of osteoarthritis

GlcN is present in the connective and cartilage tissues and it contributes in the maintenance of the strength and flexibility of these tissues (Hua *et al.* 2005). The ability to synthesize GlcN decreases with age. Consequently, replenishing the levels of GlcN, especially GlcN hydrochloride and GlcN sulfate, would be useful for the prevention and treatment of osteoarthritis (OA) (Xing *et al.* 2006). GlcN treats OA and rheumatoid arthritis (RH) by its chondroprotective effect through normalizing cartilage metabolism by inhibiting the degradation and stimulating the synthesis of glycosaminoglycans. In addition to that, GlcN has anti-inflammatory effect because it suppresses neutrophil functions such as phagocytosis, chemotaxis, superoxide generation, and granule enzyme release (anti-reactive properties). GlcN also reduces the expression of NF- κ B induced by proinflammatory cytokines. Moreover, GlcN reduces the production of nitric oxide and prostaglandin E₂ in plasma, hence, restores articular function (Hua *et al.* 2005; Matheu *et al.* 1999; Mendis *et al.* 2008; Nagaoka *et al.* 2011; Reginster *et al.* 2012; Xing *et al.* 2006).

1.4.2 Other Glucosamine effects

GlcN has been reported to function as an inhibitor of tumor growth since it can alter signaling molecules involved in protein translation. In addition it has been reported to alter uracil and adenine nucleotide contents, thus, results in disruption of the structure and function of cellular membranes. Moreover, GlcN has antioxidant and scavenging ability on

superoxide and hydroxyl radicals. Therefore, it is considered as a desired antioxidant food supplement because it is non-toxic and free from side effects (Xing *et al.* 2006).

1.4.3 Glucosamine Pharmacokinetics

1.4.3.1 Orally administered GlcN

GlcN is absorbed rapidly following oral administration with 26% BA as compared to I.V. administration. Its peak plasma concentration (C_{max}) can be reached after 3 hours (T_{max}). However, GlcN undergoes substantial first-pass metabolism and its elimination $t_{0.5}$ was estimated to be 15 hours (Anderson *et al.* 2005; Henrotin *et al.* 2012; Kirkham and Samarasinghe 2009; Persiani *et al.* 2005). Other studies have shown that non-serum $t_{0.5}$ of GlcN ranges from 28-58 hours (Kirkham and Samarasinghe 2009). GlcN plasma concentration was shown to remain above baseline for up to 48 hours after oral administration (Henrotin *et al.* 2012). It has been also reported that GlcN shows linear PK at the dose range of 750-1500 mg, whereas increasing the dose up to 3000 mg could deviate such linearity (Persiani *et al.* 2005)

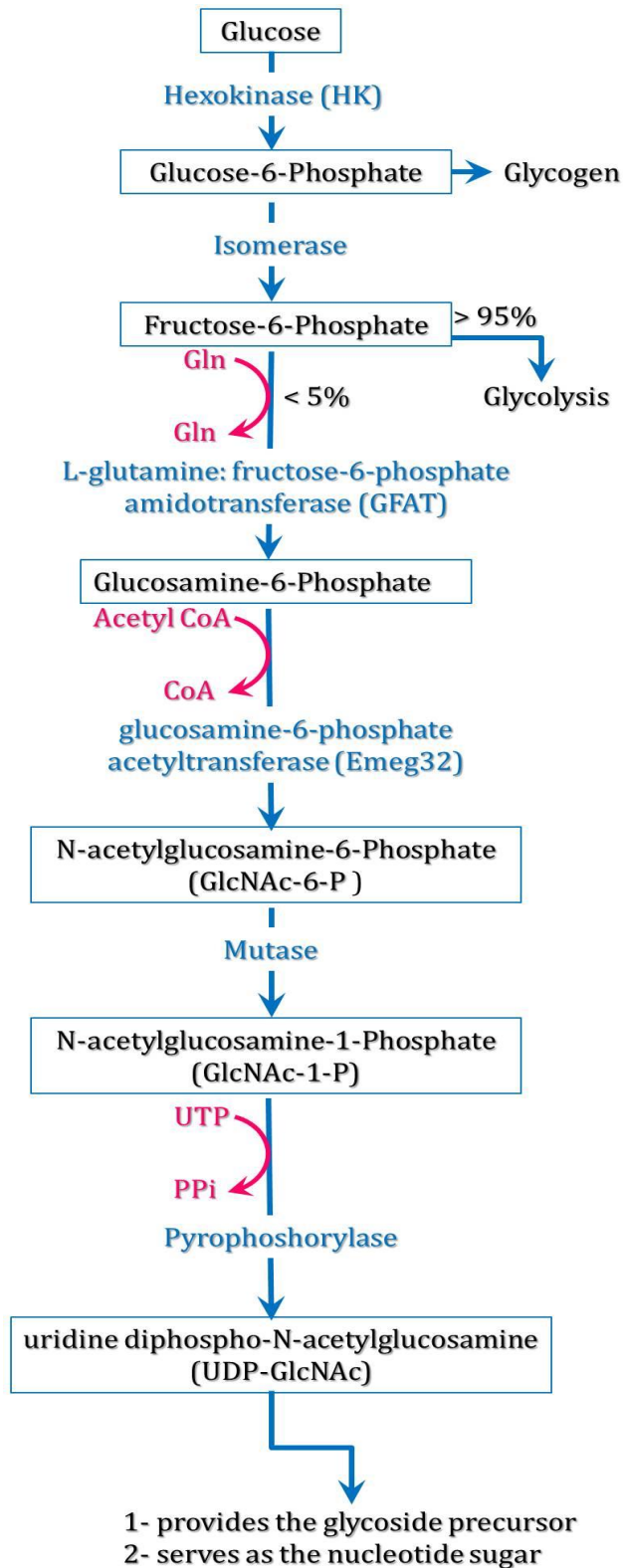
1.4.3.2 Intravenously administered GlcN

Following I.V. administration of radiolabeled GlcN, about 10% of the labeled GlcN was found as free GlcN in plasma; which was cleared by the liver and kidney and excreted in the urine. The remaining 90% was bound to plasma proteins. Peak plasma concentration was reached at 8 hours (T_{max}) (Anderson *et al.* 2005). GlcN V_d was found to be 2.12 L and its apparent terminal $t_{0.5}$ was found to be one hour (Aghazadeh-Habashi *et al.* 2002).

Following administration of radiolabeled GlcN by I.V. and oral routes, about half of radioactivity was excreted in CO₂, 40% was excreted in urine whereas the remaining 2-10% were excreted in feces. Blood levels achieved after oral GlcN are only 20% of those achieved with I.V. GlcN (Anderson *et al.* 2005; Setnikar *et al.* 1983).

1.4.4 Biochemical pathways

GlcN is naturally produced in the cells as GlcN-6-phosphate via hexosamine biosynthetic pathway through the combination of glutamine with fructose-6-phosphate in the presence of the enzyme glutamine fructose-6-phosphate amidotransferase. Ending up with the formation of uridine diphosphate-N-acetyl glucosamines, which enters in the formation of glycosaminoglycans, glycolipids and proteoglycans. This sugar will be used for O-linked glycosylation of several proteins such as RNA polymerase, transcription factors and nuclear pore proteins causing changes in the biological activity (Anderson *et al.* 2005; Roseman 2001; Uldry *et al.* 2002).



1.4.4.1 Hexosamine biosynthetic pathway

Glucose is phosphorylated by the enzyme hexokinase. Phosphorylated glucose will enter glycogen synthetic pathway or will be converted by the enzyme glucose-6-phosphate isomerase to fructose-6-phosphate. More than 95% of fructose-6-phosphate may enter glycolysis, whereas less than 5% of glucose uptake enters the hexosamine biosynthetic pathway for glucose metabolism. Fructose-6-phosphate is converted by (L-glutamine: fructose-6-phosphate amidotransferase) (GFAT) the rate-limiting enzyme. This reaction results in the production of glucosamine 6-phosphate, which is followed by the acetylation of glucosamine-6-phosphate by the enzyme (glucosamine-6-phosphate acetyl transferase) ending in the production of N-acetylglucosamine-6-phosphate.

Figure 1.6 Hexosamine biosynthetic pathway. Adapted and modified from (Ngho *et al.* 2010).

N-acetylglucosamin-6-phosphate will be converted to GlcNAc-1-P by the enzyme mutase (phosphate-acetyl glucosamine mutase), followed by production of UDP-GlcNAc by (UDP-GlcNAc pyrophosphorylase). Finally, UDP-GlcNAc molecule will act as a glycoside precursor and serves as the nucleotide sugar for the posttranslational glycosylation of many proteins (Anderson *et al.* 2005; Ngoh *et al.* 2010) **(Figure 1.6)**

1.4.5 Glucosamine safety and toxicity

1.4.5.1 Orally administered GlcN

Oral administration of very large doses (5000–15,000 mg/kg body weight) of GlcN was found to be well tolerated without toxicity. Studies on mice, rats, rabbits and dogs received GlcN orally in doses of approximately 159–8000 mg/kg/day for 12–365 days did not show any adverse effects (Setnikar *et al.* 1991; Setnikar *et al.* 1983).

1.4.5.2 Intravenously administered GlcN

Several studies established the safety and toxicity of GlcN following I.V. infusion to rats. In these studies, doses ranged from 240 to 9937 mg/kg body weight. Meininger *et al.* reported that infusion of 564 mg/kg did not affect blood glucose levels (Meininger *et al.* 2000), whereas other studies used average infusion rates of 2496 mg/kg detected GlcN adverse effects on glucose metabolism. However, these results were difficult to be explained because of different GlcN oral BA which is 26% as compared to I.V. route. In addition to that oral GlcN administration did not induce alteration on glucose metabolism at very high doses (300–2149 mg/kg body weight) on rats, rabbits and dogs which is different from that of parenteral administration (Anderson *et al.* 2005).

1.4.5.3 Glucosamine safety on human

Administration of GlcN to more than 800 patients who were monitored continuously following infusion of large amounts of GlcN did not lead to any adverse effects. Other human clinical studies indicated that there were no adverse effects of GlcN administration on liver and kidney function, blood chemistries (white blood count, red

blood count, and hemoglobin), urinalyses, and on cardiovascular parameters (pressure and pulse rate) (Monauni *et al.* 2000; Pouwels *et al.* 2001). Interestingly, GlcN exerts an inhibitory effect on platelets *in vivo* by suppressing thromboxane A₂ production, ATP release and platelet aggregation, so it is considered as safe anti-platelet agent (Lu-Suguro *et al.* 2005).

Nevertheless, the reported adverse effects of GlcN are generally uncommon and minor, such as nausea, vomiting, headache, dyspepsia and skin allergies (Delafuente 2000). However, it should be taken into consideration that GlcN is made from the shells of crab, lobster, and shrimp. Thus, it should be avoided in people with shellfish allergies since it can develop facial and throat swelling (Dahmer and Schiller 2008; Matheu *et al.* 1999).

1.5 Cimetidine

Cimetidine is the first histamine type 2 (H₂) receptor antagonists. It inhibits gastric acid secretion by reversibly competing with histamine for binding to H₂ receptors on the basolateral membrane of parietal cells. It is used in the treatment of peptic ulcer disease (Brunton *et al.* 2006; Pelkonen and Puurunen 1980; Puurunen and Pelkonen 1979) as well as duodenal ulcers, and uncomplicated gastroesophageal reflux disease (Brunton *et al.* 2006).

1.5.1 Cimetidine drug interactions

Cimetidine is an imidazole-containing drug that binds to CYP450 heme iron and effectively reduce metabolism of endogenous substrates (e.g., testosterone) or other concomitant used drugs metabolized by CYP1A2, CYP2C9, CYP2D6, and CYP3A4 through competitive inhibition. Thus, the half-lives of these drugs will be prolonged (Brunton *et al.* 2006; Katzung *et al.* 2004). As a result, it is used as a control in many of literature studies documenting its role in drug interactions due to its clear effect and role in drug interactions (Piyapolrunroj *et al.* 2000).

Pharmacokinetic drug interaction between PRN and cimetidine may lead to reinforcement of the β -adrenoceptor blocking effects of PRN due to changes in the therapeutic levels of PRN in blood. Such interaction may also lead to pharmacodynamic effects where cimetidine was reported capable of causing dangerous reduction in blood pressure and heart rate in patients receiving PRN for coronary heart disease (Reimann *et al.* 1981).

1.6 Rifampin (Rifampicin)

Rifampin is a semisynthetic derivative of macrocyclic antibiotic produced by *Streptomyces mediterranei*. Rifampin is a bactericidal, large lipid-soluble molecule active against gram-negative and gram-positive cocci, mycobacteria, enteric bacteria, and chlamydiae. It is used in the treatment of mycobacterial Infections (Katzung *et al.* 2004). Rifampin's mechanism of action is through binding to the β -subunit of bacterial DNA-dependent RNA polymerase and thereby inhibits RNA synthesis. However, it does not affect mammalian polymerases (Craig and Stitzel 2004).

1.6.1 Rifampin drug interactions

Rifampin is an enzyme inducer which potently induces CYP1A2, 3A4, 2D6, 2C8, 2C9, and 2C19. Therefore, reduces the $t_{0.5}$ of many compounds, such as digoxin, digitoxin, mexiletine, PRN, metoprolol, disopyramide, quinidine, tocainide and ketoconazole as well as non-nucleoside reverse transcriptase inhibitors, and HIV protease (Brunton *et al.* 2006).

1.7 Bioanalytical HPLC method validation parameters definitions (EMEA)

1.7.1 Accuracy

The accuracy of an analytical method describes the closeness of the mean of test value obtained by the method to the actual concentration of the analyte (expressed in percentage) (FDA 2013). Any bias or systematic error in the method is usually indicated by the accuracy (Bliesner 2006). Accuracy samples and quality control samples (QC samples) should be spiked with a specified amount of analyte and the resultant concentrations of the analyzed samples will be compared with the actual value. Accuracy evaluation should be done for values of QC samples obtained within a single run (intra-day accuracy or within run accuracy) and in different runs (inter-day accuracy or between-run accuracy) (EMEA 2011).

Accuracy % is calculated as follows:

$$\text{Accuracy}\% = \frac{\text{Measured (calculated) concentration}}{\text{Theoretical (true) concentration}} \times 100\%$$

Intra-day accuracy (within-run accuracy) should be measured using a minimum of five samples per level for each single run with a minimum of four concentration levels which are covering the calibration curve range: the lower limit of quantification (LLOQ), within three times the LLOQ (QC low), around 50% of the calibration curve range (QC mid), and at least at 75% of the upper calibration curve range (QC high). On the other hand, inter-day accuracy (between-run accuracy) is measured using samples of LLOQ, QC low, mid and

high obtained from at least three runs analyzed on at least two different days to be evaluated for the validation of the inter-day accuracy. In both intra-day and inter-day accuracy, accuracy % of QC (low, mid and high) should be within 85-115% while LLOQ should be within 85-120%, according to EMEA guidelines (EMEA 2011).

1.7.2 Precision

The precision of an analytical method describes the closeness of repeated individual measures of analyte which is usually determines the degree of repeatability under normal conditions (Shabir 2003; Taverniers *et al.* 2004) and is usually expressed as the coefficient of variation (CV %). CV% is calculated as follows:

$$CV \% = \frac{\text{Standard deviation}}{\text{Mean}} \times 100\%$$

Precision should be determined for samples of LLOQ, QC low, mid and high, within a single run and between different runs, i.e. using the same runs and data as for the demonstration of accuracy (Taverniers *et al.* 2004). Intra-day precision (within-run precision) is the minimum of five samples per concentration level of LLOQ, QC low, mid and high for each single run which will be evaluated for intra-day precision validation. Inter-day precision (between-run precision) is usually validated for all QC samples (LLOQ, QC low, mid and high) from at least three runs analyzed on at least two different days. In both intra-day and inter-day precision, CV% value should not exceed 15% for all QC samples (QC low, mid and high), except for the LLOQ which should not exceed 20% (EMEA 2011).

1.7.3 Linearity

The linearity of an analytical method is its ability to obtain test results (area response) that are directly proportional to the concentration of analytes in samples within the given range. It involves six calibration curves or more over the concentration range (from LLOQ to ULOQ) where the standard curves are repeated in three or more runs randomly (Huber 2007; Shabir 2003; Shah *et al.* 2000). Linearity for each calibration curve is usually evaluated by examining y-intercept and the regression factor (R^2) which is a value that is used to evaluate closeness between predicted and target data. The best linear relationship must be more than 0.99 (closer to 1) which is considered sufficient evidence to conclude that the method has a perfect linear calibration (Kazakevich and Lobrutto 2007; Shabir 2003).

1.7.4 Stability

Evaluation of stability conditions should be conducted to ensure that every step taken during sample preparation, analysis and storage conditions will not affect analyte concentration. The stability of every step in the analytical method is ensured by applying conditions to the stability tests such as sample matrix, storage, container materials and analytical conditions which should be similar to those used for the actual study samples. Analyte stability is studied using QC low and QC high samples which are analyzed immediately after preparation then after applying storage conditions to the samples to be evaluated. QC samples are analyzed against a calibration curve, obtained from freshly spiked calibration standards, and the resultant concentrations are compared to the actual

concentrations where accuracy % of QC (low and high) should be within 85-115% according to EMEA guidelines (EMEA 2011).

Stability tests should be evaluated as follow:

1.7.4.1 Freeze and thaw stability test

QC samples are stored and frozen in the freezer at the intended temperature and thereafter thawed at room processing temperature (room temperature) where freezing and thawing of stability samples should be similar to sample handling conditions. Stability should be assessed for a minimum of three freeze-thaw cycles (EMEA 2011; FDA 2013).

1.7.4.2 Sample stability after preparation at room temperature (bench-top stability)

Bench-top stability is the short term stability of the analyte in the matrix at room temperature or laboratory handling conditions which are expected for study samples and under storage conditions used during the study (EMEA 2011; FDA 2013).

1.7.4.3 Autosampler stability

On-instrument/ autosampler stability of the processed sample at injector or autosampler temperature (EMEA 2011; FDA 2013).

1.7.5 Recovery

Recovery is not considered among the validation parameters regarded as essential for method validation. Recovery describes method ability to detect the sample to be tested in the presence of internal standard and drug in order to obtain results with less error or bias (Peters *et al.* 2007). Recovery is the extraction efficiency of an analytical process,

reported as a percentage of the known amount of an analyte carried through the sample extraction and processing steps of the method (Huber 2007; Shah *et al.* 2000). Recovery depends on sample processing procedure, sample matrix and analyte concentration (Huber 2007). Recovery is calculated as follows:

$$\text{Absolute recovery of the drug or internal standard} = \left(\frac{\text{AUC mean of serum/krebs buffer}}{\text{AUC mean of the mobile phase}} \right) \times 100\%$$

1.7.6 Range

Range is defined as the range of concentration between the upper and lower levels (ULOQ and LLOQ) that can be reproducibly and reliably quantified with accuracy, precision and linearity using concentration-response relationship since the range is derived from linearity (FDA 2013 ; Huber 2007).

1.7.7 Reproducibility

Reproducibility is the degree of reproducibility of results obtained under different conditions, such as different laboratories, environmental conditions, analysts, operators, instruments, and materials. It is also considered a measurement of test results reproducibility under normal, expected operational conditions from laboratory to laboratory and from analyst to analyst (Huber 2007).

2.3.8 Selectivity

Selectivity of an analytical method is defined as the ability of a method to measure the analyte of interest accurately in the presence of interference, such as synthetic precursors, excipients, enantiomers, or degradation products that may be expected to be

present in the sample matrix (Araujo 2009; EMEA 2011; Huber 2007; Shah *et al.* 2000). Selectivity may also investigate interference from degradation products formed during sample preparation, interferences caused by metabolites of the drug(s) and interference from possible co-administered medications (EMEA 2011).

1.7.9 Sensitivity

The sensitivity of an analytical method is defined as the method capability to discriminate small differences in concentration or mass of the test analyte and is dependent on the signal-to-noise ratio in a given detector (Huber 2007; Kupiec 2004).

1.7.10 Limit of detection

It is the lowest amount of analyte in a sample that can be detected but not necessarily quantitated as an exact value (Huber 2007), the limit of detection is expressed as the concentration of analyte in the sample based on a signal-to-noise (S/N) ratio (3:1) (Bliesner 2006). At each concentration level six to ten independent replicates will be measured randomly at the various level (Armbruster and Pry 2008).

1.7.11 Lower limit of quantification

The LLOQ of an analytical procedure is the lowest concentration of analyte in a sample that can be quantitatively determined with acceptable accuracy and precision and is considered the lowest calibration standards (Bliesner 2006; EMEA 2011). The analyte signal of the LLOQ sample should be at least five times the signal of a blank sample. The LLOQ should be suitable with the desired concentrations required for the aim of the study (EMEA 2011).

1.8 Aim and objectives of the study

1.8.1 Aim

The aim of this study was to evaluate the effect of GlcN on PRN concentration levels in rats and to investigate whether there is a possible drug-drug interaction. PRN-GlcN drug interaction was compared with the known interactions of cimetidine and rifampin with PRN.

1.8.2 Objectives

The two main practical objectives of the current study were; to define the doses of GlcN that can affect PRN BA *in vivo* and *in situ* as well as PRN concentration levels *in vitro* and to uncover the mechanism by which GlcN affects PRN serum concentration. In order to achieve these objectives, a validated HPLC method of PRN in rat serum and Krebs buffer was developed. Later, several *in vivo*, *in situ* and *in vitro* tests were conducted. Finally, this work might reveal whether PRN dose adjustment should be necessary with GlcN administration in patients with OA and RA by determining the effect of GlcN on PRN BA. Consequently, recommend whether health care professionals should be aware of such PRN dose adjustment.

Chapter Two

Materials and method

Chapter Two

2. Materials and methods

2.1 Materials

Chemicals and drugs

Potassium chloride and ethylene diamine tetra acetic acid were purchased from (Acros organics, BVBA Geel, Belgium). Deionized water (Nanopur™), methanol advanced gradient grade, and acetonitrile were obtained from (Fisher Scientific Ltd., Loughborough, UK). Potassium dihydrophosphate, penicillin, streptomycin, fetal bovine serum, sodium lauryl sulphate, and magnesium sulfate were all purchased from (Sigma-Aldrich, St. Louis, Missouri), sodium bicarbonate (Merck, Darmstadt, Germany), phosphoric acid (Kyowa Medex Co., Tokyo, Japan), and triethylamine (Tedia Company, Inc., USA) were also used. All chemicals were of analytical grade, whereas solvents were of HPLC grade.

HBSS (Ca²⁺, and Mg²⁺ free), HBSS (with Ca²⁺, and Mg²⁺), and Williams's Medium E were obtained from (Invitrogen, Carlsbad, CA, USA). Collagenase II and L-glutamine were purchased from (Gibco BRL, Gaithersburg, MD, USA).

Propranolol hydrochloride was a kind gift from The Arab Pharmaceutical Manufacturing (APM, Salt, Jordan), whereas Glucosamine hydrochloride was obtained from Biocon (Bangalore, India; batch No: DA-B10-04-000650/02493). Rifampin and Florane® (isoflurane) was a kind gift from Hikma Pharmaceuticals (Amman, Jordan), whereas

cimetidine kindly donated by Jordan Sweden Medical and Sterilization Company (JOSWE, Naur, Jordan).

2.2 Methodology

2.2.1 Chromatographic conditions

The HPLC system FINNIGAN SURVEYOR (Thermo Electron Corporation, San Jose, CA, USA) was used. The detector (UV-VIS Plus Detector), the pump (solvent delivery systems pump) (LC Pump) and the autosampler (Autosampler Plus). Computer system used was Windows XP and the software used was ChromQuest software 4.2.34. HPLC system was set at a wavelength of 214 nm and coupled with a hypersil™ BDS C-18 Column (Thermo Electron Corporation, San Jose, CA, USA); (150 mm x 4.6 mm, 5µm) with a flow rate of 1 ml/min using a 15 µl injection volume and 7 ml/min run time. Sildenafil citrate was used as an internal standard (IS) in this method.

2.2.2 HPLC analysis procedure

2.2.2.1 Preparation of mobile phase

Mobile phase used at a ratio of 15% acetonitrile HPLC gradient, 32.5% methanol HPLC gradient and 52.5% water. Water was prepared by the addition of triethylamine where 1 L of water contains 900 µl of triethylamine then pH was adjusted to 2.75 using phosphoric acid. Water 525 ml was mixed with 150 ml of acetonitrile and 325 ml of methanol to obtain a final volume of 1000 ml.

Preparation of stock solutions and working solutions

2.2.2.2 Preparation of stock solutions

Preparation of stock solutions of propranolol

PRN (10 mg) was dissolved in 50 ml methanol to obtain a final concentration of 200 µg/ml stock solution of PRN.

Preparation of stock solutions of sildenafil IS

Sildenafil (10 mg) was dissolved in 10 ml acetonitrile to obtain a final concentration of 1000 µg/ml stock solution of sildenafil.

2.2.2.3 Preparation of working solutions

Preparation of working solution of sildenafil (IS)

Sildenafil (250 µl) from stock solution (1000 µg/ml) was diluted to 50 ml of acetonitrile to obtain 5 µg/ml of sildenafil working solution.

Preparation of propranolol serial spiking samples and quality control (QC) samples in serum and buffer.

Calibration curve and QC samples were prepared by taking different volumes (µl) from PRN stock solution (200 µg/ml) as shown in **tables 2.1 and 2.2** to reach 1 ml final volume. Consequently, concentrations of working solutions (µg/ml) were obtained to be used later for serum and Krebs buffer spiking solutions which were prepared by taking 25 µl of each working solution to be spiked in 975 µl of serum or Krebs buffer (final volume 1 ml). Spiked serum and Krebs buffer of PRN serial samples and QC samples were prepared as shown in **table 2.1 and 2.2** respectively.

Table 2.1 Spiked serum or Krebs buffer of PRN serial spiking samples.

Serial dilutions of Propranolol from Stock solution of 200 µg/ml					Serum and Buffer spiking solution			
Solution No:	Working Solution conc(µg/ml)	Stock Conc (µg/ml)	Volume taken from stock (µl)	Total Volume (ml)	Cal ID	Volume taken from working solutions (µl)	Total Volume	Final concentration (ng/ml)
1	2	200	10	1	C1	25	1	50
2	4	200	20	1	C2	25	1	100
3	8	200	40	1	C3	25	1	200
4	20	200	100	1	C4	25	1	500
5	40	200	200	1	C5	25	1	1000
6	80	200	400	1	C6	25	1	2000
7	120	200	600	1	C7	25	1	3000

Table 2.2 Spiked serum or Krebs buffer of PRN quality control samples.

Serial dilutions of Propranolol from Stock solution of 200 µg/ml					Serum and Buffer spiking solution			
Solution No:	Working Solution conc(µg/ml)	Stock Conc (µg/ml)	Volume taken from stock (µl)	Total Volume (ml)	Cal ID	Volume taken from working solutions (µl)	Total Volume	Final concentration (ng/ml)
8	6	200	30	1	QCL	25	1	150
9	60	200	300	1	QCM	25	1	1500
10	100	200	500	1	QCH	25	1	2500

2.2.2.4 Method of extraction

An appropriate number of Eppendorf tubes were placed in a rack and labeled properly, 100 μ l aliquots of each test sample (*In vivo* rat samples, *in situ* SPIP, everted gut samples) was pipetted into the appropriate labeled tube followed by the addition of 150 μ l IS (5 μ g/ml of Sildenafil). Finally, each sample was vortexed vigorously for 1 min then centrifuged at 14000 rpm for 15 minutes. The procedure described was applied for subject samples, calibrator and quality control samples.

2.2.2.5 Method development

By referring to previous studies, PRN was detected in plasma using reverse phase HPLC method. PRN wavelength was determined after several trials on different wavelength of 250, 280 and 214 nm resulting in the best detection for 214 nm wavelength. IS selection depends on chemical similarity of this IS to PRN, comparable retention times and similarly in the derivatization procedures of both drugs. Good separation between PRN HCl and sildenafil was obtained after the examination of different mobile phases and columns. Among serum extraction methods, protein precipitation method with acetonitrile was found to be optimal in our method for the extraction of serum and Krebs buffer. Mobile phase composition was selected after several trials to obtain symmetric shapes of analyte and good resolution with short run time (7 min).

2.2.3 Method Validation

Validation in this thesis was conducted in accordance with EMEA guidelines of bioanalytical method validation.

2.2.3.1 Intra-day accuracy and precision

Intra-day accuracy and precision were calculated by analyzing six replicates of each QC concentration mentioned in **table 2.3** on three different days accompanied by a calibration curve for each day in order to calculate the concentration per each. Accuracy level was determined by accuracy % while coefficient of variation (CV%) was calculated to determine precision. As mentioned previously in **1.7.1 and 1.7.2** Accuracy % of QC (low, mid and high) should be within 85-115% while LLOQ should be within 85-120%, in regard to CV% value it should not exceed 15% for all QC samples (QC low, mid and high), except for the LLOQ which should not exceed 20%.

Table 2.3 Quality control concentrations used for method validation

QC solution	Final concentration (ng/ml)
LLOQ	50
QC low	150
QC mid	1500
QC high	2500

2.2.3.2 Inter-day accuracy and precision

Inter-day accuracy and precision were calculated by using data of measured concentrations obtained from days 1, 2 and 3 to calculate CV% and accuracy % for each QC concentration (LLOQ, QC low, QC mid and QC high) separately.

2.2.3.3 Linearity

Each calibration curve contained seven standard concentrations (50, 100, 200, 500, 1000, 2000, and 3000 ng/ml). Six calibration curves were performed throughout method validation (three from intra-day 1, 2 and 3 validations while the remaining three were obtained from stability tests). Depending on the data obtained from those six calibrations; mean of measured concentrations as well as mean ratios of standard points for each level (concentration) were calculated followed by accuracy % and CV% calculation which should be within the acceptance criteria of EMEA guidelines (**sections 1.7.1 and 1.7.2**). Linearity test was performed to determine the acceptability of linearity data by plotting a seventh calibration curve (linearity curve) which was obtained by using the mean ratios of the six calibration curves versus each concentration level to obtain R² value.

2.2.3.4 Stability

Freeze and thaw stability

Six samples for each (QC low and QC high) were spiked properly in serum or Krebs buffer without carrying out the extraction procedure.

At zero time: With corresponding calibration curve, three samples for each (QC low and QC high) were extracted then injected to be analyzed and the resultant concentrations were calculated, the remaining three spiked samples for each (QC low and QC high) were stored and frozen at -20°C for 24 hours.

After 24 hours (Cycle 1): Following the first 24 hours of freezing, samples were thawed at room temperature (25°C) which was the sample processing temperature during analysis stages. After complete thawing, samples were refrozen again for 24 hours.

After 48 hours (Cycle 2): Following the second 24 hours of freezing samples were thawed at room temperature 25°C then were refrozen for the last 24 hours analysis.

After 72 hours (Cycle 3): Finally, the spiked samples were thawed after the last 24 hours of freezing then extracted to be analyzed and the resultant concentrations were calculated.

Sample stability after preparation at room temperature (bench-top stability)

Six samples for each (QC low and QC high) were spiked properly in serum or Krebs buffer without carrying out the extraction procedure.

At zero time: With corresponding calibration curve, three samples for each (QC low and QC high) were extracted then injected to be analyzed and the resultant concentrations were calculated, the remaining three spiked samples for each (QC low and QC high) were left on the bench.

After 24 hours Samples were left on the bench at room temperature 25°C, they were then extracted and injected to be analyzed. The resultant concentrations were calculated.

Autosampler stability

At zero time: With corresponding freshly prepared calibration curve three samples for each (QC low and QC high) were prepared with sufficient volume for the test. They were spiked properly in serum or Krebs buffer, extracted then analyzed and the resultant concentrations were calculated.

After 24 hours of leaving the samples in the autosampler the same three samples for each (QC low and QC high) were injected to be analyzed again and the resultant concentrations were also calculated.

2.2.3.5 Recovery

Drug and IS recovery

Two groups of QC low, mid and high were prepared. In the first group both the drug and the IS were prepared in the mobile phase while the second group was spiked in serum or Krebs buffer. CV% values were calculated from the resultant AUC of both the drug and the IS followed by absolute recovery calculation for each of them.

2.2.4 Animal handling

The protocols for the animal study were approved by the Ethical Committee of the Higher Research Council at the Faculty of Pharmacy and Medical Sciences, University of Petra (Amman, Jordan). Adult males and non-pregnant females Sprague Dawley rats were supplied and housed at the University of Petra's Animal House. Rats with average weight of (220 ± 20 g) were used. Rats were kept in air-conditioned environment under controlled temperatures (22-24 °C), humidity (55-65%), and photoperiod cycles (12 light/12 h dark). Rats were fasted overnight (for 18 to 22 h) with free access to water, unless otherwise stated. All experiments were achieved in accordance with University of Petra's Institutional Guidelines on Animal Use which adopts the guidelines of the Federation of European Laboratory Animal Science Association (FELASA).

2.2.5 *In vivo* Glucosamine, cimetidine and rifampin effect on propranolol bioavailability

2.2.5.1 Drugs preparation

PRN reference solution, cimetidine, rifampin and GlcN solutions were all prepared by dissolving an accurately weighed amount of PRN, cimetidine, rifampin and GlcN in distilled water to obtain 4, 1, 2 and 40 mg/ml, respectively.

2.2.5.2 Study protocol

All solutions were freshly prepared on the day of experiment and were administered to fasting rats by stainless steel oral gavage needles (Harvard Apparatus, Kent, UK). For all experiments, rats were marked on tail for identification, weighed, and randomized into four groups (n=7). Zero blood samples were pooled from rat's tail for all groups.

Control group received 4 mg/ml of PRN reference solution preceded by water 30 min before the administration of PRN. Rats were divided into 3 groups and received GlcN or cimetidine or rifampin tested solutions at concentration of 40, 1 and 2 mg/ml, respectively. After 30 min all groups received 4 mg/ml of PRN solution. Rats in GlcN group were maintained on drinking water containing 25 g/L GlcN for three days prior to GlcN administration. Rats in rifampin experiment received a daily single dose of rifampin solution (2 mg/ml) for two weeks before the day of experiment. For all groups, blood samples were pooled from rat's tail at different time intervals (0.25, 0.5, 1, 2, 3, 6, 8 and 10 hr). Blood was left to clot, centrifuged for 10 min at 14000 rpm. Then, serum was separated, transferred directly into eppendorf tubes, and kept in freezer at -20 °C till HPLC analysis.

2.2.5.3 Pharmacokinetics and statistical analysis

Pharmacokinetics

Individual PK parameters for drug concentration of *in vivo* plasma samples were calculated by noncompartmental analysis (NCA) using the Kinetica program (used under academic license from Innaphase Ltd, France (Lic. # K 201009)). Pharmacokinetic parameters used were AUC, C_{\max} , AUMC, MRT, $t_{0.5}$, T_{\max} and Kel.

BA is determined by the rate (T_{\max} and C_{\max}) and extent (AUC) of an active drug to reach its site of action in the blood. The time (T_{\max}) of the maximum observed concentration (C_{\max}) were deduced directly from the serum concentration-time curves, whereas the AUC was calculated using the trapezoidal rule:

$$M_0 = \int_0^{\infty} t^0 \cdot C_p dt = \int_0^{\infty} C_p dt = AUC$$

AUMC is the area under moment curve which is simply $C_p \times t$.

$$M_1 = \int_0^{\infty} t \cdot C_p dt = AUMC$$

MRT (Mean residence time) is the mean time that drug molecules remain in the body after dosing and is calculated by the following equation:

$$MRT = \frac{AUMC}{AUC}$$

Kel, represents the fraction of drug eliminated per time and is determined by the slopes of the terminal segments of logarithmically transformed plasma levels against their

corresponding times, where slope equals K_{el} . $t_{0.5}$ was then calculated using the following equation $t_{0.5} = 0.693 / K_{el}$ which is defined as the time required for a drug to fall half of its initial value.

Statistical analysis

Statistical comparisons were obtained using one-way ANOVA followed by Tukey's to compare between more than two groups using SPSS statistical software, (IBM, USP); version 22. Each data point represents the mean \pm SEM. P-value less than 0.05 was considered statistical significant ($p < 0.05$).

2.2.5.4 Data analysis (Optimized effective intestinal permeability)

Effective intestinal permeability (P_{eff}) values were estimated by Nelder–Mead algorithm of the Parameter Estimation module using SimCYP program. The Nelder–Mead method, which is also called downhill simplex, is a commonly used nonlinear optimization algorithm. This was done by searching for the best parameter values that produce plasma concentration that matches the actual plasma concentration at the same time. The objective function is the weighted sum of squared differences of observed and model predicted values. Polar surface area was used first to predict an initial estimate of P_{eff} . SimCYP program was used under academic license from SimCYP Ltd, Sheffield, U.K. (Lic. # CLCLID – AKDI – LEEE – FECI).

2.2.6 Anaesthesia and surgical protocol

A perfusion system consisting of an anaesthesia system (SomnoSuite small Animal Anesthesia System, Kent Scientific Corporation Torrington, USA) that is linked to an oxygen

concentrator (Dual flow oxygen concentrator for oxygen bar, Hebei, China), a water bath (Elmasonic S, Elma, Germany), and a peristaltic perfusion pump (BT100-2J, Hebei, China). The rat was placed on a surgical board (Plas Labs, Lansing, MI, USA) above a heating pad maintained at 37 °C, and anaesthetized by isoflurane (5% for induction and 2.5% for maintenance). Anaesthesia was maintained for the duration of the experiment and was monitored by toe pinch. The skin of the abdomen was then sterilized with 70% ethanol-containing cotton wool, opened using sterile scissors and non-toothed forceps. A midline longitudinal incision was made 1 cm below rat's sternum till 1 cm above rat's tail in the pelvic region followed by two mid-transverse incisions to left and right of the midline to expose rat's viscera.



Figure 2.1 Anesthesia system linked to an oxygen concentrator and a peristaltic perfusion pump.

2.2.7 *In Situ* Single-Pass Intestinal Perfusion (SPIP)

2.2.7.1 Washing and perfusion solution preparation

All drugs used in SPIP experiment (GlcN, cimetidine, and rifampin) were dissolved in normal saline solution (NaCl, 9 mg/ml). Washing solution was prepared by dissolving GlcN, cimetidine or rifampin (according to the experiment) in saline solution to obtain a concentration of 10, 1, and 2 mg/ml, respectively. Perfusion solution was prepared by dissolving PRN in saline solution to give 1 mg/ml concentration together with GlcN or cimetidine or rifampin to obtain a final concentration of 10, 1, and 2 mg/ml, respectively.

2.2.7.2 Intestinal perfusion

A fasted female non pregnant rat was anaesthetized and its intestine was exposed surgically as described in **(section 2.2.6)**. A semi-circular incision was made and an inlet silicon tube (0.3 cm diameter) was inserted into the duodenum 4 cm away from the pylorus. A second incision was made in the ileocecal end and an outflow silicon tube was fitted. Both tube ends were tied securely using surgical suture (Atramat®, Mexico City, Mexico) and linked with suitable tube fittings and inserted in the peristaltic pump at a flow rate preset to 3.6 ml/min. Initially, intestinal segments were rinsed with pre-warmed (37 °C) saline washing solution for 20 min until the outlet solution was clear then perfusion solution was switched. A pre-sample drug was drawn from perfusion solution as well as zero-time blood sample was drawn from rat's tail before perfusion solution was switched. Perfusion solution was perfused for 60 min and blood samples were quantitatively pooled from rat's tail at different time intervals namely; at 10, 20, 30 and 60 min. All blood samples were left to clot, centrifuged for 10 min at 14000 rpm, then serum was separated,

transferred directly into eppendorf tubes, and kept in freezer at -20°C till HPLC analysis. Care was taken throughout the experiment to avoid disturbance in the circulatory system, and the exposed intestinal segments were kept moist with body tempered saline (37 °C) .

2.2.8 GlcN effect on PRN absorption by Everted rat intestinal sac (ERIS)

A simulated physiological solution, Krebs buffer, was prepared by mixing the following volumes (in ml) of 1 M: NaCl 118, KCL 4.5, KH₂PO₄ 1.2, NaHCO₃ 25, MgSo₄ 1.6, Glucose 5.5, CaCl₂ 2.5 and 0.25 ml of 0.1 M EDTA, the volume was completed to 1 L by distilled water then the buffer was oxygenated with oxygen concentrator. CaCl₂ was added after oxygenation to prevent turbidity, and then the pH was adjusted to 7.4 using 1M HCl (0.08 mg/ml). Krebs buffer is known to be a physiological solution that helps in maintaining intracellular and extracellular osmotic balance. Moreover, glucose serves as an energy source of the cell.

Three PRN solutions were prepared by dissolving 10 mg PRN in 100 ml Krebs buffer to obtain a final concentration of 0.1 mg/ml, whereas two soaking solutions were prepared by dissolving 100 mg GlcN, and 1 mg sodium lauryl sulphate (SLS) in two of PRN solutions prepared to give a final concentration of 1 and 0.01 mg/ml, respectively.

SLS is known to be an anionic surfactant that is used as an emulsifier (Lee and Maibach 2006). SLS is used to improve the absorption of many drugs, such as acyclovir due to its ability to enhance the permeability of mucoadhesive tablets of acyclovir, thus enhance its bioavailability (Dias *et al.* 2010).

Fasting male rats were killed by high dose of inhaled ether. The small intestine was removed and washed by Krebs buffer then placed in oxygenated Krebs buffer at 37 °C. The

intestine was everted on a glass rod; one end of the intestine was clamped whereas the whole intestine was filled with oxygenated Krebs buffer through the other end which was then sealed. The everted intestine was divided into sacs of 2.5-3 cm length by using silk sutures; few centimeters of duodenum and ileum were discarded (Zhou *et al.* 2010). Sacs, were divided into three groups (n=6 in each group) and soaked in Krebs buffer in a shaking water bath (60 cycles/min) for 10 min at 37 °C. The sacs were then transferred to the soaking solutions prepared (PRN only, PRN with GlcN and PRN with SLS) and were incubated as above. At the appropriate time points (20, 40 and 60 min) of incubation, sacs were removed (Chan *et al.* 2006; Qinna *et al.* 2015). Samples were drawn from inside the sacs by a needle and placed in Eppendorf tubes then kept in freezer at -20°C till HPLC analysis. All samples were diluted in distilled water (1/25) times before analysis.

2.2.9 Isolation and primary culture of rat hepatic cells

2.2.9.1 Preparation of buffers

All perfusion buffers were freshly prepared using sterile technique and were warmed for 30 minutes in a water bath (Elmasonic S, Elma, Germany) at 42 °C with an optimal temperature. Perfusion buffer I was prepared by adding 0.9 and 0.5 mM of MgCl₂ and EDTA, respectively, to Hank's Balanced Salt Solution (HBSS, without Ca²⁺ and Mg²⁺). Perfusion buffer II was prepared by adding 0.5 mM Tris base to HBSS (with Ca²⁺ and Mg²⁺). Perfusion buffer II plus collagenase II was prepared by dissolving 1000 U of collagenase II in 300 ml of perfusion buffer II. This buffer was kept warm in water-bath and used within 30 min after preparation. William's complete Medium was prepared by the addition of 2 mM of L-glutamine, 5% fetal bovine serum, 100 IU/ml penicillin and 100 mg/ml of streptomycin to Williams' Medium E.

2.2.9.2 Rat perfusion for liver isolation

Male Sprague Dawley rat was anaesthetized (**section 2.2.6**) and the abdominal contents were displaced to the animal's left to expose the liver. Hepatic portal vein (HPV) was exposed and two loose ligatures were passed, one around the PV, while the other was around the inferior vena cava (IVC). A 18-gauge angiocath (Becton Dickinson, Mountain View, CA, USA) was inserted into the HPV, whereas the perfusate tubing was connected to the needle and the infusion was initiated with pre-warmed 37 °C Perfusion buffer I. Once the liver was blanched to a light-brown color and all lobes began to swell a cut at IVC was made to allow buffer efflux. Thereafter, rat's chest was cut to place a second cannula of 18-gauge connected to a soft tube into the vena cava above the liver in order to enable a recirculating system. All loose ligatures were tied securely.

Perfusion solution was switched to perfusion buffer II plus collagenase II, and the flow rate was increased to 25 ml/min and the liver became pale in color. The recirculating perfusion mode with collagenase solution lasted for 15 minutes. Later, the liver was dissected. Once the liver looked mushy, it was minced and placed in pre-chilled sterile beaker with 20 ml collagenase to be transferred to the tissue cell culture hood.

2.2.9.3 Hepatocyte cell isolation

Within the cell culture hood, liver cells were dispersed gently using cell scraper (Fisher Scientific Ltd., Loughborough, UK) in a sterile petri dish containing collagenase solution. Cell suspension was filtered and dispensed through a 100 µm cell strainer (Becton Dickinson, Mountain View, CA, USA) into a centrifugation tube to remove connective tissues and undigested tissue fragments. Later, cells were suspended in 40 ml

collagenase solution and were centrifuged at 100 x g for 3 min at 4 °C. The supernatant was aspirated, then cells were resuspended in 40 ml cold William's complete medium, washed and centrifugation was repeated. The supernatant was aspirated again; cells were resuspended in 40 ml cold William's complete medium then were centrifuged at 200 x g for 10 min at 4 °C. Finally, cells in the suspension were counted using a hemocytometer.

2.2.9.4 Hepatocyte culture

Hepatocytes were maintained in tissue culture flasks or plastic dishes in a humidified atmosphere of 5% CO₂ at 37°C. Hepatocytes were seeded in the required format for experiments to reach 70-80% confluence by the end of the treatment. Hepatocytes were diluted with 30 ml warm William's complete medium to the desired concentration. Upon plating, the plates were left inside the cell culture hood for 30 minutes before being placed into the incubator to form an even monolayer of hepatocytes. Cells were allowed to recover and grow at least overnight prior to the day of experimentation (Shen *et al.* 2012).

2.2.9.5 Treatment of the cultured cells

After 20 h incubation, rat hepatocytes were pre-treated (200, 40 and 4 mM) GlcN, (5 µM) cimetidine and (50 µM) rifampin which were dissolved in the incubation medium to obtain a final concentrations of (2.87, 28.6 and 143.4 mg/ml) GlcN, (0.005 mg/ml) cimetidine, and (0.164 mg/ml) rifampin dissolved in the incubation medium. After 30 min, 0.0236 mg/ml PRN was added. Samples were pooled after 15, 30, 60 and 120 min of incubation and placed in Eppendorf tubes then kept in freezer at -20°C till HPLC analysis.

Chapter Three

Results

Chapter Three

3. Results

Table 3.1 Summary of chromatographic conditions applied.

HPLC Conditions	Pump Flow Rate	Autosampler Injection Volum	Autosampler temp	Column Oven Temp
	1.00 ml/ min	15 μ l	4°C	40°C
Chromatography	Mobile phase	mixture of (15% ACN, 32.5% Methanol, 52.5% water) (Water contain 0.9ml of Triethylamine /L), pH=2.75 adjust with phosphoric acid		
	Column type	Hypersil Thermo Electron Corporation BDS C-18 Column (150 mm x 4.6 mm, 5 μ m)		
	Expected Retention times (minutes)	Propranolol	4.2	
		Sildenafil	5.5	
Detection Conditions	Wavelength	214 nm		

3.1 Krebs buffer validation

3.1.1 Intra-day validation

3.1.1.1 Accuracy

Validation for days 1-3

Accuracy % range of the six replicates of LLOQ for days 1, 2 and 3 were (96.15%-108.02%), (102.91%-109.26%) and (98.26%-112.40%), respectively. Regarding accuracy % values of QC low six replicates for days 1, 2 and 3 they were (98.92%-109.64%), (98.80%-110.47%), and (100.20%-111.75%), respectively. The accuracy % values of the six replicates of QC mid were (105.64%-109.09%), (98.40%-109.02%), and (104.92%-108.94%) for days 1, 2 and 3, respectively, whereas accuracy % values of QC high were (101.00%-105.16%), (99.39%-105.93%) and (98.27%-106.01%) for day 1, 2 and 3, respectively. Highest accuracy % of mean predicted values was shown by QC mid for day 1 and day 3 of 107.36% and 106.90%, respectively, while LLOQ had the highest accuracy % on the second day of validation of 105.69%. By contrast, the lowest accuracy % of mean predicted value was obtained by LLOQ, QC low and QC high of 103.38%, 104.29% and 103.21% for day 1, 2 and 3, respectively (**Tables 3.2, 3.3 and 3.4**).

3.1.1.2 Precision

Validation for days 1-3

The highest coefficient of variation in predicted concentrations (CV%) was obtained by QC low being 4.54% and 4.04% for both day 1 and 2, respectively, while it was 5.49% for LLOQ. By contrast, the lowest variability of errors was shown by QC mid for both day 1 and day 3 of 1.30% and 1.39%, respectively. On the other hand, LLOQ had the lowest (CV%) on the second day of validation 2.25% **(Tables 3.2, 3.3 and 3.4)**.

Table 3.2 Intra-day accuracy & precision data for all QC samples LLOQ, QC low, QC mid, and QC high of propranolol based on the standard calibration curves of the first day of validation (n=6). Corresponding calibration curve used in the calculation of measured concentration of intra-day one is shown in **table 3.13**.

Theo. Conc.	Propranolol Area	Sildenafil Area	Ratios	Measured Conc.	Accuracy %	Mean accuracy %	Precision %
50 ng/ml LLOQ	1589	123453	0.0129	53.458	106.92	103.38%	4.03%
	1622	124379	0.0130	54.009	108.02		
	1565	126954	0.0123	51.689	103.38		
	1562	127006	0.0123	51.596	103.19		
	1549	126823	0.0122	51.320	102.64		
	1415	126159	0.0112	48.075	96.15		
Mean	1550	125796	0.0123	51.691	103.38		
STD	71.13	1515.86	0.0006	2.084	4.17		
CV%	4.59	1.21	5.1986	4.032	4.03		
150 ng/ml QCL	5900	128544	0.0459	160.876	107.25	104.43%	4.54%
	6099	129768	0.0470	164.455	109.64		
	5962	128186	0.0465	162.866	108.58		
	5529	125814	0.0439	154.524	103.02		
	5420	128544	0.0422	148.731	99.15		
	5456	129725	0.0421	148.385	98.92		
Mean	5728	128430	0.0446	156.640	104.43		
STD	293.40	1441.96	0.0022	7.113	4.74		
CV%	5.12	1.12	4.9038	4.541	4.54		
1500 ng/ml QC Mid	61574	124557	0.4943	1619.388	107.96	107.36%	1.30%
	65070	130250	0.4996	1636.410	109.09		
	62409	128688	0.4850	1588.879	105.93		
	56234	113223	0.4967	1626.939	108.46		
	58976	120308	0.4902	1605.938	107.06		
	56200	116198	0.4837	1584.630	105.64		
Mean	60077	122204	0.4916	1610.364	107.36		
STD	3567.11	6821.18	0.0064	20.871	1.39		
CV%	5.94	5.58	1.3054	1.296	1.30		
2500 ng/ml QC High	91595	114601	0.7993	2611.061	104.44	103.86%	1.44%
	92441	116069	0.7964	2601.889	104.08		
	92910	115448	0.8048	2629.035	105.16		
	90568	114138	0.7935	2592.341	103.69		
	90857	117566	0.7728	2525.086	101.00		
	89658	111795	0.8020	2619.954	104.80		
Mean	91338	114936	0.7948	2596.561	103.86		
STD	1216.59	1953.34	0.0115	37.328	1.49		
CV%	1.33	1.70	1.4440	1.438	1.44		

Table 3.3 Intra-day accuracy & precision data for all QC samples LLOQ, QC low, QC mid, and QC high of propranolol based on the standard calibration curves of the second day of validation (n=6). Corresponding calibration curve used in the calculation of measured concentration of intra-day two is shown in **table 3.14**.

Theo. Conc.	Propranolol Area	Sildenafil Area	Ratios	Measured Conc.	Accuracy %	Mean accuracy %	Precision %
50 ng/ml LLOQ	1177	110614	0.0106	53.391	106.78	105.70%	2.25%
	1211	109994	0.0110	54.632	109.26		
	1125	110920	0.0101	51.716	103.43		
	1159	111622	0.0104	52.526	105.05		
	1183	111291	0.0106	53.355	106.71		
	1131	112374	0.0101	51.455	102.91		
Mean	1164	111136	0.0105	52.846	105.69		
STD	32.78	826.58	0.0004	1.188	2.38		
CV%	2.82	0.74	3.3732	2.249	2.25		
150 ng/ml QCL	5029	117504	0.0428	161.496	107.66	104.29%	4.04%
	5296	120226	0.0441	165.704	110.47		
	5070	124957	0.0406	154.017	102.68		
	4892	118344	0.0413	156.583	104.39		
	4584	114145	0.0402	152.624	101.75		
	4585	118033	0.0388	148.205	98.80		
Mean	4909	118868	0.0413	156.438	104.29		
STD	283.19	3579.36	0.0019	6.319	4.21		
CV%	5.77	3.01	4.5519	4.039	4.04		
1500 ng/ml QC Mid	57782	120080	0.4812	1635.247	109.02	105.40%	3.53%
	58053	133823	0.4338	1475.932	98.40		
	58278	125775	0.4634	1575.259	105.02		
	56382	119660	0.4712	1601.593	106.77		
	56367	120965	0.4660	1584.088	105.61		
	57561	121195	0.4749	1614.234	107.62		
Mean	57404	123583	0.4651	1581.059	105.40		
STD	833.36	5475.03	0.0166	55.773	3.72		
CV%	1.45	4.43	3.5673	3.528	3.53		
2500 ng/ml QC High	96709	124386	0.7775	2631.296	105.25	104.50%	2.43%
	95362	122212	0.7803	2640.738	105.63		
	95930	122617	0.7824	2647.646	105.91		
	94371	120593	0.7826	2648.329	105.93		
	85468	116457	0.7339	2484.763	99.39		
	93351	120468	0.7749	2622.595	104.90		
Mean	93532	121122	0.7719	2612.561	104.50		
STD	4122.07	2703.58	0.0189	63.385	2.54		
CV%	4.41	2.23	2.4426	2.426	2.43		

Table 3.4 Intra-day accuracy & precision data for all QC samples LLOQ, QC low, QC mid, and QC high of propranolol based on the standard calibration curves of the third day of validation (n=6). Corresponding calibration curve used in the calculation of measured concentration of intra-day three is shown in **table 3.15**.

Theo. Conc.	Propranolol Area	Sildenafil Area	Ratios	Measured Conc.	Accuracy %	Mean accuracy %	Precision %
50 ng/ml LLOQ	1239	111803	0.0111	56.198	112.40	105.19%	5.49%
	1009	111484	0.0091	49.209	98.42		
	1140	107131	0.0106	54.682	109.36		
	1144	111057	0.0103	53.511	107.02		
	997	110437	0.0090	49.130	98.26		
	1144	113170	0.0101	52.850	105.70		
Mean	1112	110847	0.0100	52.597	105.19		
STD	92.51	2036.51	0.0008	2.888	5.78		
CV%	8.32	1.84	8.3650	5.491	5.49		
150 ng/ml QCL	5019	121882	0.0412	159.757	106.50	104.34%	4.51%
	5127	124471	0.0412	159.795	106.53		
	5276	121383	0.0435	167.625	111.75		
	4596	118817	0.0387	151.162	100.77		
	4321	112355	0.0385	150.396	100.26		
	4560	118652	0.0384	150.304	100.20		
Mean	4817	119593	0.0402	156.507	104.34		
STD	376.43	4150.06	0.0021	7.062	4.71		
CV%	7.82	3.47	5.1013	4.512	4.51		
1500 ng/ml QC Mid	57045	121463	0.4696	1634.039	108.94	106.90%	1.39%
	57298	126727	0.4521	1573.784	104.92		
	57722	125076	0.4615	1605.984	107.07		
	56166	121892	0.4608	1603.539	106.90		
	56046	123184	0.4550	1583.558	105.57		
	56813	122013	0.4656	1620.212	108.01		
Mean	56848	123393	0.4608	1603.519	106.90		
STD	650.34	2091.60	0.0065	22.355	1.49		
CV%	1.14	1.70	1.4100	1.394	1.39		
2500 ng/ml QC High	95415	124731	0.7650	2650.168	106.01	103.21%	2.65%
	95070	127233	0.7472	2589.078	103.56		
	95348	127964	0.7451	2581.866	103.27		
	93808	123323	0.7607	2635.382	105.42		
	84993	119920	0.7087	2456.730	98.27		
	92508	124800	0.7413	2568.565	102.74		
Mean	92857	124662	0.7447	2580.298	103.21		
STD	4012.84	2891.94	0.0199	68.414	2.74		
CV%	4.32	2.32	2.6701	2.651	2.65		

3.1.2 Inter-day validation

3.1.2.1 Accuracy

The highest accuracy % of all QC samples was obtained by QC mid of 106.55% while QC high showed the lowest accuracy % of 103.86 %, medium accuracy % was shown by LLOQ and QC low 104.76% and 104.35% respectively **(Table 3.5)**.

3.1.2.2 Precision

The highest coefficient of variation in predicted concentration (CV%) was obtained by QC low of 4.106% while QC high showed the lowest variability of errors of 2.162% **(Table 3.5)**.

Table 3.5 Inter-day accuracy & precision data for the three days of QC samples validation (LLOQ, QC low, QC mid, and QC high) of propranolol based on the standard calibration curves of the three days of validation (n=6).

	50			150			1500			2500		
	Day One	Day Two	Day Three	Day One	Day Two	Day Three	Day One	Day Two	Day Three	Day One	Day Two	Day Three
	53.458	53.391	56.198	160.876	161.496	159.757	1619.388	1635.247	1634.039	2611.061	2631.296	2650.168
	54.009	54.632	49.209	164.455	165.704	159.795	1636.410	1475.932	1573.784	2601.889	2640.738	2589.078
	51.689	51.716	54.682	162.866	154.017	167.625	1588.879	1575.259	1605.984	2629.035	2647.646	2581.866
	51.596	52.526	53.511	154.524	156.583	151.162	1626.939	1601.593	1603.539	2592.341	2648.329	2635.382
	51.320	53.355	49.130	148.731	152.624	150.396	1605.938	1584.088	1583.558	2525.086	2484.763	2456.730
	48.075	51.455	52.850	148.385	148.205	150.304	1584.630	1614.234	1620.212	2619.954	2622.595	2568.565
Mean	52.378			156.528			1598.314			2596.473		
STD	2.099			6.427			36.822			56.141		
CV%	4.008			4.106			2.304			2.162		
Accuracy %	104.76			104.35			106.55			103.86		

3.1.3 Stability

3.1.3.1 Freeze- Thaw stability

QC low (150 ng/ml)

The highest accuracy % of mean predicted value was 104.38% at zero hour while the lowest accuracy % was 100.56% obtained at 72 hours (**Table 3.6**).

Table 3.6 Propranolol QC low samples (150 ng/ml) results for freeze-thaw stability test (n=3).

Time (hour)	Propranolol Area	Sildenafil Area	Ratios	Measured Conc.	Mean Measured	Accuracy %	Mean accuracy %
Zero	5123	124634	0.0411	159.203	156.575	106.14	104.38
	5130	129186	0.0397	154.332		102.89	
	5071	126013	0.0402	156.189		104.13	
72.00	4325	115789	0.0374	151.208	150.841	100.81	100.56
	4110	112736	0.0365	147.964		98.64	
	4451	117306	0.0379	153.350		102.23	

QC high (2500 ng/ml)

The highest accuracy % of mean predicted values was 102.83% at 72 hours while the lowest accuracy % was 102.61% obtained at zero hour (**Table 3.7**).

Table 3.7 Propranolol QC high samples (2500 ng/ml) results for freeze-thaw stability test (n=3).

Time (hour)	Propranolol Area	Sildenafil Area	Ratios	Measured Conc.	Mean Measured	Accuracy %	Mean accuracy %
Zero	94337	127516	0.7398	2600.243	2565.135	104.01	102.61
	93414	126369	0.7392	2598.185		103.93	
	86246	121431	0.7102	2496.976		99.88	
72.00	87258	124607	0.7003	2552.855	2570.843	102.11	102.83
	87323	121718	0.7174	2615.005		104.60	
	87858	125870	0.6980	2544.668		101.79	

* Corresponding calibration curve used in the calculation of measured concentrations of freeze- thaw stability test is shown in **table 3.16**.

3.1.3.2 Sample stability after preparation at room temperature (Bench- Top stability)

QC low (150 ng/ml)

The highest accuracy % of mean predicted value was 104.38% at zero hour while the lowest accuracy % was 103.28% obtained at 24 hours (**Table 3.8**).

Table 3.8 Propranolol QC low samples (150 ng/ml) results for bench-top stability test (n=3).

Time (hour)	Propranolol Area	Sildenafil Area	Ratios	Measured Conc.	Mean Measured	Accuracy %	Mean accuracy %
Zero	5123	124634	0.0411	159.203	156.575	106.14	104.38
	5130	129186	0.0397	154.332		102.89	
	5071	126013	0.0402	156.189		104.13	
24.00	4979	127195	0.0391	159.776	154.922	106.52	103.28
	4854	131560	0.0369	151.622		101.08	
	4793	128234	0.0374	153.367		102.24	

QC high (2500 ng/ml)

The highest accuracy % of mean predicted value was 103.24% at 24 hour while the lowest accuracy % was 102.61% obtained at zero hour (**Table 3.9**).

Table 3.9 Propranolol QC high samples (2500 ng/ml) results for bench-top stability test (n=3).

Time (hour)	Propranolol Area	Sildenafil Area	Ratios	Measured Conc.	Mean Measured	Accuracy %	Mean accuracy %
Zero	94337	127516	0.73981	2600.243	2565.135	104.01	102.61
	93414	126369	0.73922	2598.185		103.93	
	86246	121431	0.71025	2496.976		99.88	
24.00	91069	129382	0.70388	2569.946	2581.067	102.80	103.24
	91102	127189	0.71627	2614.890		104.60	
	92083	131419	0.70068	2558.364		102.33	

* Corresponding calibration curve used in the calculation of measured concentrations of bench-top stability test is shown in **table 3.17**.

3.1.3.3 Autosampler stability

QC low (150 ng/ml)

The highest accuracy % of mean predicted value was 104.38% at zero hour while the lowest accuracy % was 100.94% obtained at 24 hours (**Table 3.10**).

Table 3.10 Propranolol QC low samples (150 ng/ml) results for autosampler stability test (n=3).

Time (hour)	Propranolol Area	Sildenafil Area	Ratios	Measured Conc.	Mean Measured	Accuracy %	Mean accuracy %
Zero	5123	124634	0.0411	159.203	156.575	106.14	104.38
	5130	129186	0.0397	154.332		102.89	
	5071	126013	0.0402	156.189		104.13	
24.00	4541	117343	0.0387	150.797	151.412	100.53	100.94
	4461	113077	0.0395	153.426		102.28	
	4582	119094	0.0385	150.012		100.01	

QC high (2500 ng/ml)

The highest accuracy % of mean predicted value was 102.61% at zero hour while the lowest accuracy % was 100.71% obtained at 24 hours (**Table 3.11**).

Table 3.11 Propranolol QC high samples (2500 ng/ml) results for autosampler stability test (n=3).

Time (hour)	Propranolol Area	Sildenafil Area	Ratios	Measured Conc.	Mean Measured	Accuracy %	Mean accuracy %
Zero	94337	127516	0.7398	2600.243	2565.135	104.01	102.61
	93414	126369	0.7392	2598.185		103.93	
	86246	121431	0.7102	2496.976		99.88	
24.00	92564	123385	0.7502	2636.575	2517.642	105.46	100.71
	65132	96297	0.6764	2378.606		95.14	
	91308	126480	0.7219	2537.746		101.51	

* Corresponding calibration curve used in the calculation of measured concentrations of autosampler stability test is shown in **table 3.18**.

3.1.4 Linearity

Linearity of any calibration curve is evaluated through regression factor (R^2) which reflects the strength of the correlation coefficient of a standard calibration curve where the best linear relationship must be more than 0.99 according to EMEA guidelines. Summary of all R^2 , slope and intercept data of the six calibration curves are shown in **table 3.12**.

Table 3.12 Summary of all R^2 , slope and intercept data of the six calibration curves.

Calibration Curve	R squared	Slope	Intercept
1	0.998979	0.000291	-0.009599
2	0.999557	0.000280	-0.009433
3	0.999717	0.000280	-0.008644
4	0.997693	0.000314	-0.010435
5	0.998913	0.000302	-0.010204
6	0.999025	0.000297	-0.011663
Mean	0.998981	0.000294	-0.009996
STD	0.000713	0.000013	0.001031
CV%	0.071333	4.497005	

Intra-day validation

Calibration curve of the first, second, and third day of validation are shown in **tables 3.13, 3.14 and 3.15**, respectively representing an accuracy range of (96.20%-108.68%), (94.17%-106.11%) and (92.23%-114.74%), respectively.

Stability validation

Calibration curve of freeze-thaw test, bench-top test, and autosampler test of stability are shown in **tables 3.16, 3.17 and 3.18**, respectively representing an accuracy range of (90.61%-111.71%), (92.15%-114.55%) and (93.13%-113.52%), respectively.

Ratios, factors and correlations in **figures 3-1 to 3-6** for Krebs buffer validation and **figures 3-8 to 3-13** for serum validation were calculated as follows:

$$\text{Ratio} = \frac{\text{Propranolol area}}{\text{Sildenafil area}}$$

$$\text{Factor} = \frac{1}{\text{Slope}}$$

$$\text{Correlation} = \text{SQRT}(R^2)$$

3.1.4.1 Calibration curve 1

Table 3.13 Calibration curve data of intra-day one of validation.

Theoretical conc. (ng/ml)	Propranolol Area	Sildenafil Area	Ratio	Measured Conc.	Accuracy %
50	1513	114520	0.0132	54.340	108.68
100	3193	120265	0.0265	97.798	97.80
200	6307	109714	0.0575	198.594	99.30
500	17316	118528	0.1461	487.290	97.46
1000	29741	101657	0.2926	964.517	96.45
2000	62571	106590	0.5870	1923.933	96.20
3000	113668	118999	0.9552	3123.520	104.12

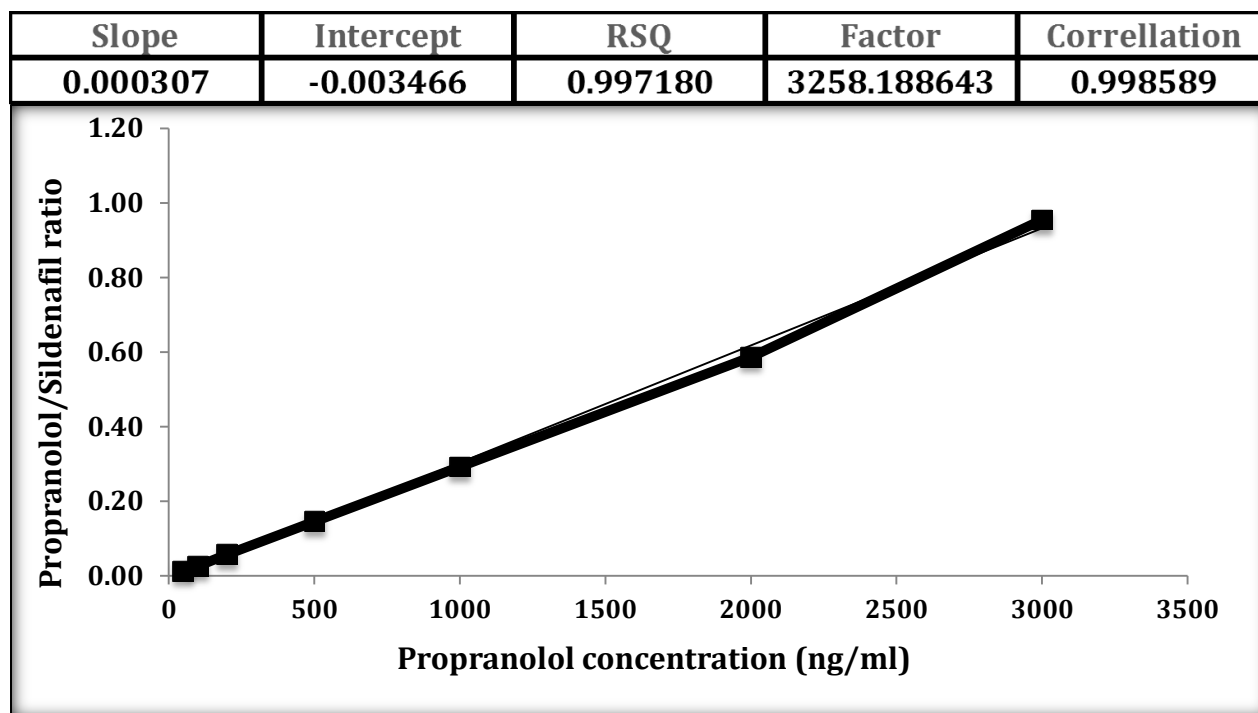


Figure 3.1 Intra-day one calibration curve of propranolol in Krebs buffer.

Measured Conc. = (Ratio +0.003466)/ 0.000307

Function is $Y = 0.000307X - 0.003466$ ($R^2 = 0.997180$)

3.1.4.2 Calibration curve 2

Table 3.14 Calibration curve data of intra-day two of validation.

Theoretical conc. (ng/ml)	Propranolol Area	Sildenafil Area	Ratio	Measured Conc.	Accuracy %
50	1180	111556	0.0106	53.056	106.11
100	3095	121657	0.0254	103.068	103.07
200	5848	115159	0.0508	188.341	94.17
500	16946	119581	0.1417	494.315	98.86
1000	29014	102128	0.2841	973.427	97.34
2000	61319	106711	0.5746	1951.055	97.55
3000	111458	122195	0.9121	3086.744	102.89

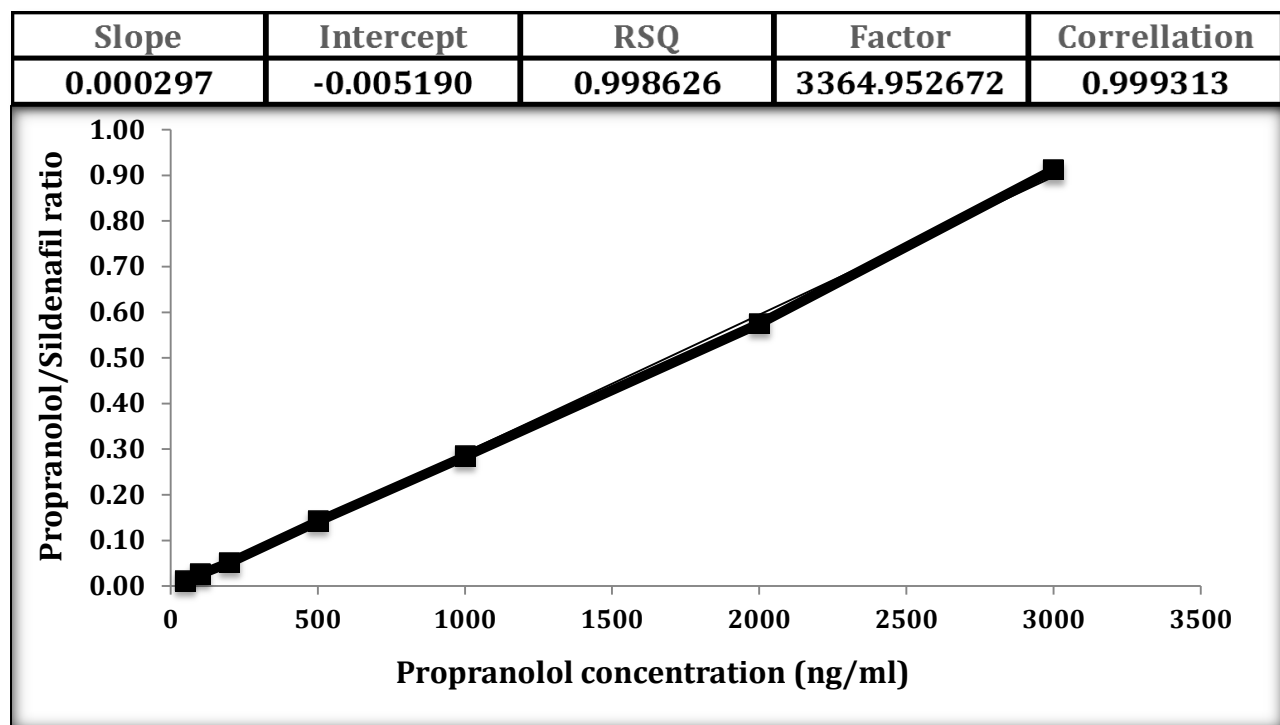


Figure 3.2 Intra-day two calibration curve of propranolol in Krebs buffer.

Measured Conc. = (Ratio +0.005190)/ 0.000297
 Function is $Y = 0.000297X - 0.005190$ ($R^2 = 0.9978626$)

3.1.4.3 Calibration curve 3

Table 3.15 Calibration curve data of intra-day three of validation.

Theoretical conc. (ng/ml)	Propranolol Area	Sildenafil Area	Ratio	Measured Conc.	Accuracy %
50	1188	103554	0.0115	57.370	114.74
100	2764	116986	0.0236	99.249	99.25
200	5296	109525	0.0484	184.451	92.23
500	15312	115447	0.1326	474.840	94.97
1000	26690	96204	0.2774	973.762	97.38
2000	56921	100683	0.5653	1965.814	98.29
3000	102703	115019	0.8929	3094.506	103.15

Slope	Intercept	RSQ	Factor	Correllation
0.000290	-0.005178	0.998527	33445.614422	0.999263

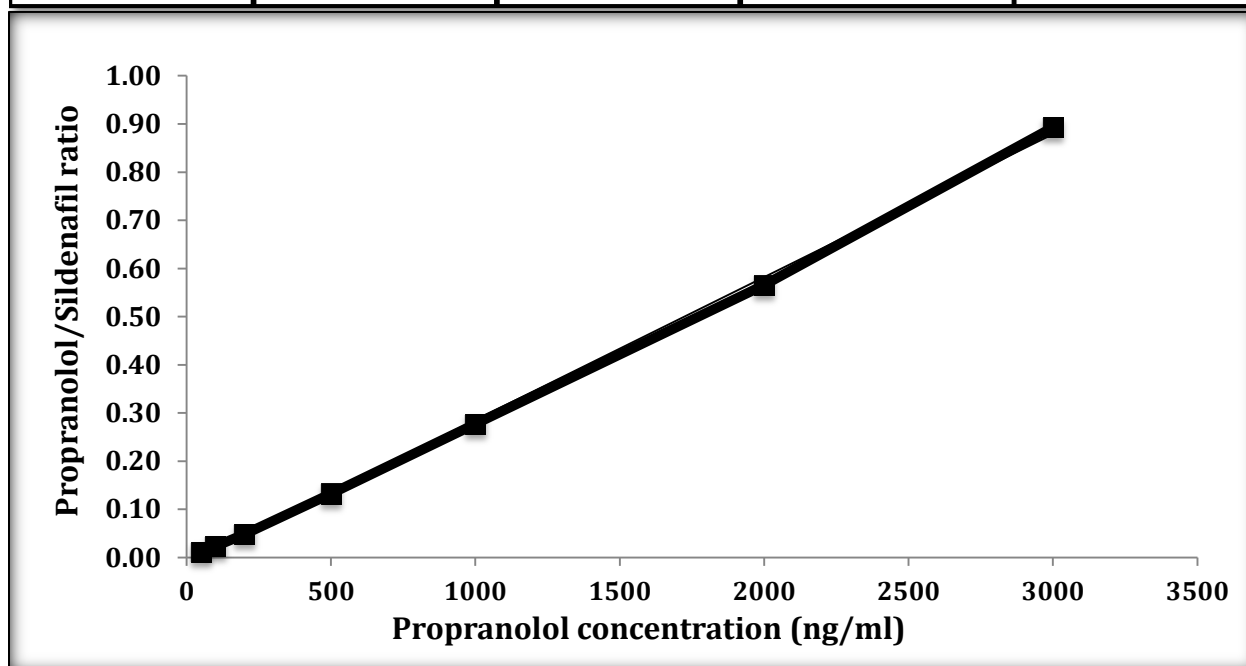


Figure 3.3 Intra-day three calibration curve of propranolol in Krebs buffer.

Measured Conc. = (Ratio +0.005178)/ 0.000290
 Function is $Y = 0.000290X - 0.005178$ ($R^2 = 0.9978626$)

3.1.4.4 Calibration curve 4

Table 3.16 Calibration curve data of freeze-thaw test of stability.

Theoretical conc. (ng/ml)	Propranolol Area	Sildenafil Area	Ratio	Measured Conc.	Accuracy %
50	1179	106597	0.0111	55.855	111.71
100	2741	115879	0.0237	101.517	101.52
200	4998	109522	0.0456	181.214	90.61
500	14560	112487	0.1294	485.066	97.01
1000	25296	95650	0.2645	974.647	97.46
2000	53710	98247	0.5467	1997.918	99.90
3000	94598	112900	0.8379	3053.783	101.79

Slope	Intercept	RSQ	Factor	Correllation
0.000276	-0.004344	0.999471	3625.802662	0.999735

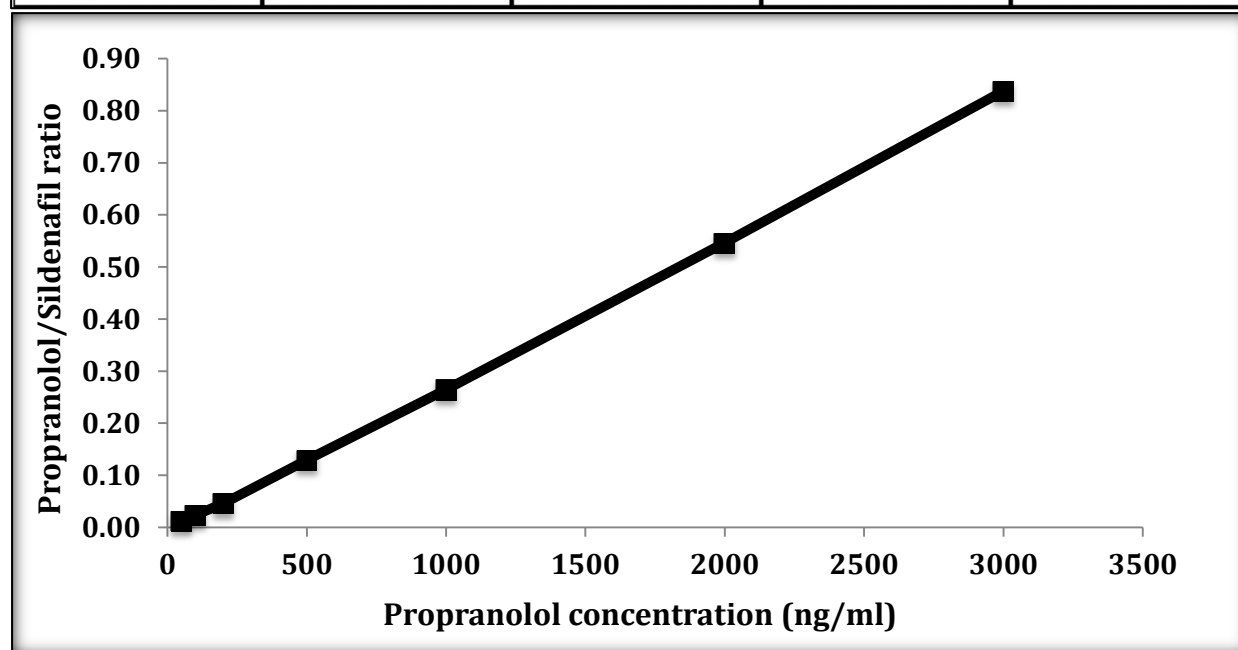


Figure 3.4 Freeze-thaw stability test calibration curve of propranolol in Krebs buffer.

Measured Conc. = (Ratio +0.004344)/ 0.000276
 Function is $Y = 0.000276X - 0.004344$ ($R^2 = 0.999471$)

3.1.4.5 Calibration curve 5

Table 3.17 Calibration curve data of bench-top test of stability.

Theoretical conc. (ng/ml)	Propranolol Area	Sildenafil Area	Ratio	Measured Conc.	Accuracy %
50	1165	106838	0.0109	57.276	114.55
100	2596	118426	0.0219	97.254	97.25
200	5068	110394	0.0459	184.303	92.15
500	14967	116673	0.1283	483.233	96.65
1000	25907	97499	0.2657	981.975	98.20
2000	54549	100876	0.5408	1980.075	99.00
3000	97098	115598	0.8400	3065.895	102.20

Slope	Intercept	RSQ	Factor	Correllation
0.000276	-0.004879	0.999281	3628.96056	0.999640

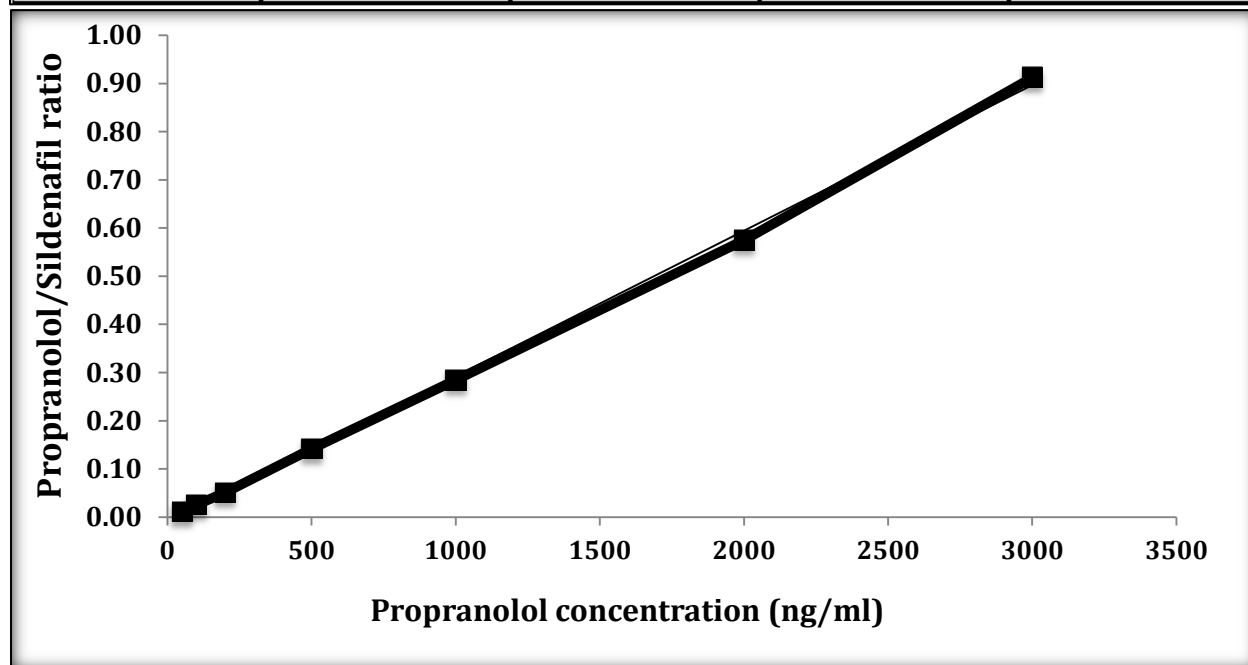


Figure 3.5 Bench-top stability test calibration curve of propranolol in Krebs buffer.

Measured Conc. = (Ratio +0.004879)/ 0.000276
 Function is $Y = 0.000276X - 0.004879$ ($R^2 = 0.999281$)

3.1.4.6 Calibration curve 6

Table 3.18 Calibration curve data of autosampler test of stability.

Theoretical conc. (ng/ml)	Propranolol Area	Sildenafil Area	Ratio	Measured Conc.	Accuracy %
50	1267	107182	0.0118	56.758	113.52
100	2721	116959	0.0233	96.782	96.78
200	5339	109306	0.0488	186.251	93.13
500	15537	114318	0.1359	490.771	98.15
1000	26315	95590	0.2753	978.266	97.83
2000	55654	100442	0.5541	1953.396	97.67
3000	100731	114673	0.8784	3087.765	102.93

Slope	Intercept	RSQ	Factor	Correllation
0.000286	-0.004407	0.998647	3497.59191	0.999323

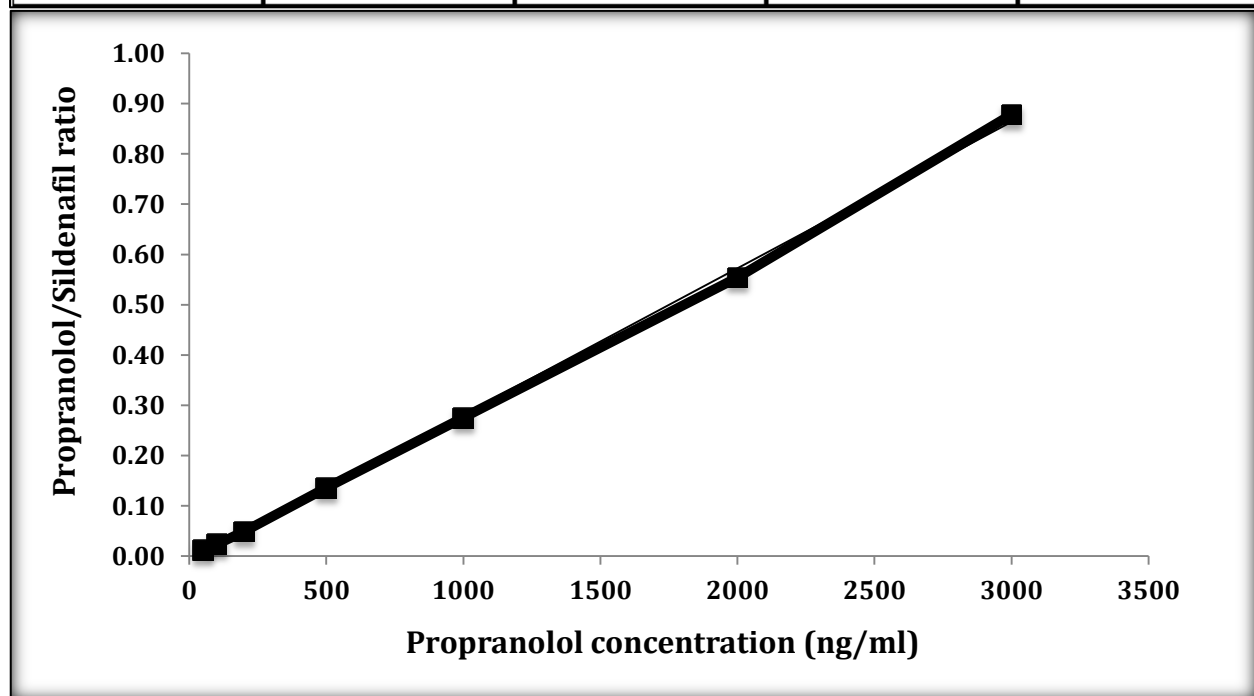


Figure 3.6 Autosampler stability test calibration curve of propranolol in Krebs buffer.

Measured Conc. = (Ratio +0.004407)/ 0.000286
 Function is $Y = 0.000286X - 0.004407$ ($R^2 = 0.998647$)

Table 3.19 Calculated Accuracy % based on measured concentration mean for each concentration of standard points.

Concentration	Calibration Curve number						Mean	STD	CV%	Accuracy %
	1	2	3	4	5	6				
50	56.758	57.276	55.855	54.340	53.056	57.370	55.776	1.745	3.128	111.55
100	96.782	97.254	101.517	97.798	103.068	99.249	99.278	2.526	2.544	99.28
200	186.251	184.303	181.214	198.594	188.341	184.451	187.192	6.063	3.239	93.60
500	490.771	483.233	485.066	487.290	494.315	474.840	485.919	6.732	1.385	97.18
1000	978.266	981.975	974.647	964.517	973.427	973.762	974.432	5.855	0.601	97.44
2000	1953.396	1980.075	1997.918	1923.933	1951.055	1965.814	1962.032	25.590	1.304	98.10
3000	3087.765	3065.895	3053.783	3123.520	3086.744	3094.506	3085.369	24.181	0.784	102.85

Table 3.20 Calculated Accuracy % based on area ratios mean for each concentration of standard points.

Concentration	Ratio for Standard Point						Mean ratio	STD	CV%
	1	2	3	4	5	6			
50	0.0118	0.0109	0.0111	0.0132	0.0106	0.0115	0.012	0.001	8.18
100	0.0233	0.0219	0.0237	0.0265	0.0254	0.0236	0.024	0.002	6.87
200	0.0488	0.0459	0.0456	0.0575	0.0508	0.0484	0.050	0.004	8.81
500	0.1359	0.1283	0.1294	0.1461	0.1417	0.1326	0.136	0.007	5.19
1000	0.2753	0.2657	0.2645	0.2926	0.2841	0.2774	0.277	0.011	3.89
2000	0.5541	0.5408	0.5467	0.5870	0.5746	0.5653	0.561	0.018	3.13
3000	0.8784	0.8400	0.8379	0.9552	0.9121	0.8929	0.886	0.045	5.05

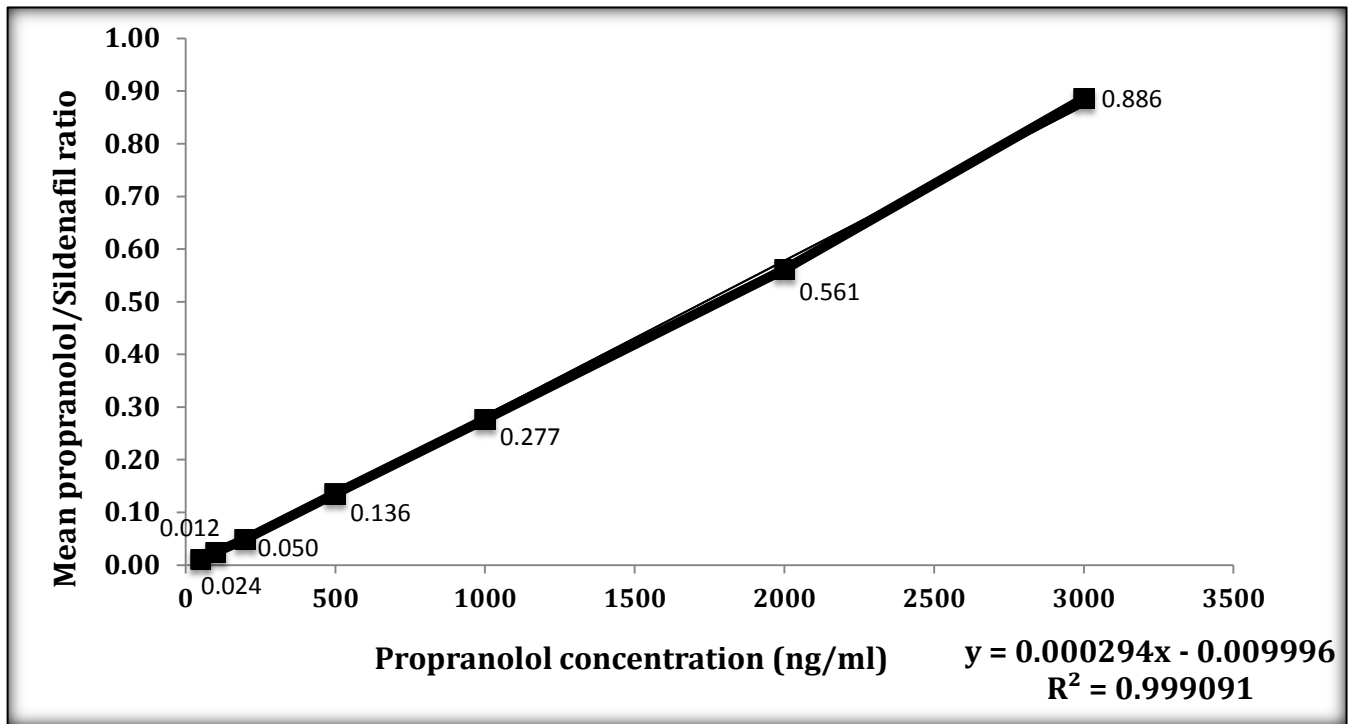


Figure 3.7 Propranolol concentrations versus mean area ratios for each concentration of standard points.

Linearity accuracy % is shown in **table 3.19** which represents an accepted accuracy range according to EMEA guidelines of (93.60%-111.55%) in addition to a linear relationship of correlation coefficient equals 0.999091.

3.1.5 Recovery

3.1.5.1 Recovery in the mobile phase

CV% of AUC mean of PRN was 0.20%, 4.60% and 0.56% for QC mid, QC low and QC high respectively while it was 1.17%, 2.20% and 2.84% for QC high, QC mid and QC low respectively for AUC mean of sildenafil as shown in **table 3.21**.

Table 3.21 CV% values of AUC mean of propranolol and sildenafil (internal standard) in mobile phase.

Concentration	Propranolol Area	Sildenafil Area	Mean (Propranolol)	C.V % (Propranolol)	Mean (Sildenafil)	C.V % (Sildenafil)
150 ng/ml QC Low	4778	125107	4538	4.60	128104	2.84
	4436	132151				
	4399	127053				
1500 ng/ml QC Mid	54697	123858	54748	0.20	126548	2.20
	54675	129408				
	54873	126377				
2500 ng/ml QC High	88668	126850	89162	0.56	126990	1.17
	89665	125580				
	89154	128540				

3.1.5.2 Recovery in Krebs buffer

CV% of AUC mean of PRN was 1.56%, 4.06% and 4.88% for QC mid, QC high and QC low respectively while it was 0.32%, 0.80% and 3.23% for QC mid, QC low and QC high respectively for AUC mean of sildenafil as shown in **table 3.22**.

Table 3.22 CV% values of AUC mean of propranolol and sildenafil (internal standard) in Krebs buffer.

Concentration	Propranolol Area	Sildenafil Area	Mean (Propranolol)	C.V % (Propranolol)	Mean (Sildenafil)	C.V % (Sildenafil)
150 ng/ml QC Low	4501	117975	4315	4.88	117372	0.80
	4086	116289				
	4357	117852				
1500 ng/ml QC Mid	52908	119786	52646	1.56	120085	0.32
	51724	120520				
	53307	119950				
2500 ng/ml QC High	87460	124771	83599	4.06	120330	3.23
	81097	117573				
	82240	118645				

The highest recovery of PRN in Krebs buffer was shown by QC mid of 96.16% while the lowest recovery was obtained by QC high of 93.76% which are considered acceptable recovery ratios of PRN between mobile phase and Krebs buffer as shown in **table 3.23**.

Table 3.23 Absolute recovery ratios of propranolol in Krebs buffer.

Concentration	AUC mean in Krebs buffer	AUC mean mobile phase	Absolute Recovery
150 ng/ml QC Low	4315	4538	95.09
1500 ng/ml QC Mid	52646	54748	96.16
2500 ng/ml QC High	83599	89162	93.76

The highest recovery of sildenafil (IS) in Krebs buffer was shown by QC mid of 94.89% while the lowest recovery was obtained by QC low of 91.62% which are considered acceptable recovery ratios according to EMEA guidelines for sildenafil between mobile phase and Krebs buffer as shown in **table 3.24**.

Table 3.24 Absolute recovery ratios of sildenafil citrate (internal standard) in Krebs buffer.

Concentration	AUC mean in Krebs buffer	AUC mean mobile phase	Absolute Recovery
150 ng/ml QC Low	117372	128104	91.62
1500 ng/ml QC Mid	120085	126548	94.89
2500 ng/ml QC High	120330	126990	94.76

3.2 Serum validation

3.2.1 Intra-day validation

3.2.1.1 Accuracy

Validation for days 1-3

Accuracy % range of the six replicates of LLOQ for days 1, 2 and 3 were (100.16%-107.06%), (104.78%-110.15%) and (101.24%-103.96%), respectively. Regarding accuracy % values of QC low six replicates for days 1, 2 and 3 they were (98.36%-101.84%), (98.27%-104.24%), and (98.75%-104.24%), respectively. The accuracy % values of the six replicates of QC mid were (101.98%-103.43%), (99.28%-101.62%), and (97.00%-101.85%) for days 1, 2 and 3, respectively, whereas accuracy % values of QC high were (103.17%/105.59%), (100.49%-102.36%) and (96.43%-104.40%) for day 1, 2 and 3, respectively. Highest accuracy % of mean predicted value was shown by QC high, LLOQ and QC low of 104.43%, 107.46% and 102.40% for day 1, 2 and 3, respectively. By contrast, the lowest accuracy % of mean predicted value was obtained by QC mid for both day 2 and day 3 of 100.32%, 100.28%, respectively, while QC low was the lowest accuracy % for day 1 of 99.52% (**Tables 3.25, 3.26 and 3.27**).

3.2.1.2 Precision

Validation for days 1-3

The highest coefficient of variation in predicted concentration (CV%) was obtained by LLOQ of 2.21% and 2.13% for both day 1 and 2, respectively, while it was 2.81% for QC high. By contrast, the lowest variability of errors was shown by QC mid, QC high and LLOQ of 0.71%, 0.67% and 0.98% for day 1, 2 and 3, respectively (**Tables 3.25, 3.26 and 3.27**).

Table 3.25 Intra-day accuracy & precision data for all QC samples LLOQ, QC low, QC mid, and QC high of propranolol based on the standard calibration curves of the first day of validation (n=6). Corresponding calibration curve used in the calculation of measured concentration of intra-day one is shown in **table 3.36**.

Theo. Conc.	Propranolol Area	Sildenafil Area	Ratios	Measured Conc.	Accuracy %	Mean accuracy %	Precision %
50 ng/ml LLOQ	1141	131440	0.0087	51.764	103.53	104.19%	2.21%
	1179	127441	0.0093	53.529	107.06		
	1133	126631	0.0089	52.588	105.18		
	1177	132027	0.0089	52.488	104.98		
	1131	128599	0.0088	52.117	104.23		
	775	95254	0.0081	50.080	100.16		
Mean	1089	123565	0.009	52.094	104.19		
STD	155.46	14034.95	0.000	1.151	2.30		
CV%	14.27	11.36	4.235	2.209	2.21		
150 ng/ml QCL	5230	126497	0.0413	152.764	101.84	99.52%	1.24%
	5248	130523	0.0402	149.247	99.50		
	5167	129940	0.0398	147.878	98.59		
	5308	132326	0.0401	148.955	99.30		
	5200	131124	0.0397	147.545	98.36		
	5335	132641	0.0402	149.290	99.53		
Mean	5248	130509	0.040	149.280	99.52		
STD	63.81	2220.15	0.001	1.856	1.24		
CV%	1.22	1.70	1.492	1.243	1.24		
1500 ng/ml QC Mid	64378	132174	0.487	1530.978	102.07	102.92%	0.71%
	65197	131975	0.494	1552.438	103.50		
	65687	133058	0.494	1551.392	103.43		
	64436	132409	0.487	1529.660	101.98		
	65050	132366	0.491	1544.492	102.97		
	65126	131673	0.495	1554.274	103.62		
Mean	64979	132276	0.491	1543.872	102.92		
STD	496.28	469.45	0.004	11.016	0.73		
CV%	0.76	0.35	0.725	0.714	0.71		
2500 ng/ml QC High	109990	130820	0.841	2624.655	104.99	104.43%	0.86%
	109147	131450	0.830	2592.366	103.69		
	115116	137060	0.840	2621.938	104.88		
	110207	132030	0.835	2605.912	104.24		
	107327	129927	0.826	2579.148	103.17		
	107847	127526	0.846	2639.846	105.59		
Mean	109939	131469	0.836	2610.644	104.43		
STD	2782.16	3159.77	0.007	22.473	0.90		
CV%	2.53	2.40	0.869	0.861	0.86		

Table 3.26 Intra-day accuracy & precision data for all QC samples LLOQ, QC low, QC mid, and QC high of propranolol based on the standard calibration curves of the second day of validation (n=6). Corresponding calibration curve used in the calculation of measured concentration of intra-day two is shown in **table 3.37**.

Theo. Conc.	Propranolol Area	Sildenafil Area	Ratios	Measured Conc.	Accuracy %	Mean accuracy %	Precision %
50 ng/ml LLOQ	1129	133557	0.008	54.071	108.14	107.46%	2.13%
	1073	130131	0.008	53.444	106.89		
	1021	116204	0.009	55.075	110.15		
	1024	128918	0.008	52.532	105.06		
	1005	127291	0.008	52.388	104.78		
	934	107151	0.009	54.865	109.73		
Mean	1031	123875	0.008	53.729	107.46		
STD	65.73	10084.80	0.000	1.143	2.29		
CV%	6.38	8.14	4.544	2.127	2.13		
150 ng/ml QCL	5180	126442	0.041	152.134	101.42	101.30%	1.94%
	5539	130739	0.042	156.355	104.24		
	5419	131073	0.041	153.268	102.18		
	5154	130808	0.039	147.411	98.27		
	5347	132078	0.040	150.675	100.45		
	5352	130959	0.041	151.834	101.22		
Mean	5332	130350	0.041	151.946	101.30		
STD	145.49	1975.51	0.001	2.947	1.96		
CV%	2.73	1.52	2.389	1.939	1.94		
1500 ng/ml QC Mid	61875	125424	0.493	1516.459	101.10	100.32%	0.94%
	65225	133918	0.487	1497.534	99.84		
	64699	133347	0.485	1491.927	99.46		
	65119	134460	0.484	1489.235	99.28		
	64856	132099	0.491	1509.337	100.62		
	65123	131315	0.496	1524.310	101.62		
Mean	64483	131761	0.489	1504.800	100.32		
STD	1292.45	3314.31	0.005	14.128	0.94		
CV%	2.00	2.52	0.957	0.939	0.94		
2500 ng/ml QC High	109531	130907	0.837	2552.107	102.08	101.53%	0.67%
	107446	130472	0.824	2512.323	100.49		
	114363	137764	0.830	2532.287	101.29		
	102402	122055	0.839	2558.965	102.36		
	108531	130871	0.829	2529.755	101.19		
	108178	129738	0.834	2543.392	101.74		
Mean	108409	130301	0.832	2538.138	101.53		
STD	3841.58	4994.62	0.006	16.896	0.68		
CV%	3.54	3.83	0.673	0.666	0.67		

Table 3.27 Intra-day accuracy & precision data for all QC samples LLOQ, QC low, QC mid, and QC high of propranolol based on the standard calibration curves of the third day of validation (n=6). Corresponding calibration curve used in the calculation of measured concentration of intra-day three is shown in **table 3.38**.

Theo. Conc.	Propranolol Area	Sildenafil Area	Ratios	Measured Conc.	Accuracy %	Mean accuracy %	Precision %
50 ng/ml LLOQ	1022	122525	0.008	50.619	101.24	102.34%	0.98%
	1098	127138	0.009	51.528	103.06		
	908	103390	0.009	51.978	103.96		
	699	83077	0.008	50.843	101.69		
	1057	124175	0.009	51.146	102.29		
	1026	121622	0.008	50.911	101.82		
Mean	968	113655	0.009	51.171	102.34		
STD	146.33	17175.54	0.000	0.502	1.00		
CV%	15.11	15.11	1.912	0.981	0.98		
150 ng/ml QCL	4990	116969	0.043	156.355	104.24	102.40%	2.15%
	5043	123152	0.041	151.082	100.72		
	5049	118438	0.043	156.260	104.17		
	4930	117136	0.042	154.590	103.06		
	5320	125795	0.042	155.216	103.48		
	4893	122354	0.040	148.128	98.75		
Mean	5038	120641	0.042	153.605	102.40		
STD	151.43	3644.86	0.001	3.303	2.20		
CV%	3.01	3.02	2.566	2.150	2.15		
1500 ng/ml QC Mid	62703	135088	0.464	1454.968	97.00	100.28%	1.81%
	59652	124996	0.477	1495.227	99.68		
	59804	123754	0.483	1513.767	100.92		
	60072	123146	0.488	1527.823	101.85		
	61535	128007	0.481	1505.963	100.40		
	61902	126920	0.488	1527.556	101.84		
Mean	60945	126985	0.480	1504.217	100.28		
STD	1272.04	4378.14	0.009	27.212	1.81		
CV%	2.09	3.45	1.840	1.809	1.81		
2500 ng/ml QC High	100550	122364	0.822	2556.592	102.26	101.63%	2.81%
	97165	120118	0.809	2517.108	100.68		
	104802	135334	0.774	2410.762	96.43		
	102722	123296	0.833	2591.729	103.67		
	100730	120046	0.839	2610.097	104.40		
	99598	121141	0.822	2557.940	102.32		
Mean	100928	123717	0.817	2540.705	101.63		
STD	2620.59	5831.42	0.023	71.288	2.85		
CV%	2.60	4.71	2.834	2.806	2.81		

3.2.2 Inter-day validation

3.2.2.1 Accuracy

The highest accuracy % of all QC samples was obtained by LLOQ of 104.66% while QC low showed the lowest accuracy % of 101.07 %, medium accuracy % was shown by QC high and QC mid 102.53% and 101.18% respectively **(Table 3.28)**.

3.2.2.2 Precision

The highest coefficient of variation in predicted concentration (CV%) was obtained by LLOQ of 2.724% while QC mid showed the lowest variability of errors of 1.714% **(Table 3.28)**.

Table 3.28 Inter-day accuracy & precision data for the three days of QC samples validation (LLOQ, QC low, QC mid, and QC high) of propranolol based on the standard calibration curves for the three days of validation (n=6).

	50			150			1500			2500		
	Day One	Day Two	Day Three	Day One	Day Two	Day Three	Day One	Day Two	Day Three	Day One	Day Two	Day Three
	51.764	54.071	50.619	152.764	152.134	156.355	1530.978	1516.459	1454.968	2624.655	2552.107	2556.592
	53.529	53.444	51.528	149.247	156.355	151.082	1552.438	1497.534	1495.227	2592.366	2512.323	2517.108
	52.588	55.075	51.978	147.878	153.268	156.260	1551.392	1491.927	1513.767	2621.938	2532.287	2410.762
	52.488	52.532	50.843	148.955	147.411	154.590	1529.660	1489.235	1527.823	2605.912	2558.965	2591.729
	52.117	52.388	51.146	147.545	150.675	155.216	1544.492	1509.337	1505.963	2579.148	2529.755	2610.097
	50.080	54.865	50.911	149.290	151.834	148.128	1554.274	1524.310	1527.556	2639.846	2543.392	2557.940
Mean	52.331			151.610			1517.630			2563.162		
STD	1.426			3.184			26.016			54.055		
CV%	2.724			2.100			1.714			2.109		
Accuracy %	104.66			101.07			101.18			102.53		

3.2.3 Stability

3.2.3.1 Freeze- Thaw stability

QC low (150 ng/ml)

The highest accuracy % of mean predicted value was 98.96% at zero hour while the lowest accuracy % was 98.27% obtained at 72 hours (**Table 3.29**).

Table 3.29 Propranolol QC low samples (150 ng/ml) results for freeze-thaw stability test (n=3).

Time (hour)	Propranolol Area	Sildenafil Area	Ratios	Measured Conc.	Mean Measured	Accuracy %	Mean accuracy %
Zero	4786	119515	0.040	150.291	148.441	100.19	98.96
	4943	128620	0.038	145.270		96.85	
	4917	123311	0.040	149.761		99.84	
72.00	4598	113255	0.041	148.827	147.398	99.22	98.27
	4403	113121	0.039	143.606		95.74	
	4720	115408	0.041	149.761		99.84	

QC high (2500 ng/ml)

The highest accuracy % of mean predicted value was 103.19% at 72 hours while the lowest accuracy % was 102.34% obtained at zero hour (**Table 3.30**).

Table 3.30 Propranolol QC high samples (2500 ng/ml) results for freeze-thaw stability test (n=3).

Time (hour)	Propranolol Area	Sildenafil Area	Ratios	Measured Conc.	Mean Measured	Accuracy %	Mean accuracy %
Zero	104325	126295	0.826	2595.004	2558.516	103.80	102.34
	102268	127144	0.804	2527.527		101.10	
	101134	124466	0.813	2553.017		102.12	
72.00	93132	112674	0.827	2597.677	2579.657	103.91	103.19
	93376	113766	0.821	2579.639		103.19	
	98800	121227	0.815	2561.654		102.47	

* Corresponding calibration curve used in the calculation of measured concentrations of freeze- thaw stability test is shown in **table 3.41**

3.2.3.2 Sample stability after preparation at room temperature (Bench- Top stability)

QC low (150 ng/ml)

The highest accuracy % of mean predicted value was 98.96% at zero hour while the lowest accuracy % was 96.50% obtained at 24 hours (**Table 3.31**).

Table 3.31 Propranolol QC low samples (150 ng/ml) results for bench-top stability test (n=3).

Time (hour)	Propranolol Area	Sildenafil Area	Ratios	Measured Conc.	Mean Measured	Accuracy %	Mean accuracy %
Zero	4786	119515	0.040	150.291	148.441	100.19	98.96
	4943	128620	0.038	145.270		96.85	
	4917	123311	0.040	149.761		99.84	
24.00	4654	118101	0.039	146.751	144.755	97.83	96.50
	4857	127290	0.038	142.849		95.23	
	4897	126412	0.039	144.664		96.44	

QC high (2500 ng/ml)

The highest accuracy % of mean predicted value was 102.34% at zero hour while the lowest accuracy % was 102.07% obtained at 24 hours (**Table 3.32**).

Table 3.32 Propranolol QC high samples (2500 ng/ml) results for bench-top stability test (n=3).

Time (hour)	Propranolol Area	Sildenafil Area	Ratios	Measured Conc.	Mean Measured	Accuracy %	Mean accuracy %
Zero	104325	126295	0.826	2595.004	2558.516	103.80	102.34
	102268	127144	0.804	2527.527		101.10	
	101134	124466	0.813	2553.017		102.12	
24.00	100547	125607	0.800	2522.625	2551.872	100.91	102.07
	97368	120500	0.808	2546.176		101.85	
	97192	118375	0.821	2586.816		103.47	

* Corresponding calibration curve used in the calculation of measured concentrations of bench-top stability test is shown in **table 3.42**.

3.2.3.3 Autosampler stability

QC low (150 ng/ml)

The highest accuracy % of mean predicted value was 98.96% at zero hour while the lowest accuracy % was 98.52% obtained at 24 hours (**Table 3.33**).

Table 3.33 Propranolol QC low samples (150 ng/ml) results for autosampler stability test (n=3).

Time (hour)	Propranolol Area	Sildenafil Area	Ratios	Measured Conc.	Mean Measured	Accuracy %	Mean accuracy %
Zero	4786	119515	0.040	150.291	148.441	100.19	98.96
	4943	128620	0.038	145.270		96.85	
	4917	123311	0.040	149.761		99.84	
24.00	4655	120946	0.038	145.448	147.777	96.97	98.52
	4973	126479	0.039	148.032		98.69	
	4912	123096	0.040	149.851		99.90	

QC high (2500 ng/ml)

The highest accuracy % of mean predicted value was 102.93% at 24 hours while the lowest accuracy % was 102.34% obtained at zero hour (**Table 3.34**).

Table 3.34 Propranolol QC high samples (2500 ng/ml) results for autosampler stability test (n=3).

Time (hour)	Propranolol Area	Sildenafil Area	Ratios	Measured Conc.	Mean Measured	Accuracy %	Mean accuracy %
Zero	104325	126295	0.826	2595.004	2558.516	103.80	102.34
	102268	127144	0.804	2527.527		101.10	
	101134	124466	0.813	2553.017		102.12	
24.00	101981	125771	0.811	2547.741	2573.283	101.91	102.93
	100354	121960	0.823	2585.055		103.40	
	99114	120359	0.823	2587.054		103.48	

* Corresponding calibration curve used in the calculation of measured concentrations of autosampler stability test is shown in **table 3.43**.

3.2.4 Linearity

Summary of all R², slope and intercept data of the six calibration curves are shown in **table 3.35**.

Table 3.35 Summary of all R², slope and intercept data of the six calibration curves.

Calibration Curve	R squared	Slope	Intercept
1	0.999740	0.000321	-0.008211
2	0.999573	0.000320	-0.007532
3	0.999343	0.000321	-0.007127
4	0.998461	0.000323	-0.007974
5	0.999725	0.000331	-0.009446
6	0.999740	0.000324	-0.008066
Mean	0.999430	0.000323	-0.008059
STD	0.000499	0.000004	0.000788
CV%	0.049952	1.308656	

Intra-day validation

Calibration curve of the first, second, and third day of validation are shown in **tables 3.36, 3.37 and 3.38**, respectively representing an accuracy range of (89.65%-112.99%), (93.24%-109.98%) and (94.22%-106.75%), respectively.

Stability validation

Calibration curve of freeze-thaw test, bench-top test, and autosampler test of stability are shown in **tables 3.39, 3.40 and 3.41**, respectively representing an accuracy range of (91.23-105.67%), (85.82-113.81%) and (85.84%-114.27%), respectively.

3.2.4.1 Calibration curve 1

Table 3.36 Calibration curve data of intra-day one of validation.

Theoretical conc. (ng/ml)	Propranolol Area	Sildenafil Area	Ratio	Measured Conc.	Accuracy %
50	1355	131945	0.0103	56.493	112.99
100	2749	131045	0.0210	89.652	89.65
200	7050	132634	0.0532	189.292	94.65
500	18503	123242	0.1501	489.612	97.92
1000	41271	125214	0.3296	1045.365	104.54
2000	84902	129415	0.6560	2056.242	102.81
3000	111972	119621	0.9361	2923.346	97.44

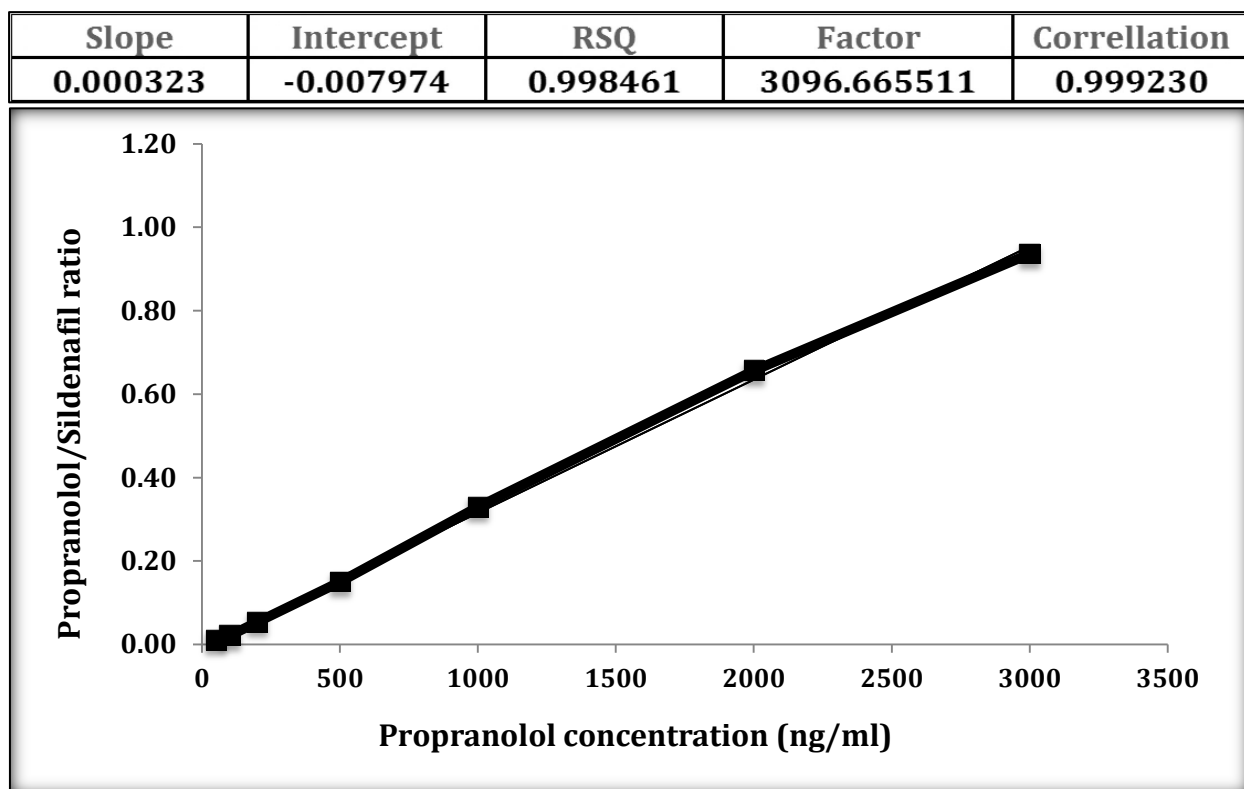


Figure 3.8 Intra-day one calibration curve of propranolol in serum.

Measured Conc. = (Ratio +0.007974)/ 0.000323
 Function is $Y = 0.000323X - 0.007974$ ($R^2 = 0.998461$).

3.2.4.2 Calibration curve 2

Table 3.37 Calibration curve data of intra-day two of validation.

Theoretical conc. (ng/ml)	Propranolol Area	Sildenafil Area	Ratio	Measured Conc.	Accuracy %
50	1154	131469	0.0088	54.990	109.98
100	2658	123895	0.0215	93.239	93.24
200	7058	131618	0.0536	190.314	95.16
500	18740	117309	0.1597	510.538	102.11
1000	40905	129244	0.3165	983.509	98.35
2000	85807	129035	0.6650	2035.076	101.75
3000	114505	116971	0.9789	2982.337	99.41

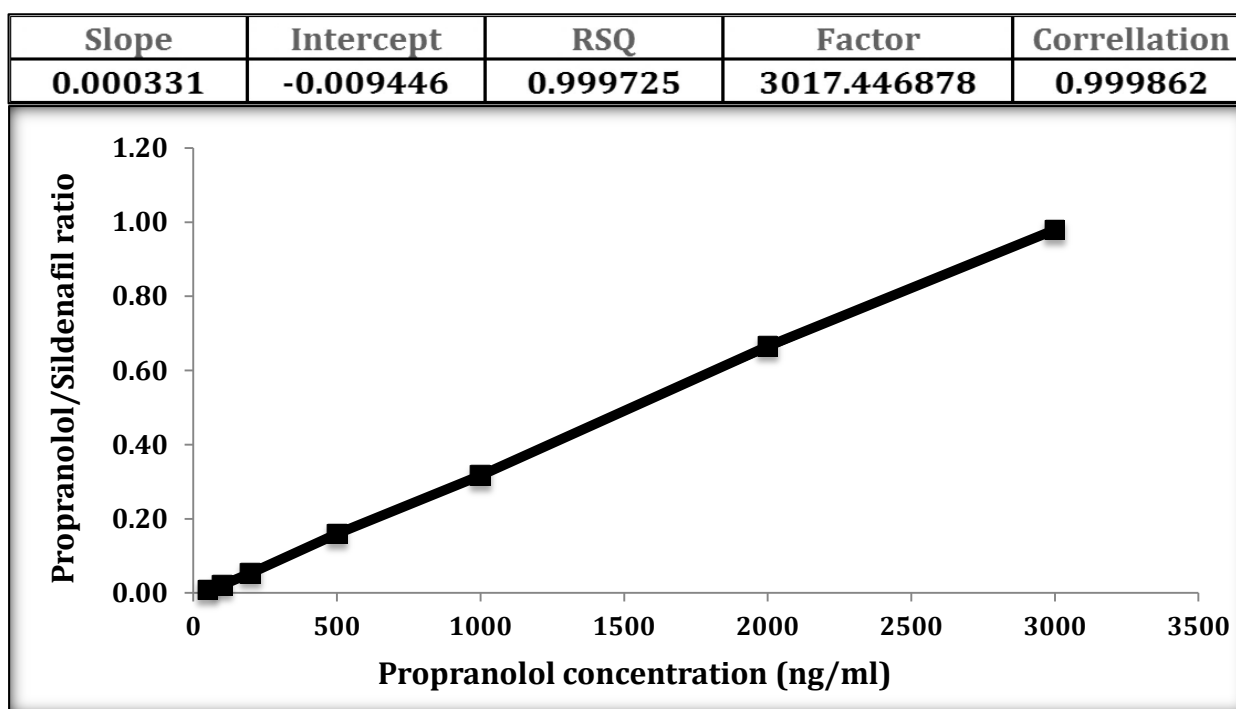


Figure 3.9 Intra-day two calibration curve of propranolol in serum.

Measured Conc. = (Ratio +0.009446)/ 0.000331
 Function is $Y = 0.000331X - 0.009446$ ($R^2 = 0.999725$).

3.2.4.3 Calibration curve 3

Table 3.38 Calibration curve data of intra-day three of validation.

Theoretical conc. (ng/ml)	Propranolol Area	Sildenafil Area	Ratio	Measured Conc.	Accuracy %
50	1204	130123	0.0093	53.377	106.75
100	2792	124068	0.0225	94.219	94.22
200	7177	129954	0.0552	195.077	97.54
500	18044	113631	0.1588	514.286	102.86
1000	40210	130393	0.3084	975.315	97.53
2000	84639	130065	0.6507	2030.542	101.53
3000	113617	118212	0.9611	2987.193	99.57

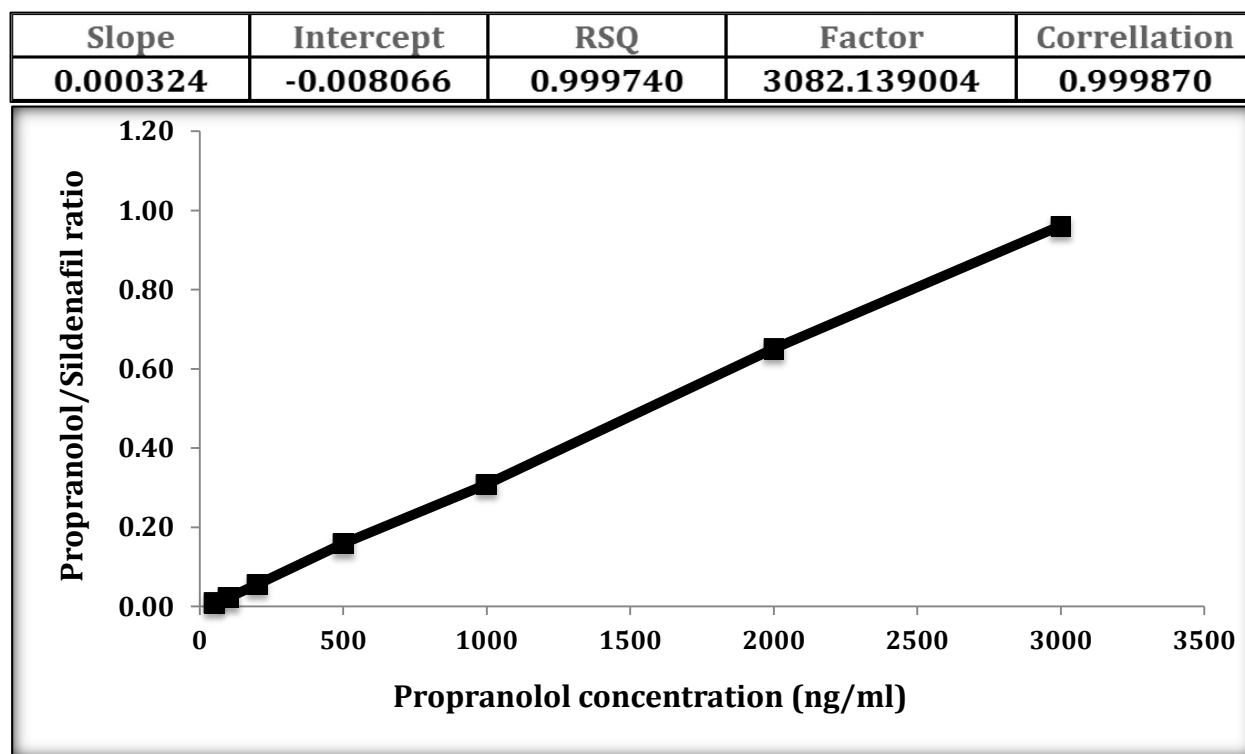


Figure 3.10 Intra-day three calibration curve of propranolol in serum.

Measured Conc. = (Ratio + 0.008066) / 0.000324
 Function is $Y = 0.000324X - 0.008066$ ($R^2 = 0.999740$).

3.2.4.4 Calibration curve 4

Table 3.39 Calibration curve data of freeze-thaw test of stability.

Theoretical conc. (ng/ml)	Propranolol Area	Sildenafil Area	Ratio	Measured Conc.	Accuracy %
50	1058	107749	0.0098	52.836	105.67
100	1859	83997	0.0221	91.226	91.23
200	7177	129276	0.0555	195.320	97.66
500	18972	120356	0.1576	513.711	102.74
1000	40891	125378	0.3261	1039.116	103.91
2000	76271	119531	0.6381	2011.743	100.59
3000	101532	108273	0.9377	2946.054	98.20

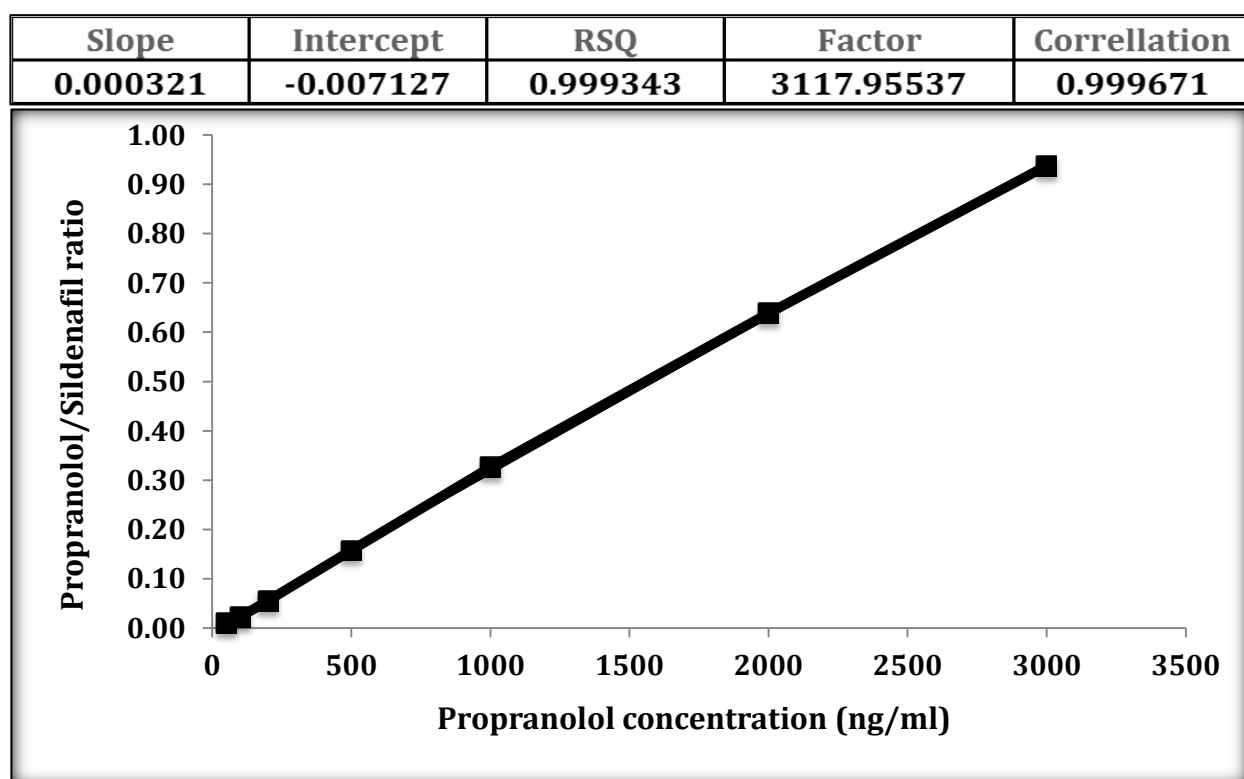


Figure 3.11 Freeze-thaw stability test calibration curve of propranolol in serum.

Measured Conc. = (Ratio +0.007127)/ 0.000321
 Function is $Y = 0.000321X - 0.007127$ ($R^2 = 0.999343$).

3.2.4.5 Calibration curve 5

Table 3.40 Calibration curve data of bench-top test of stability.

Theoretical conc. (ng/ml)	Propranolol Area	Sildenafil Area	Ratio	Measured Conc.	Accuracy %
50	1331	124691	0.0107	56.904	113.81
100	2672	114670	0.0233	96.372	96.37
200	5921	124954	0.0474	171.647	85.82
500	19088	124566	0.1532	502.489	100.50
1000	40808	125700	0.3246	1038.240	103.82
2000	79345	124735	0.6361	2011.734	100.59
3000	107927	114386	0.9435	2972.608	99.09

Slope	Intercept	RSQ	Factor	Correllation
0.000320	-0.007532	0.999573	3125.556740	0.999786

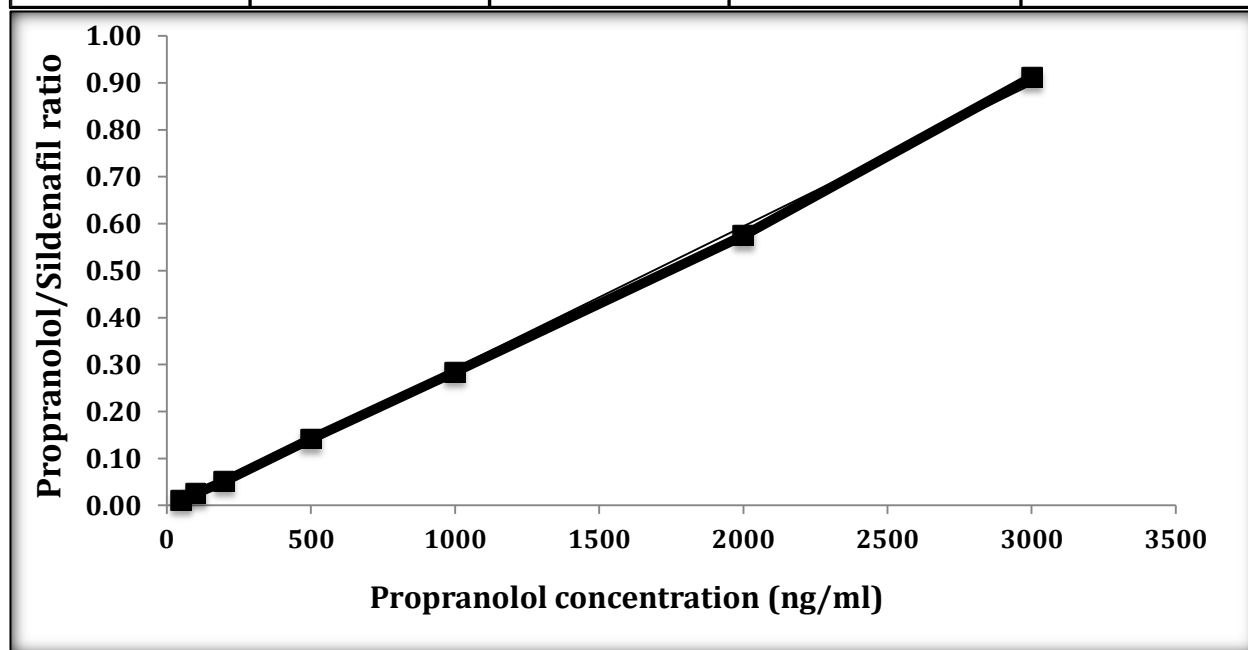


Figure 3.12 Bench-top stability test calibration curve of propranolol in serum.

Measured Conc. = (Ratio +0.007532)/ 0.000320
 Function is $Y = 0.000320X - 0.007532$ ($R^2 = 0.999573$)

3.2.4.6 Calibration curve 6

Table 3.41 Calibration curve data of autosampler test of stability.

Theoretical conc. (ng/ml)	Propranolol Area	Sildenafil Area	Ratio	Measured Conc.	Accuracy %
50	1249	123202	0.010	57.133	114.27
100	2924	123509	0.024	99.283	99.28
200	5843	124510	0.047	171.689	85.84
500	18637	125684	0.148	487.291	97.46
1000	40384	125700	0.321	1025.937	102.59
2000	80293	125614	0.639	2015.902	100.80
3000	109707	115126	0.953	2992.772	99.76

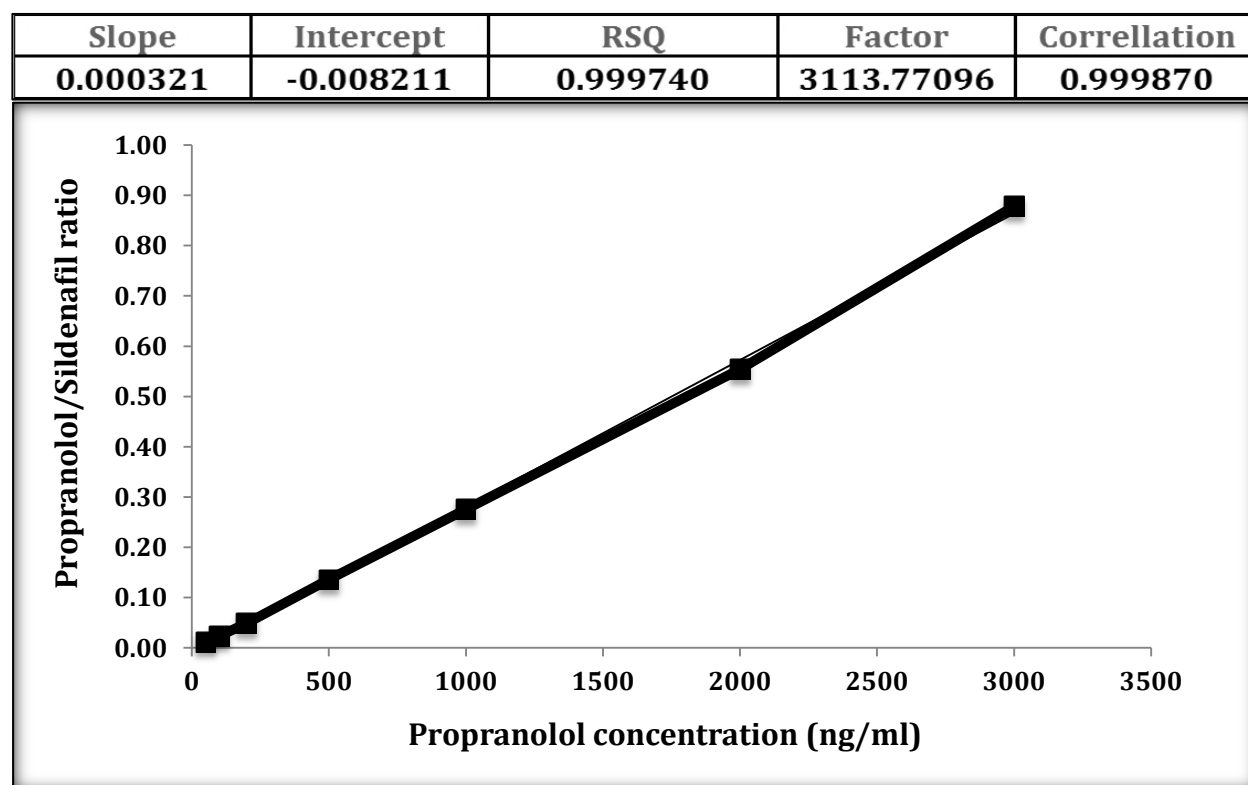


Figure 3.13 Autosampler stability test calibration curve of propranolol in serum.

Measured Conc. = (Ratio +0.008211)/ 0.000321
 Function is $Y = 0.000321X - 0.008211$ ($R^2 = 0.999740$).

Table 3.42 Calculated Accuracy % based on measured concentration mean for each concentration of standard points.

Concentration	Calibration Curve number						Mean	STD	CV%	Accuracy
	1	2	3	4	5	6				
50	57.133	56.904	52.836	56.493	54.990	53.377	55.289	1.856	3.357	110.58
100	99.283	96.372	91.226	89.652	93.239	94.219	93.999	3.486	3.709	94.00
200	171.689	171.647	195.320	189.292	190.314	195.077	185.556	11.030	5.944	92.78
500	487.291	502.489	513.711	489.612	510.538	514.286	502.988	12.043	2.394	100.60
1000	1025.937	1038.240	1039.116	1045.365	983.509	975.315	1017.914	30.591	3.005	101.79
2000	2015.902	2011.734	2011.743	2056.242	2035.076	2030.542	2026.873	17.446	0.861	101.34
3000	2992.772	2972.608	2946.054	2923.346	2982.337	2987.193	2967.385	27.137	0.915	98.91

Table 3.43 Calculated Accuracy % based on area ratios mean for each concentration of standard points.

Concentration	Ratio for Standard Point						Mean	STD	CV%
	1	2	3	4	5	6			
50	0.0101	0.0107	0.0098	0.0103	0.0088	0.0093	0.010	0.001	7.11
100	0.0237	0.0233	0.0221	0.0210	0.0215	0.0225	0.022	0.001	4.66
200	0.0469	0.0474	0.0555	0.0532	0.0536	0.0552	0.052	0.004	7.39
500	0.1483	0.1532	0.1576	0.1501	0.1597	0.1588	0.155	0.005	3.10
1000	0.3213	0.3246	0.3261	0.3296	0.3165	0.3084	0.321	0.008	2.39
2000	0.6392	0.6361	0.6381	0.6560	0.6650	0.6507	0.648	0.012	1.80
3000	0.9529	0.9435	0.9377	0.9361	0.9789	0.9611	0.952	0.016	1.72

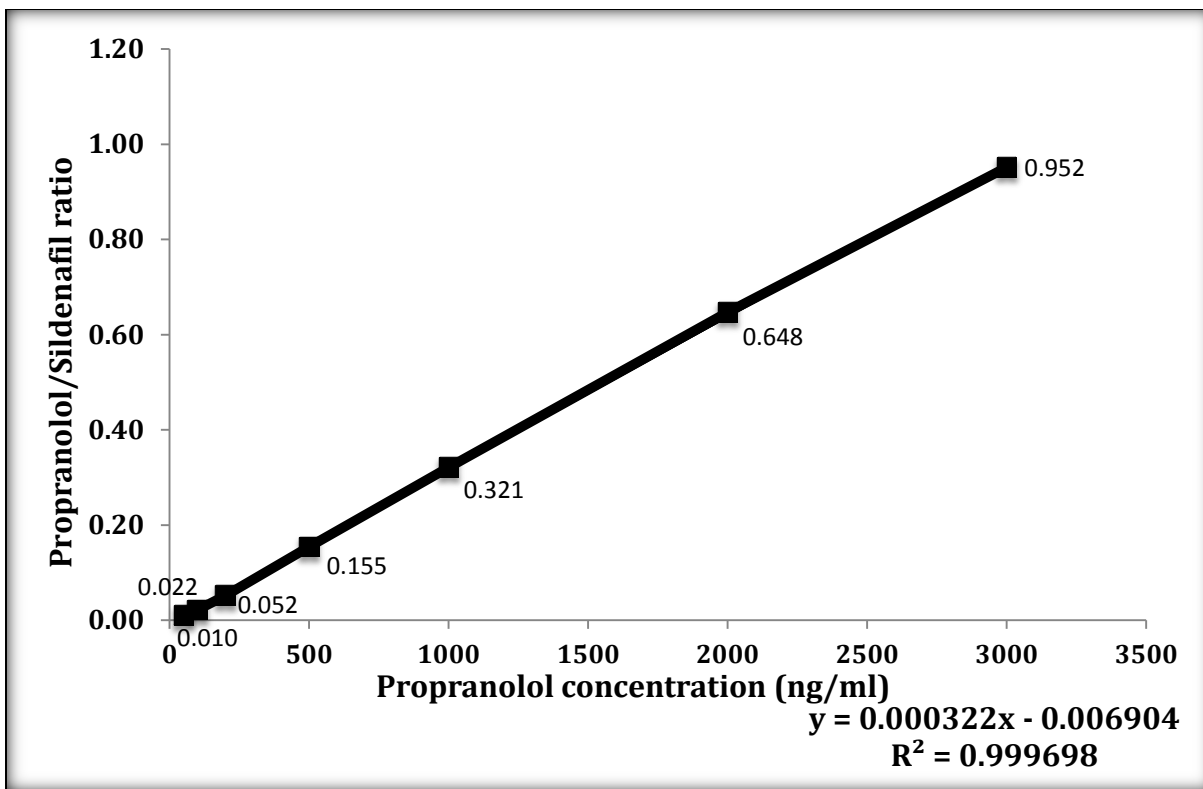


Figure 3.14 Propranolol concentrations versus mean area ratios for each concentration of standard points.

Linearity accuracy % is shown in **table 3.42** which represents an accepted accuracy range according to EMEA guidelines of (92.78%-110.58%) in addition to a linear relationship of correlation coefficient equals 0.999698.

3.2.5 Recovery

3.2.5.1 Recovery in mobile phase

CV% of AUC mean of PRN was 1.02%, 9.49% and 10.12% for QC mid, QC high and QC low respectively while it was 1.19%, 5.76% and 8.43% for QC mid, QC low, and QC high respectively for AUC mean of sildenafil as shown in **table 3.44**.

Table 3.44 CV% values of AUC mean of propranolol and sildenafil (internal standard) in mobile phase.

Concentration	Propranolol Area	Sildenafil Area	Mean (Propranolol)	C.V % (Propranolol)	Mean (Sildenafil)	C.V % (Sildenafil)
150 ng/ml QC Low	5025	120636	4617	10.12	114053	5.76
	4107	107496				
	4718	114026				
1500 ng/ml QC Mid	62281	129680	61572	1.02	128046	1.19
	61349	127789				
	61087	126668				
2500 ng/ml QC High	89158	110825	100128	9.49	122717	8.43
	105514	127644				
	105713	129682				

3.2.5.2 Recovery in the serum

CV% of AUC mean of PRN was 2.25%, 2.49% and 2.88% for, QC high, QC mid and QC low respectively while it was 1.88%, 4.12% and 4.38% for QC high, QC low and QC mid respectively for AUC mean of sildenafil as shown in **table 3.45**.

Table 3.45 CV% values of AUC mean of propranolol and sildenafil (internal standard) in serum blood.

Concentration	Propranolol Area	Sildenafil Area	Mean (Propranolol)	C.V % (Propranolol)	Mean (Sildenafil)	C.V % (Sildenafil)
150 ng/ml QC Low	4483	112051	4582	2.88	117653	4.12
	4531	120438				
	4732	120471				
1500 ng/ml QC Mid	63470	134955	61805	2.49	128485	4.38
	60429	124779				
	61515	125721				
2500 ng/ml QC High	98807	119284	101061	2.25	121769	1.88
	101027	123803				
	103348	122220				

The highest recovery of PRN in serum was shown by QC high of 100.93% while the lowest recovery was obtained by QC low of 99.25% which are considered acceptable recovery ratios of PRN between mobile phase and serum as shown in **table 3.46**.

Table 3.46 Absolute recovery ratios of propranolol in serum.

Concentration	AUC mean in serum	AUC mean in mobile phase	Absolute Recovery
150 ng/ml QC Low	4582	4617	99.25
1500 ng/ml QC Mid	61805	61572	100.38
2500 ng/ml QC High	101061	100128	100.93

The highest recovery of sildenafil (IS) in serum was shown by QC low of 103.16% while the lowest recovery was obtained by QC high of 99.23% which are considered acceptable recovery ratios of sildenafil between mobile phase and serum as shown in **table 3.47**.

Table 3.47 Absolute recovery ratios of sildenafil citrate (internal standard) in serum.

Concentration	AUC mean in serum	AUC mean in mobile phase	Absolute Recovery
150 ng/ml QC Low	117653	114053	103.16
1500 ng/ml QC Mid	128485	128046	100.34
2500 ng/ml QC High	121769	122717	99.23

3.3 Representative HPLC chromatograms of analyzed Sprague-Dawley rat serum.

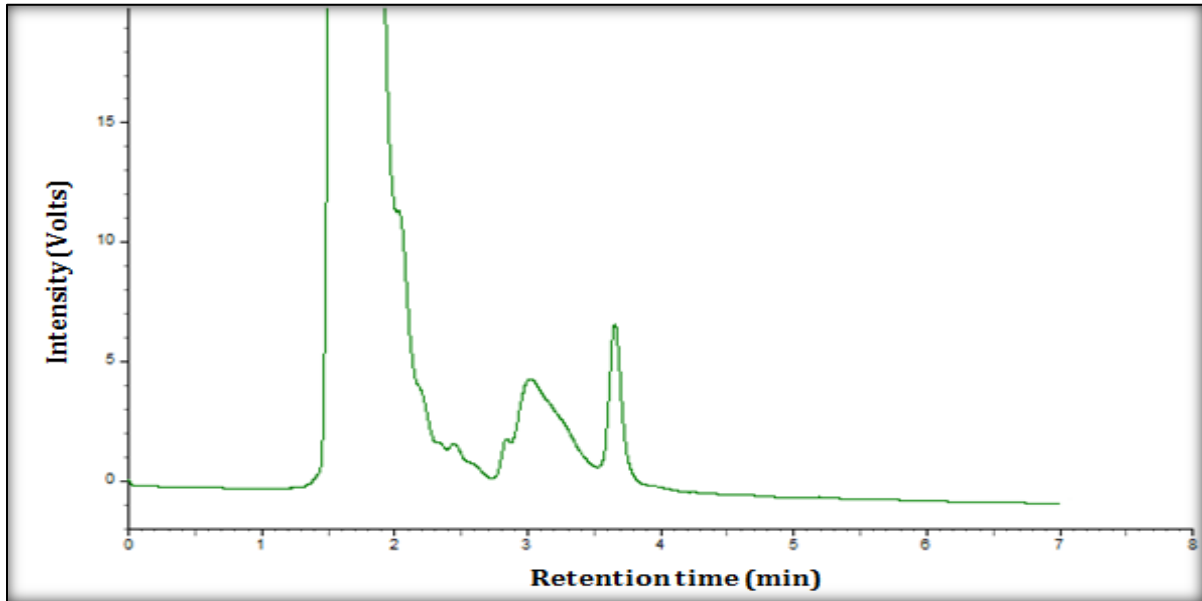


Figure 3.15 A processed blank serum sample.

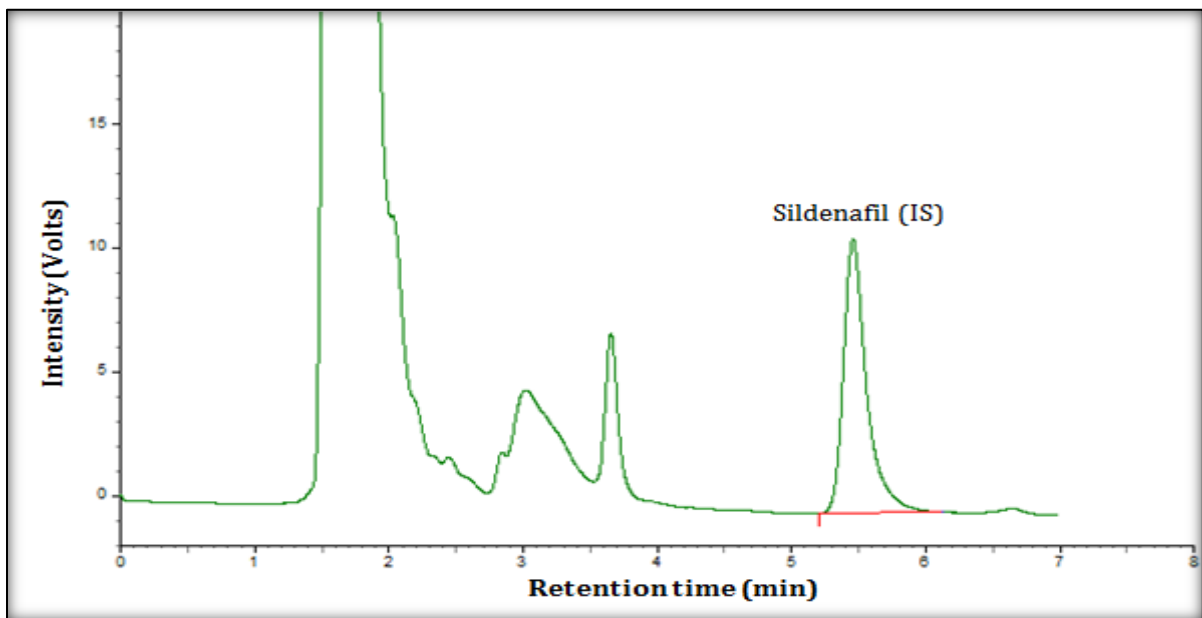


Figure 3.16 A processed zero serum sample spiked with sildenafil; the internal standard of propranolol analysis.

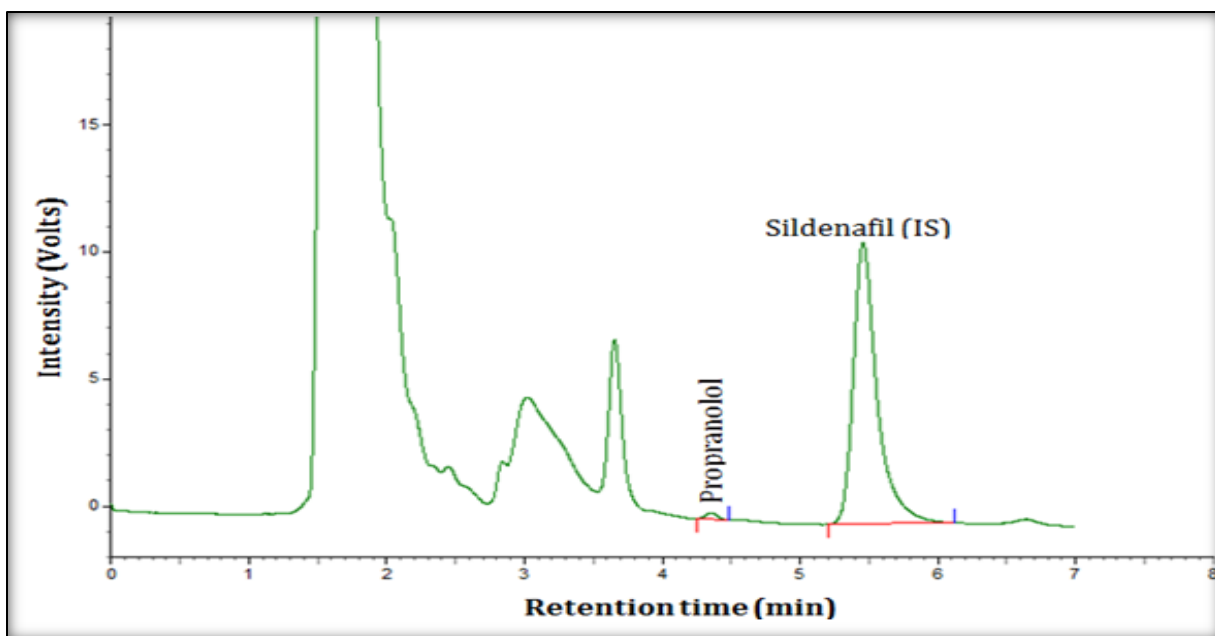


Figure 3.17 A processed lower limit of quantification (50 ng/ml) for serum sample spiked with sildenafil; the internal standard of propranolol analysis.

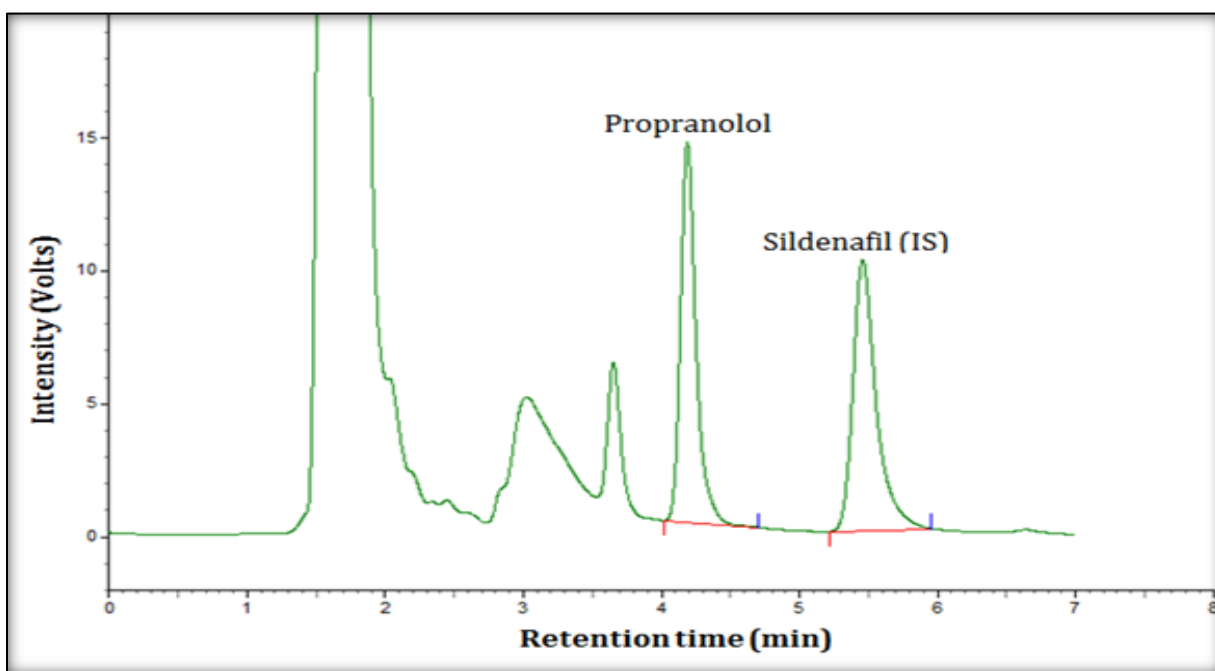


Figure 3.18 A processed upper limit of quantification (3000 ng/ml) for serum sample spiked with sildenafil; the internal standard of propranolol analysis.

3.4 In vivo experiments

3.4.1 Effect of GlcN on PRN BA

Different sets of experiments were done to study the effect of GlcN on PRN BA. The experiments were performed to compare the effect of 100 and 200 mg/kg GlcN on PRN BA using a single dose of 20 mg/kg PRN. The results showed that 100 mg/kg did not change PRN AUC and C_{max} ($p>0.05$). On the other hand, higher GlcN 200 mg/kg dose decreased PRN AUC and C_{max} significantly by 43% ($p<0.01$) and 34% ($p<0.05$), respectively (**Table 3.48, Figure 3.19**). Conversely, none of the above mentioned tested combinations affected T_{max} values of PRN.

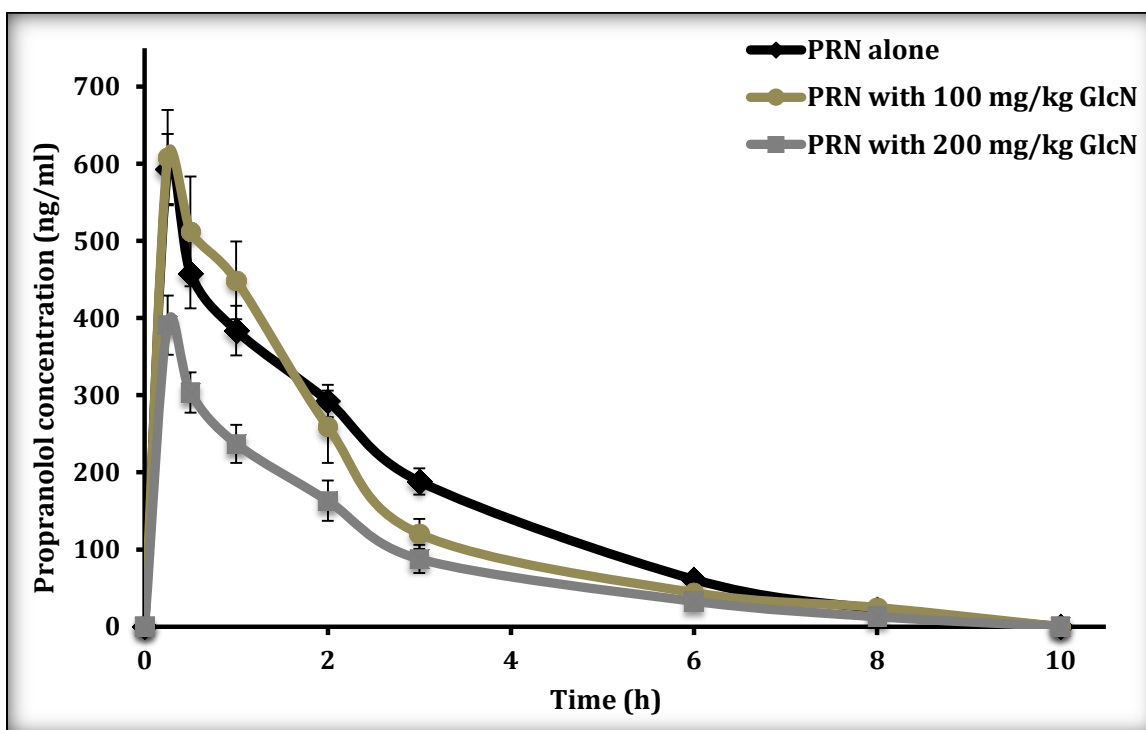


Figure 3.19 *In vivo* serum concentration versus time curves of propranolol in rats after a single oral dose of 20 mg/kg of propranolol, propranolol with 100 and 200 mg/kg of glucosamine. Each data point represents the mean \pm SEM ($n=7$).

3.4.2 Effect of cimetidine and rifampin on PRN BA

Another set of experiments were carried out to study the effect of cimetidine and rifampin, as controls, on PRN BA using a single dose of 20 mg/kg PRN. The results showed that rifampin 9 mg/kg did not change PRN AUC and C_{max} ($p>0.05$), whereas 5 mg/kg of cimetidine increased PRN C_{max} significantly by 86% ($p<0.01$) and AUC by 20% ($p>0.05$) (Table 3.49, Figure 3.20).

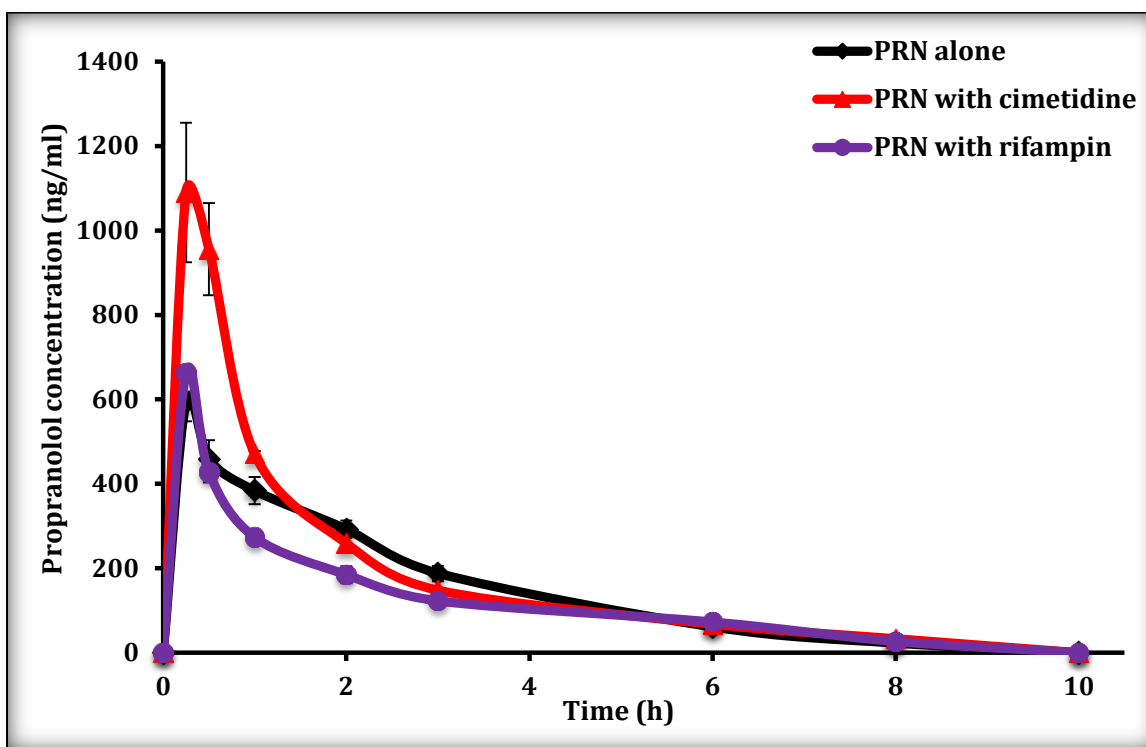


Figure 3.20 *In vivo* serum concentration versus time curves of propranolol in rats after a single oral dose of 20 mg/kg of propranolol, propranolol with 5 and 9 mg/kg of cimetidine and rifampin, respectively. Each data point represents the mean \pm SEM ($n=5$).

Table 3.48 Glucosamine effect on propranolol AUC, C_{max} , and other pharmacokinetic parameters after an oral dose of 20 mg/kg PRN, PRN with GlcN 100 or PRN with GlcN 200 mg/kg in rats. The data are presented as mean \pm SEM (n=7).

Treatment	AUC (ng/ml*h)	C_{max} (ng/ml)	AUMC (ng/mL*h ²)	MRT (h)	$t_{0.5}$ (h)	Kel (1/h)	% change in AUC of PRN	% change in C_{max} of PRN
PRN (20 mg/kg)	1539.92 \pm 98.89	593.35 \pm 45.42	4171.57 \pm 387.35	2.69 \pm 0.15	1.84 \pm 0.16	0.40 \pm 0.04	100%	100%
PRN with GlcN (100 mg/kg)	1427.39 \pm 170.32	615.07 \pm 62.98	4096.52 \pm 775.53	2.73 \pm 0.30	2.44 \pm 0.44	0.34 \pm 0.07	93%	104%
PRN with GlcN (200 mg/kg)	880.79 \pm 122.66**	393.77 \pm 36.82*	2374.64 \pm 498.52	2.54 \pm 0.30	1.92 \pm 0.26	0.41 \pm 0.07	57%	66%

*, p<0.05 and **, p<0.01

Table 3.49 Cimetidine and rifampin effect on propranolol AUC, C_{max} , and other pharmacokinetic parameters after an oral dose of 20 mg/kg of propranolol, propranolol with 5 and 9 mg/kg of cimetidine and rifampin, respectively in rats. The data are presented as mean \pm SEM (n=5).

Treatment	AUC (ng/ml*h)	C_{max} (ng/ml)	AUMC (ng/mL*h ²)	MRT (h)	$t_{0.5}$ (h)	Kel (1/h)	% change in AUC of PRN	% change in C_{max} of PRN
PRN (20 mg/kg)	1539.92 \pm 98.89	593.35 \pm 45.42	4171.57 \pm 387.35	2.69 \pm 0.15	1.84 \pm 0.16	0.40 \pm 0.04	100%	100%
PRN with cimetidine (5 mg/kg)	1853.73 \pm 151.19	1105.17 \pm 157.70**	4586.12 \pm 302.71	2.49 \pm 0.05	2.42 \pm 0.14	0.29 \pm 0.02	120%	186%
PRN with rifampin (9 mg/kg)	1323.52 \pm 32.63	663.72 \pm 14.29	4594.33 \pm 409.48	3.46 \pm 0.25*	2.82 \pm 0.24*	0.25 \pm 0.02*	86%	112%

*, p<0.05 and **, p<0.01

3.4.3 Effect of GlcN on PRN effective intestinal permeability (P_{eff}) and clearance

Effective intestinal permeability (P_{eff}) values were estimated by the Nelder–Mead algorithm of the Parameter Estimation module using the SimCYP program. PRN plasma mean concentration profiles were used to estimate P_{eff} , V_d and clearance values as shown in **table 3.50**. Permeability of PRN with 200 mg/kg GlcN was reduced by 50% with GlcN, whereas clearance increased while V_d almost did not changed.

Table 3.50 P_{eff} , Clearance, and V_d results of propranolol 20 mg/kg, propranolol with 100 and 200 mg/kg GlcN estimated by the Nelder–Mead algorithm using the SimCYP program.

Treatment	effective intestinal permeability (P_{eff}) (10^{-4} cm/sec)	Clearance (CL) (L/hr)	Volume (V_d) (L/kg)
PRN (20 mg/kg)	25.28	23.88	0.49
PRN with GlcN (100 mg/kg)	23.99	25.11	0.43
PRN with GlcN (200 mg/kg)	12.65	35.75	0.55

Figure 3.21 shows the observed (measured) plasma mean concentration profiles of PRN, PRN with 100 mg/kg and 200 mg/kg GlcN versus SimCYP-predicted values. The results indicated good fitting of observed PRN plasma concentrations values with those estimated by SimCYP program.

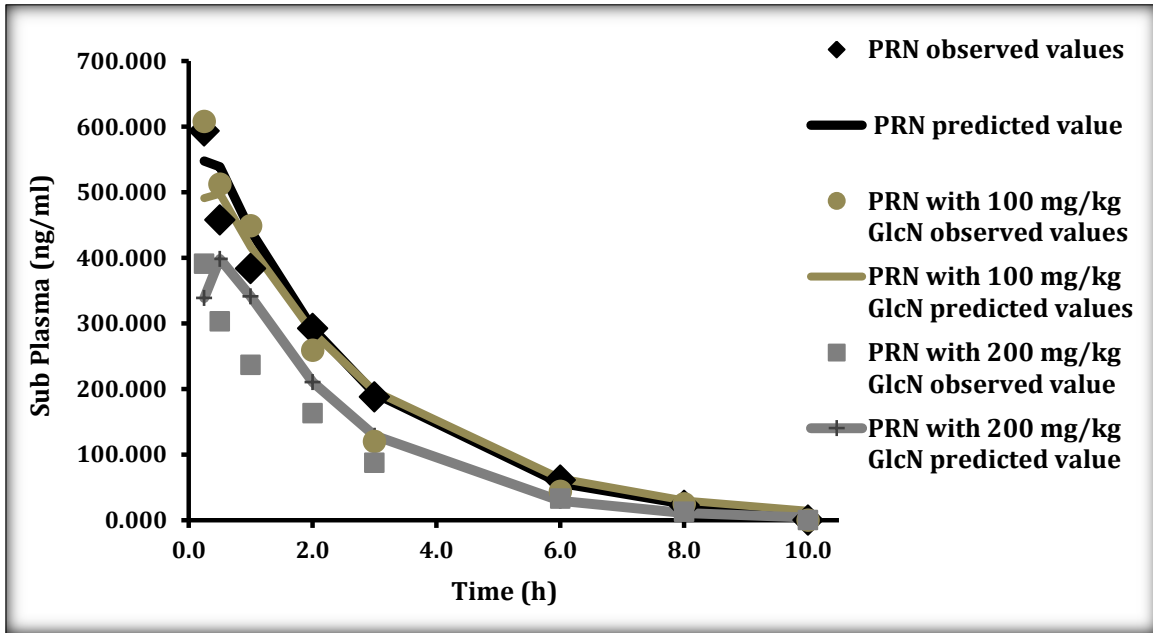


Figure 3.21 Observed versus SimCYP-predicted propranolol plasma concentrations of 20 mg/kg propranolol, propranolol with 100 mg/kg glucosamine and propranolol with 200 mg/kg glucosamine.

3.5 Effect of GlcN on PRN *in situ* single-pass intestinal perfusion (SPIP)

As seen in **figure 3.22**, cimetidine, an enzyme inhibitor increased the BA of PRN whereas; rifampin, an enzyme inducer decreased PRN BA. For all conditions, the concentration of PRN increased in a time-dependent manner. The highest increase in PRN concentration of 286 ± 20 ng/ml was observed at 60 min. Administering PRN with the enzyme inducer rifampin decreased its BA and achieved the lowest concentration of 237 ± 60 ng/ml at 60 min. By contrast, administering PRN with the enzyme inhibitor cimetidine increased its BA and achieved a higher concentration of 511 ± 138 ng/ml at 60 min, however, such increase was not statistically significant. Meanwhile, combining PRN with GlcN significantly enhanced the BA of PRN by two-fold to reach 842 ± 150 ng/ml ($p < 0.05$).

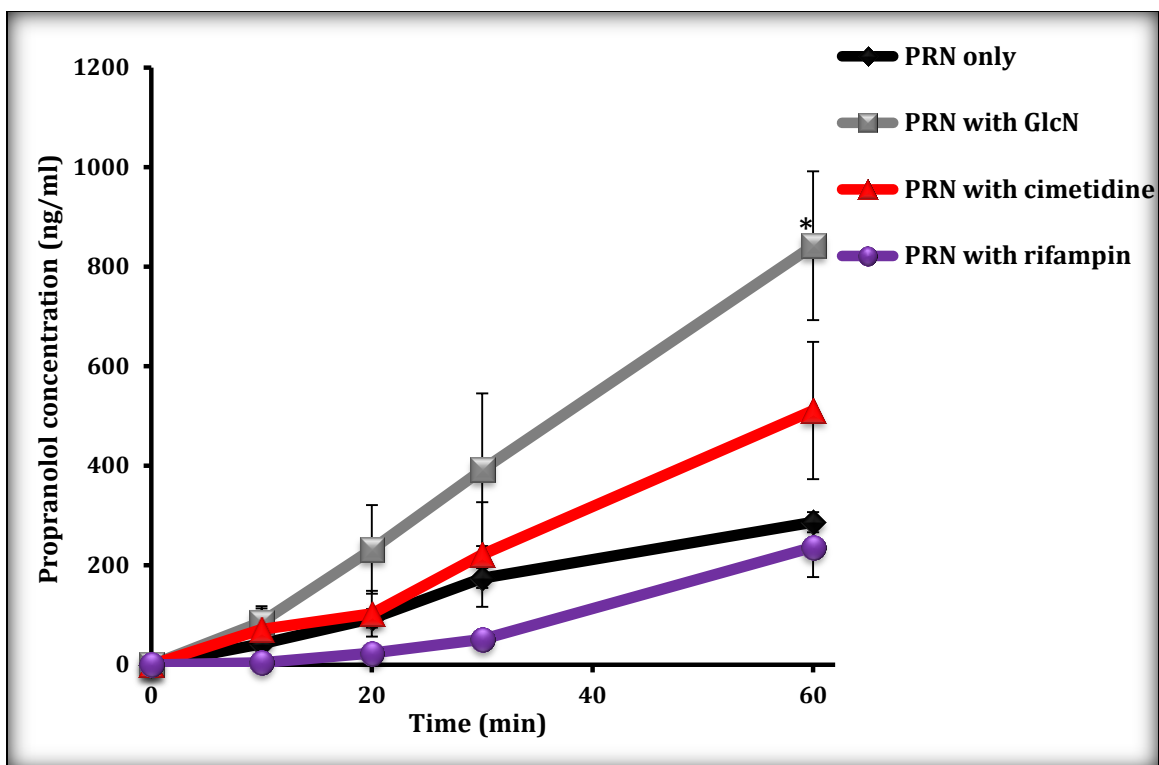


Figure 3.22 Time dependence curves of propranolol serum concentration in rats using *in situ* single pass intestinal perfusion. Rats were administered propranolol alone 1 mg/ml, propranolol with glucosamine 10 mg/ml, propranolol with cimetidine 1 mg/ml, and propranolol with rifampin 2 mg/ml. The data are presented as mean \pm SEM (n=6). Significant effect was seen between propranolol only and propranolol with GlcN ($p < 0.05$).

3.6 Effect of GlcN on PRN absorption in everted rat intestine sac (ERIS)

To measure the effect of GlcN on PRN absorption, the everted rat intestinal sac (ERIS) *in vitro* technique was used to measure the amount of PRN absorbed over time. Both GlcN and SLS increased PRN concentration level by increasing its absorption insignificantly at 40 and 60 min in a time-dependent manner GlcN. The maximum value for PRN with GlcN at 60 min was 51484 ± 3619 ng/ml, whereas PRN with SLS gave the lowest value of 38605.91 ± 2541.20 ng/ml (Figure 3.23).

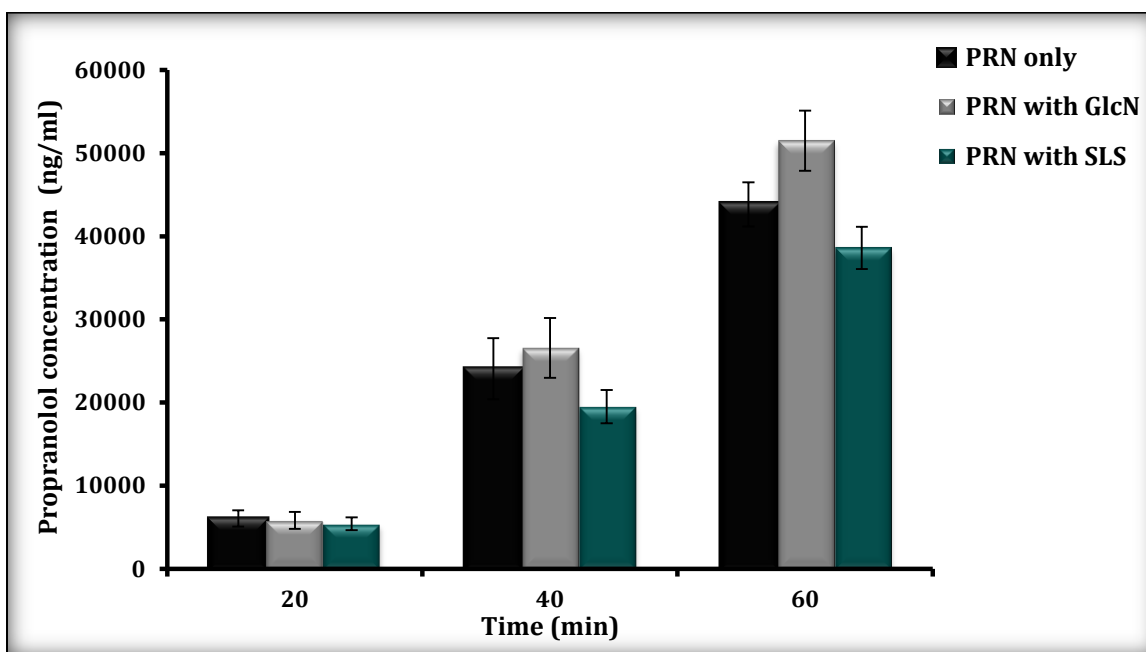


Figure 3.23 Absorption of propranolol in the everted rat intestinal sac versus time. Rats were administered 0.1 mg/ml propranolol, propranolol with 1 mg/ml glucosamine and propranolol with 0.01 mg/ml sodium lauryl sulfate for 60 min. The data are presented as mean \pm SEM (n=6).

3.7 Hepatocyte cell isolation and culture

3.7.1 Effect of GlcN on PRN metabolism

Interestingly, dose dependent increase in PRN was only significant at 200 mM of post incubation ($p < 0.001$). The maximum value for PRN with GlcN at 60 min was 6728 ± 143 ng/ml, whereas PRN with 40 mM GlcN gave the lowest value of 6011 ± 99 ng/ml at 30 min (**Figure 3.24**).

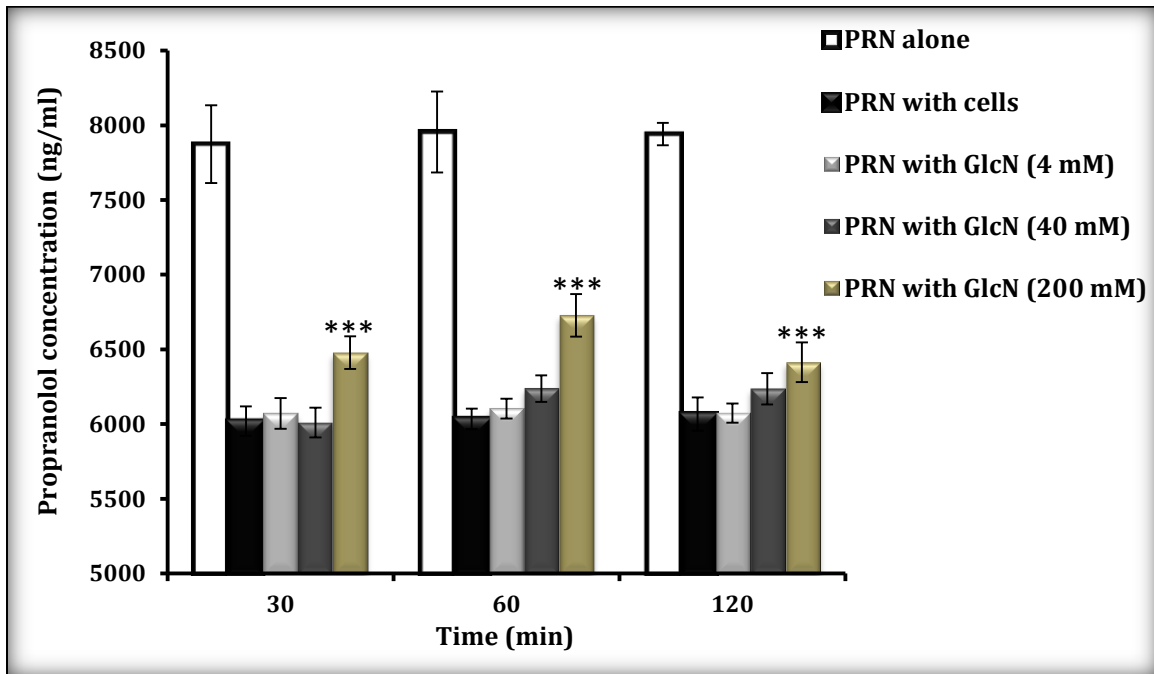


Figure 3.24 Propranolol concentration versus time profiles in hepatocyte cell isolation and culture. Cells were cultured with 20 μ M of propranolol with 40 mM glucosamine, glucosamine high and low concentrations of 200 mM and 4 mM, respectively, for 120 min. The data are presented as mean \pm SEM (***, $p < 0.001$).

3.7.2 Effect of cimetidine and rifampin on PRN metabolism

Cimetidine (5 μM), decreased PRN metabolism and increased PRN concentrations at 30, 60, and 120 min significantly ($p < 0.01$), whereas rifampin (50 μM) increased PRN metabolism and decreased PRN concentrations at 30, 60 and 120 min ($p > 0.05$). The maximum value for PRN with cimetidine at 60 min was 6525 ± 160 ng/ml, whereas PRN with rifampin GlcN obtained the lowest value of 5877 ± 230 ng/ml at 30 min (**Figure 3.25**).

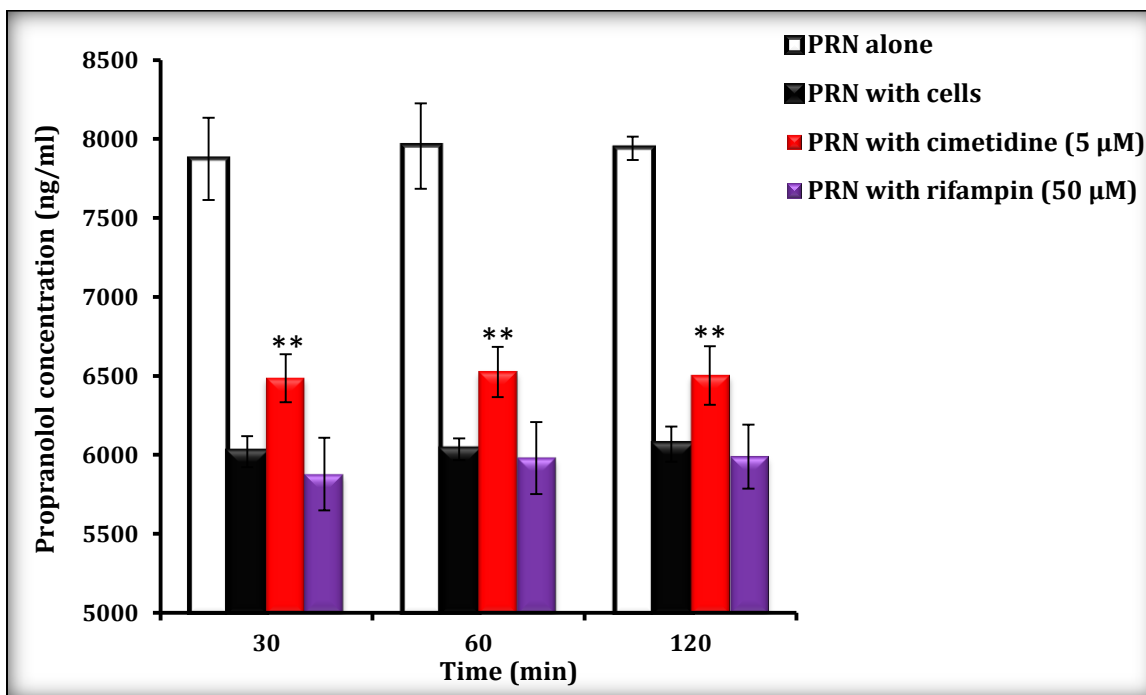


Figure 3.25 Propranolol concentration versus time profiles in hepatocyte cell isolation and culture. Cells were cultured with 20 μM propranolol with 5 μM cimetidine and 50 μM rifampin for 120 min. The data are presented as mean \pm SEM (**, $p < 0.01$).

Chapter Four

Discussion

Chapter Four

4. Discussion

PRN has been used widely to treat hypertension, cardiac arrhythmias, and many other diseases (Routledge and Shand 1978). According to the Biopharmaceutics Classification System (BCS) PRN is classified as class 1 drug with rapid dissolution, high solubility, high permeability and an extensive metabolism (Custodio *et al.* 2008). Dissolution and GIT permeability are fundamental and major parameters controlling the rate and extent of drug absorption (Amidon *et al.* 1995). PRN undergoes extensive first-pass effect by the liver resulting in a relatively low oral BA of 13-23% (Cid *et al.* 1986; Sastry *et al.* 1993) and short plasma $t_{0.5}$ ranging from 3 to 6 hours (Castleden and George 1979; Ismail *et al.* 2004; Leahey *et al.* 1980). As a result, PRN has to be given in high doses to solve this problem, which inevitably increases PRN side effects (Partani *et al.* 2009). Ryu *et al.* have shown a strategy to overcome PRN low BA by using a route of drug delivery (rectal route) other than oral (Ryu *et al.* 1999). Rectal infusion of PRN induced a 4-5 fold increase in PRN BA. Another study in dogs has shown that PRN oral BA was increased by the administration of PRN laurate salt. This salt is a lipid vehicle containing fatty acids that increases the intestinal absorption of many drugs by various mechanisms (Aungst and Hussain 1992).

A study has shown that GlcN combination with ibuprofen produced a significant antinociceptive synergistic effect; a racemic mixture of GlcN with

ibuprofen reduced ibuprofen effective dose by 58% (Raffa *et al.* 2010). However, increasing GlcN dose did not increase the antinociceptive effect when combined with ibuprofen (Tallarida *et al.* 2003). A recent study by Qinna *et al.* has shown that GlcN increases paracetamol BA by reducing its metabolism in addition to a reduction in hepatocyte injury after administration of high doses of paracetamol (Qinna *et al.* 2015). Therefore, this study was conducted to investigate the effect of GlcN on PRN PK and metabolism since GlcN has been reported to alter the BA of many drugs. To study such interaction, a validated, sensitive, precise and simple reversed phase HPLC method was developed for the estimation of small concentrations of PRN HCl in serum and Krebs buffer. This chromatographic method was validated using EMEA guidelines with acceptable ranges of accuracy, precision, linearity, recovery, limits of quantitation, and detection.

Cimetidine is a CYP450 enzyme inhibitor which affects PRN PK by decreasing its hepatic first-pass metabolism, therefore increasing PRN plasma concentration and its pharmacological effect in humans (Heagerty *et al.* 1981; Reimann *et al.* 1981). On the other hand, Herman *et al.* has reported that chronic administration of rifampin (a CYP450 inducer) led to a marked reduction in PRN steady-state concentration (Herman *et al.* 1983). Based on these studies, both cimetidine and rifampin were used as controls in the experiments performed here. Our results on Sprague-Dawley rats have shown that cimetidine increased PRN concentration levels in *in vivo* (**Table 3.49, Figure 3.20**); *in situ* SPIP (**Figure 3.22**) and in hepatocyte isolation and cell culture (**Figure 3.25**). On the contrary, rifampin

showed a trend towards a decrease in PRN concentration levels *in situ* and *in vitro* (**Figure 3.22 and 3.25**) and *in vivo* experiments (**Table 3.49, Figure 3.20**) as compared to the control. Hepatocyte cell isolation and culture technique was used to study drug metabolism and drug-drug interaction between PRN and GlcN in comparison with control drugs (Hewitt *et al.* 2007).

A drug such as PRN is considered highly permeable since the extent of its absorption is greater or equal to 90% of the administered dose based on a mass balance determination or in comparison to an I.V. reference dose (Custodio *et al.* 2008). However, our results indicated that GlcN decreased PRN BA in a dose-dependent manner to a higher extent than that observed when PRN was used alone. This was emphasized by a shorter MRT of PRN with GlcN 200 mg/kg (2.54 h) as compared to PRN alone (2.69 h) meaning that higher clearance of PRN-GlcN 200 mg/kg (**Table 3.48, Figure 3.19**). Furthermore, PRN was used as powder dissolved in solution and not as tablets. Hence, dissolution parameter would be excluded and permeability is the main factor responsible for PRN BA in the current research. P_{eff} values were optimized by SimCYP program to predict the actual average plasma PRN profile in order to estimate P_{eff} , V_d and clearance. GlcN at 100 mg/kg did not change P_{eff} or clearance of PRN, whereas GlcN at 200 mg/kg decreased P_{eff} , and increased clearance (**Table 3.50**), which can be related to a dose dependent effect.

Many factors are involved in oral drug delivery, and its BA can be divided into components which reflect intestine delivery (gastric emptying, pH- pK_a), absorption from the lumen (dissolution, lipophilicity), and drug efflux pumps such

as P-gp (Song *et al.* 2004). Nevertheless, drug delivery in this study is independent of gastric emptying because there is no significant difference in T_{max} between PRN alone and PRN with 200 mg/kg of GlcN was observed (Gainsborough *et al.* 1993; Shindo *et al.* 2008). pK_a and pH have a major effect on drug permeability and solubility as well as on the rate and extent of oral drug absorption (Palm *et al.* 1999; Ungell *et al.* 1998). GlcN is a basic cation with pK_a of 7.75 (Hofer and Kunemund 1985), and PRN is also a basic drug with pK_a of 9.4 (Salman *et al.* 2010). According to the pH partition theory, absorption of oral drugs takes place mainly by a passive diffusion of the un-ionized form of the drug molecule through the lipophilic intestinal membrane (Palm *et al.* 1999; Ungell *et al.* 1998). In an empty stomach, where the pH is low (pH 2-3), only a small fraction of the weak bases such as PRN or GlcN would be taken up, as the unionized fraction would be small. Therefore, PRN given on an empty stomach would be absorbed mainly after passage into the slightly alkaline duodenum where pH is more than 7 in the un-ionized form due to higher un-ionized fraction amount (Hurst *et al.* 2007; Liedholm and Melander 1990; Palm *et al.* 1999). Moreover, GlcN has been shown to be absorbed throughout the gut, where the highest absorption occurs in the small intestine, mainly the duodenum (Ibrahim *et al.* 2012). Although it seems that pH is an important factor for PRN BA. However, such factor was not studied in the current research (Amidon *et al.* 1995).

As for PRN site of absorption in the intestine, SPIP technique in rats has been used to study PRN permeability in the intestine. This model has been well elucidated for its correlation with human absorption. PRN absorption occurs along the whole

intestine with the main absorption site in the colon with the highest permeability (Nagare *et al.* 2010). Therefore, SPIP technique was used in the current investigation to assess how PRN BA would be affected in the presence of GlcN, cimetidine and rifampin using the whole length of the small intestine. The results showed that GlcN increased PRN BA significantly to a higher extent than cimetidine and rifampin (**Figure 3.22**). Everted gut technique has been used due to its ability to evaluate intestinal absorption of drugs without the influence of hepatic first-pass effect (Li *et al.* 2011). In the current study, everted gut model was used to enable the investigation of the effects of SLS as well as GlcN on PRN. The intestinal absorption of PRN or PRN concentration levels in the presence of GlcN was higher than in the presence of SLS (**Figure 3.23**) confirming the previous *in vitro* hepatocyte isolation and culture (**Figure 3.24**) and *in situ* results (**Figure 3.22**).

P-glycoprotein (P-gp) is another factor responsible for drug permeability. PRN is said to be a substrate for the (P-gp) efflux transporter, which decreases PRN oral absorption, thus, reducing its BA. A recent study using the SPIP technique has shown that P-gp affects the intestinal absorption of PRN. Verapamil HCl, a P-gp inhibitor, increased PRN BA when it was co-perfused with PRN more than PRN perfusion alone. This indicated that P-gp is an important contributor for PRN low oral BA (Abushammala *et al.* 2013). D'Emanuele and colleagues have shown that the reduction in PRN BA could be avoided when PRN is administered in conjugation with polyamidoamine (PAMAM) dendrimers (D'Emanuele *et al.* 2004). This complex bypasses P-gp efflux transporter and consequently increases its transport. Another

study has shown that the energy-dependent efflux P-gp pump located on the apical plasma membrane of rabbit conjunctival epithelial cells plays a role in restricting PRN transport (Yang *et al.* 2000). Hirakawa *et al.* have shown that GlcN induced the expression of Multidrug Exporter Genes (*mdtEF*) in *Escherichia coli* that is stimulated through catabolite control. This result indicated that GlcN may be responsible for the increased multidrug resistance in the bacteria (Hirakawa *et al.* 2005). However, there are limited studies of the effect of GlcN on P-gp in rats, therefore, further studies are still warranted. The current study did not investigate the effect of P-gp efflux transporter on PRN-GlcN combination; however, it cannot be excluded that this could be potentially responsible for the reduction in the *in vivo* levels of PRN.

GlcN PK studies in rats have shown that GlcN undergoes extensive hepatic first pass metabolism resulting in low BA (about 19- 21%) (Adebowale *et al.* 2002; Persiani *et al.* 2005; Thakral *et al.* 2007). PK and BA of GlcN have shown that C_{max} and AUC of GlcN in human were linear only within dose range of 750-1500 mg that was preceded by a pre-saturated 750 mg phase. GlcN C_{max} and AUC at 3000 mg dose were significantly lower than the corresponding values calculated at the dose of 750 mg. This suggests the involvement of two processes; a process that is capacity limited which is saturated with low doses, and a process that is linear for higher doses (Jackson *et al.* 2010; Persiani *et al.* 2005). If GlcN doses (100 and 200 mg/kg) used in this study were converted to human adults (7000 and 14000 mg/kg, respectively), which both are higher than 3000 mg/kg, wherein GlcN absorption in

human is reduced and this may be a possible reason that GlcN did not get absorbed and consequently did not increase PRN BA as in *in vivo* results (**Figure 3.19**). However, a recent study in rats has shown a linear relation between the oral administered dose and the average AUC. Moreover, everted rat colon *in vitro* data also demonstrated a linear relationship between GlcN concentration and the accumulation rate from mucosal to serosal fluid indicating that GlcN intestinal absorption is linear and not capacity limited (Ibrahim *et al.* 2012). Transporters involved in GlcN absorption have been revealed to be (GLUT 1, 2 and 4), which also facilitate glucose absorption. In particular, GLUT2 has demonstrated a 20-fold greater affinity for GlcN than that for glucose. Transporter-regulated GlcN absorption increases the possibility of a capacity-limited intestinal absorption for the compound (Uldry *et al.* 2002), which was also addressed by Persiani *et al.* (Persiani *et al.* 2005). Nonetheless, PRN is much less influenced by cell transporter since it is a class I drug (Custodio *et al.* 2008), which most likely excludes the transporters as the potential reason of reduced PRN BA.

Chapter Five

Conclusion and future work

Chapter Five

5. Conclusion and future work

GlcN decreased PRN BA in a dose-dependent manner (200 mg/kg and not 100 mg/kg) mostly by decreasing PRN absorption and permeability in vivo, whereas GlcN increased PRN concentration levels in situ and in vitro. Moreover, In vivo results suggest that the patient may suffer complications from uncontrolled, inadequately treated hypertension, angina pectoris and other diseases treated by PRN. As a result, it might be necessary to prescribe PRN with GlcN with caution as a dosage regimen adjustment of PRN might be needed in order to achieve the required therapeutic effect in patients receiving GlcN. (with caution until further clinical investigation describes such drug-drug interaction). Finally, our results showed that cimetidine and rifampin levels were in line with the previously reported researches.

Further studies are still warranted to uncover the effect of PRN and GlcN combination by studying the effect of GlcN on P-gp efflux transporters present in small and large intestine mucosa, in renal tubule, and in biliary hepatocytes. Moreover, it might be interesting to examine the effect of high and low doses of GlcN alone or in combination with PRN on P-gp. It is also warranted to perform an investigation of the stomach absorption of PRN alone and PRN combined to GlcN. Furthermore, further studies is still needed to investigate the effect of GlcN on CYP2D6 and CYP1A2 that are responsible for PRN metabolism as well as testing

phase I and phase II metabolic reactions of PRN with or without GlcN in liver homogenate *in vitro*.

References

- Abushammala I, Ramadan M, El-Qedra A (2013) The Effect of P-Glycoprotein on Propranolol Absorption Using In Situ Rats Single-Pass Intestinal Perfusion. *International Journal of Pharmaceutical Sciences Review & Research* 22(1):161-165
- Adebowale A, Du J, Liang Z, Leslie JL, Eddington ND (2002) The bioavailability and pharmacokinetics of glucosamine hydrochloride and low molecular weight chondroitin sulfate after single and multiple doses to beagle dogs. *Biopharmaceutics & drug disposition* 23(6):217-225
- Aghazadeh-Habashi A, Sattari S, Pasutto F, Jamali F (2002) Single dose pharmacokinetics and bioavailability of glucosamine in the rat. *Journal of Pharmaceutical Sciences* 5(2):181-184
- Al-Hamidi H, Edwards AA, Mohammad MA, Nokhodchi A (2010) Glucosamine HCl as a new carrier for improved dissolution behaviour: effect of grinding. *Colloids and Surfaces B: Biointerfaces* 81(1):96-109
- Amidon GL, Lennernas H, Shah VP, Crison JR (1995) A theoretical basis for a biopharmaceutic drug classification: the correlation of in vitro drug product dissolution and in vivo bioavailability. *Pharmaceutical Research* 12(3):413-20
- Amidon GL, Sinko PJ, Fleisher D (1988) Estimating human oral fraction dose absorbed: a correlation using rat intestinal membrane permeability for passive and carrier-mediated compounds. *Pharmaceutical research* 5(10):651-654
- Anderson J, Nicolosi R, Borzelleca J (2005) Glucosamine effects in humans: a review of effects on glucose metabolism, side effects, safety considerations and efficacy. *Food and Chemical Toxicology* 43(2):187-201
- Araujo P (2009) Key aspects of analytical method validation and linearity evaluation. *Journal of chromatography B* 877(23):2224-2234
- Armbruster DA, Pry T (2008) Limit of blank, limit of detection and limit of quantitation. *The Clinical Biochemist Reviews* 29(Suppl 1):S49-S52
- Aungst BJ, Hussain MA (1992) Sustained propranolol delivery and increased oral bioavailability in dogs given a propranolol laurate salt. *Pharmaceutical research* 9(11):1507-1509
- Barthe L, Woodley J, Houin G (1999) Gastrointestinal absorption of drugs: methods and studies. *Fundamental & clinical pharmacology* 13(2):154-168
- Bauer LA (2001) *Applied clinical pharmacokinetics*, vol 2. McGraw-Hill New York:
- Beckmann M, Gerber JG, Byyny RL, LoVerde M, Nies AS (1988) Propranolol increases prostacyclin synthesis in patients with essential hypertension. *Hypertension* 12(6):582-588
- Bjornsson TD, Callaghan JT, Einolf HJ, *et al.* (2003) The conduct of in vitro and in vivo drug-drug interaction studies: a Pharmaceutical Research and Manufacturers of America (PhRMA) perspective. *Drug Metabolism and Disposition* 31(7):815-32
- Bliesner DM (2006) *Validating Chromatographic Methods: A Practical Guide*. Wiley Online Library
- Brunton L, Lazo J, Parker K (2006) *The pharmacological basis of therapeutics*. Goodman and Gilman's. New York: McGraw-Hill

- Bu SY, Mashek DG (2010) Hepatic long-chain acyl-CoA synthetase 5 mediates fatty acid channeling between anabolic and catabolic pathways. *Journal of lipid research* 51(11):3270-3280
- Caldwell J, Gardner I, Swales N (1995) An introduction to drug disposition: the basic principles of absorption, distribution, metabolism, and excretion. *Toxicologic pathology* 23(2):102-114
- Castleden CM, George CF (1979) The effect of ageing on the hepatic clearance of propranolol. *British journal of clinical pharmacology* 7(1):49-54
- Chafin CC, Soberman JE, Demirkan K, Self T (1999) Beta-blockers after myocardial infarction: do benefits ever outweigh risks in asthma? *Cardiology* 92(2):99-105
- Chan K, Liu ZQ, Jiang ZH, *et al.* (2006) The effects of sinomenine on intestinal absorption of paeoniflorin by the everted rat gut sac model. *Journal of ethnopharmacology* 103(3):425-32
- Chidsey CA, Morselli P, Bianchetti G, Morganti A, Leonetti G, Zanchetti A (1975) Studies of the absorption and removal of propranolol in hypertensive patients during therapy. *Circulation* 52(2):313-8
- Chowhan Z, Amaro A (1977) Everted rat intestinal sacs as an in vitro model for assessing absorptivity of new drugs. *Journal of pharmaceutical sciences* 66(9):1249-1253
- Cid E, Mella F, Lucchini L, Cárcamo M, Monasterio J (1986) Plasma concentrations and bioavailability of propranolol by oral, rectal and intravenous administration in man. *Biopharmaceutics & drug disposition* 7(6):559-566
- Coleman MD (2010) *Human drug metabolism: an introduction*. John Wiley & Sons
- Corrie K, Hardman JG (2011) Mechanisms of drug interactions: pharmacodynamics and pharmacokinetics. *Anaesthesia & Intensive Care Medicine* 12(4):156-159
- Craig CR, Stitzel RE (2004) *Modern pharmacology with clinical applications*. Lippincott Williams & Wilkins
- Custodio JM, Wu C-Y, Benet LZ (2008) Predicting drug disposition, absorption/elimination/transporter interplay and the role of food on drug absorption. *Advanced drug delivery reviews* 60(6):717-733
- D'Emanuele A, Jevprasesphant R, Penny J, Attwood D (2004) The use of a dendrimer-propranolol prodrug to bypass efflux transporters and enhance oral bioavailability. *Journal of Controlled Release* 95(3):447-53
- Dahmer S, Schiller RM (2008) Glucosamine. *American family physician* 78(4):471-6
- Delafuente JC (2000) Glucosamine in the treatment of osteoarthritis. *Rheumatic Disease Clinics of North America* 26(1):1-11
- Dhillon S, Gill K (2006) Basic pharmacokinetics. *Clinical pharmacokinetics*:1-44
- Dias R, Sakhare S, Mali K (2010) In-vitro absorption studies of mucoadhesive tablets of acyclovir. *Indian Journal of pharmaceutical Education and Research* 44(2):183-188
- Dobesh PP (2004) Ximelagatran: Pharmacology, pharmacokinetics, and pharmacodynamics. *Pharmacotherapy: The Journal of Human Pharmacology and Drug Therapy* 24(10P2):169S-178S
- Dressman JB, Reppas C (2010) *Oral drug absorption: Prediction and assessment*, vol 193. CRC Press
- EMA (2011) *Guidelines on bioanalytical method validation*. European Medicines Agency (EMA), Committee for Medicinal Products for Human Use (CHMP)

- Evans GH, Nies AS, Shand DG (1973) The disposition of propranolol. 3. Decreased half-life and volume of distribution as a result of plasma binding in man, monkey, dog and rat. *Journal of Pharmacology and Experimental Therapeutics* 186(1):114-22
- FDA (2013) Guidance for industry, bioanalytical method validation. Department of Health and Human Services Food and Drug Administration <http://www.fda.gov>
- Gainsborough N, Maskrey V, Nelson M, *et al.* (1993) The association of age with gastric emptying. *Age and ageing* 22(1):37-40
- Gomez-Lechon M, Donato M, Castell J, Jover R (2004) Human hepatocytes in primary culture: the choice to investigate drug metabolism in man. *Current drug metabolism* 5(5):443-462
- Gonçalves LA, Vigário AM, Penha-Gonçalves C (2007) Improved isolation of murine hepatocytes for in vitro malaria liver stage studies. *Malaria journal* 6(1):169
- Guibal E (2005) Heterogeneous catalysis on chitosan-based materials: a review. *Progress in Polymer Science* 30(1):71-109
- Heagerty A, Donovan M, Castleden C, Pohl J, Patel L, Hedges A (1981) Influence of cimetidine on pharmacokinetics of propranolol. *British medical journal* 282(6280):1917-1919
- Hebb AR, Godwin TF, Gunn RW (1968) A new beta adrenergic blocking agent, propranolol, in the treatment of angina pectoris. *Canadian Medical Association journal* 98(5):246-51
- Hedaya MA (2012) *Basic pharmacokinetics*. CRC Press
- Henrotin Y, Mobasheri A, Marty M (2012) Is there any scientific evidence for the use of glucosamine in the management of human osteoarthritis. *Arthritis Research and Therapy* 14(1):201
- Herman R, Nakamura K, Wilkinson G, Wood A (1983) Induction of propranolol metabolism by rifampicin. *British journal of clinical pharmacology* 16(5):565-569
- Hewitt NJ, Gómez Lechón MJ, Houston JB, *et al.* (2007) Primary hepatocytes: current understanding of the regulation of metabolic enzymes and transporter proteins, and pharmaceutical practice for the use of hepatocytes in metabolism, enzyme induction, transporter, clearance, and hepatotoxicity studies. *Drug metabolism reviews* 39(1):159-234
- Hirakawa H, Inazumi Y, Masaki T, Hirata T, Yamaguchi A (2005) Indole induces the expression of multidrug exporter genes in *Escherichia coli*. *Molecular microbiology* 55(4):1113-26
- Hofer M, Kunemund A (1985) Tetraphenylphosphonium ion is a true indicator of negative plasma-membrane potential in the yeast *Rhodotorula glutinis*. Experiments under osmotic stress and at low external pH values. *Biochemical Journal* 225(3):815-9
- Hua J, Suguro S, Hirano S, Sakamoto K, Nagaoka I (2005) Preventive actions of a high dose of glucosamine on adjuvant arthritis in rats. *Inflammation research : official journal of the European Histamine Research Society* 54(3):127-32
- Huber L (2007) *Validation and Qualification in Analytical Laboratories, Second Edition*. Taylor & Francis
- Hurst S, Loi CM, Brodfuehrer J, El-Kattan A (2007) Impact of physiological, physicochemical and biopharmaceutical factors in absorption and metabolism

- mechanisms on the drug oral bioavailability of rats and humans. *Expert Opinion Drug Metabolism Toxicology* 3(4):469-89
- Ibrahim A, Gilzad-kohan MH, Aghazadeh-Habashi A, Jamali F (2012) Absorption and bioavailability of glucosamine in the rat. *Journal of Pharmaceutical Sciences* 101(7):2574-83
- Ismail Z, Wahab MSA, Rahman ARA (2004) Bioequivalence study of propranolol tablets. *Eur J Gen Med* 1(4):42-47
- Ito K, Iwatsubo T, Kanamitsu S, Ueda K, Suzuki H, Sugiyama Y (1998) Prediction of pharmacokinetic alterations caused by drug-drug interactions: metabolic interaction in the liver. *Pharmacological reviews* 50(3):387-412
- Jackson CG, Plaas AH, Sandy JD, *et al.* (2010) The human pharmacokinetics of oral ingestion of glucosamine and chondroitin sulfate taken separately or in combination. *Osteoarthritis and Cartilage* 18(3):297-302
- Johnson JA, Herring VL, Wolfe MS, Relling MV (2000) CYP1A2 and CYP2D6 4-hydroxylate propranolol and both reactions exhibit racial differences. *Journal of Pharmacology and Experimental Therapeutics* 294(3):1099-105
- Jonker DM, Visser SA, van der Graaf PH, Voskuyl RA, Danhof M (2005) Towards a mechanism-based analysis of pharmacodynamic drug-drug interactions in vivo. *Pharmacology & therapeutics* 106(1):1-18
- Kashuba AD, Bertino Jr JS (2001) Mechanisms of drug interactions *Drug Interactions in Infectious Diseases*. Springer, p 13-38
- Katzung BG, Masters SB, Trevor AJ (2004) *Basic & clinical pharmacology*.
- Kazakevich YV, Lobrutto R (2007) *HPLC for pharmaceutical scientists*. John Wiley & Sons
- Kirkham SG, Samarasinghe RK (2009) Review article: Glucosamine. *Journal of Orthopaedic Surgery* 17(1):72-6
- Kubinyi H, Mannhold R, Krogsgaard L, Timmerman H (1993) Methods and principles in medicinal chemistry. Mannhold, R *et al*, eds:1-141
- Kupiec T (2004) Quality-control analytical methods: High-performance liquid chromatography. *International journal of pharmaceutical compounding* 8:223-227
- Lacombe O, Woodley J, Solleux C, Delbos J-M, Boursier-Neyret C, Houin G (2004) Localisation of drug permeability along the rat small intestine, using markers of the paracellular, transcellular and some transporter routes. *European journal of pharmaceutical sciences* 23(4):385-391
- Lafforgue G, Arellano C, Vachoux C, *et al.* (2008) Oral absorption of ampicillin: role of paracellular route vs. PepT1 transporter. *Fundamental & clinical pharmacology* 22(2):189-201
- Le Ferrec E, Chesne C, Artusson P, *et al.* (2001a) In vitro models of the intestinal barrier. *Alternatives to Laboratory Animals* 29:649-668
- Le Ferrec E, Chesne C, Artusson P, *et al.* (2001b) In vitro models of the intestinal barrier. The report and recommendations of ECVAM Workshop 46. European Centre for the Validation of Alternative methods. *Alternatives to Laboratory Animals* 29(6):649-68
- Leahey WJ, Neill JD, Varma MP, Shanks RG (1980) Comparison of the efficacy and pharmacokinetics of conventional propranolol and a long acting preparation of propranolol. *British journal of clinical pharmacology* 9(1):33-40

- Lee CH, Maibach HI (2006) Sodium lauryl sulfate Irritant Dermatitis. Springer, p 257-267
- Leucuta SE, Vlase L (2006) Pharmacokinetics and metabolic drug interactions. *Current clinical pharmacology* 1(1):5-20
- Li M, Si L, Pan H, *et al.* (2011) Excipients enhance intestinal absorption of ganciclovir by P-gp inhibition: assessed in vitro by everted gut sac and in situ by improved intestinal perfusion. *International journal of pharmaceutics* 403(1):37-45
- Liedholm H, Melander A (1990) Mechanisms and variations in the food effect on propranolol bioavailability. *European journal of clinical pharmacology* 38(5):469-475
- Liu L, Li F, Fang Ye, Guo S (2006) Regioselective grafting of poly (ethylene glycol) onto chitosan and the properties of the resulting copolymers. *Macromolecular bioscience* 6(10):855-861
- Lu-Suguro JF, Hua J, Sakamoto K, Nagaoka I (2005) Inhibitory action of glucosamine on platelet activation in guinea pigs. *Inflammation research : official journal of the European Histamine Research Society* 54(12):493-9
- Mannhold R, Kubinyi H, Timmerman H, Folkers G, Höltje H, Vacca J (2000). Wiley Online Library
- Mansoor AH, Kaul U (2009) Beta-blockers in cardiovascular medicine. *Journal of the Association of Physicians of India* 57:7-12
- Marathe PH, Shen DD, Nelson WL (1994) Metabolic kinetics of pseudoracemic propranolol in human liver microsomes. Enantioselectivity and quinidine inhibition. *Drug Metabolism and Disposition* 22(2):237-47
- Martinez MN, Amidon GL (2002) A mechanistic approach to understanding the factors affecting drug absorption: a review of fundamentals. *The Journal of Clinical Pharmacology* 42(6):620-643
- Masubuchi Y, Hosokawa S, Horie T, *et al.* (1994) Cytochrome P450 isozymes involved in propranolol metabolism in human liver microsomes. The role of CYP2D6 as ring-hydroxylase and CYP1A2 as N-desisopropylase. *Drug Metabolism and Disposition* 22(6):909-15
- Matheu V, Gracia Bara MT, Pelta R, Vivas E, Rubio M (1999) Immediate-hypersensitivity reaction to glucosamine sulfate. *Allergy* 54(6):643
- Meininger CJ, Kelly KA, Li H, Haynes TE, Wu G (2000) Glucosamine inhibits inducible nitric oxide synthesis. *Biochemical and biophysical research communications* 279(1):234-239
- Mendis E, Kim MM, Rajapakse N, Kim SK (2008) Sulfated glucosamine inhibits oxidation of biomolecules in cells via a mechanism involving intracellular free radical scavenging. *European journal of pharmacology* 579(1-3):74-85
- Monauni T, Zenti M, Cretti A, *et al.* (2000) Effects of glucosamine infusion on insulin secretion and insulin action in humans. *Diabetes* 49(6):926-935
- Nagaoka I, Igarashi M, Hua J, Ju Y, Yomogida S, Sakamoto K (2011) Recent aspects of the anti-inflammatory actions of glucosamine. *Carbohydrate polymers* 84(2):825-830
- Nagare N, Damre A, Singh KS, *et al.* (2010) Determination of site of absorption of propranolol in rat gut using in situ single-pass intestinal perfusion. *Indian journal of pharmaceutical sciences* 72(5):625-9

- Ngoh GA, Facundo HT, Zafir A, Jones SP (2010) O-GlcNAc signaling in the cardiovascular system. *Circulation research* 107(2):171-85
- Nkontchou G, Aout M, Mahmoudi A, *et al.* (2012) Effect of long-term propranolol treatment on hepatocellular carcinoma incidence in patients with HCV-associated cirrhosis. *Cancer Prevention Research* 5(8):1007-14
- Palm K, Luthman K, Ros J, Gråsjö J, Artursson P (1999) Effect of molecular charge on intestinal epithelial drug transport: pH-dependent transport of cationic drugs. *Journal of Pharmacology and Experimental Therapeutics* 291(2):435-443
- Partani P, Modhave Y, Gurule S, Khuroo A, Monif T (2009) Simultaneous determination of propranolol and 4-hydroxy propranolol in human plasma by solid phase extraction and liquid chromatography/electrospray tandem mass spectrometry. *Journal of pharmaceutical and biomedical analysis* 50(5):966-76
- Pelkonen O, Puurunen J (1980) The effect of cimetidine on in vitro and in vivo microsomal drug metabolism in the rat. *Biochemical pharmacology* 29(22):3075-3080
- Persiani S, Roda E, Rovati LC, Locatelli M, Giacobelli G, Roda A (2005) Glucosamine oral bioavailability and plasma pharmacokinetics after increasing doses of crystalline glucosamine sulfate in man. *Osteoarthritis and cartilage / OARS, Osteoarthritis Research Society* 13(12):1041-9
- Peters FT, Drummer OH, Musshoff F (2007) Validation of new methods. *Forensic science international* 165(2):216-224
- Piyapolrungraj N, Zhou Y, Li C, Liu G, Zimmermann E, Fleisher D (2000) Cimetidine absorption and elimination in rat small intestine. *Drug metabolism and disposition* 28(1):65-72
- Pleuvry BJ (2005) Pharmacodynamic and pharmacokinetic drug interactions. *Anaesthesia & Intensive Care Medicine* 6(4):129-133
- Pouwels M-JJ, Jacobs JR, Span PN, Lutterman JA, Smits P, Tack CJ (2001) Short-Term Glucosamine Infusion Does Not Affect Insulin Sensitivity in Humans 1. *The Journal of Clinical Endocrinology & Metabolism* 86(5):2099-2103
- Puurunen J, Pelkonen O (1979) Cimetidine inhibits microsomal drug metabolism in the rat. *European journal of pharmacology* 55(3):335-336
- Qinna NA, Shubbar MH, Matalka KZ, Al-Jbour N, Ghattas MA, Badwan AA (2015) Glucosamine enhances paracetamol bioavailability by reducing its metabolism. *Journal of Pharmaceutical Sciences* 104(1):257-65
- Raffa RB (2010) *Drug Disposition and Response Handbook of Drug-Nutrient Interactions*. Springer, p 27-43
- Raffa RB, Pergolizzi JV, Tallarida RJ (2010) The determination and application of fixed-dose analgesic combinations for treating multimodal pain. *The Journal of Pain* 11(8):701-709
- Reginster JY, Neuprez A, Lecart MP, Sarlet N, Bruyere O (2012) Role of glucosamine in the treatment for osteoarthritis. *Rheumatology international* 32(10):2959-67
- Reimann IW, Klotz U, Siems B, Frolich J (1981) Cimetidine increases steady state plasma levels of propranolol. *British journal of clinical pharmacology* 12(6):785-790
- Rescigno A (2010) The two faces of pharmacokinetics. *Journal of Pharmacy & Pharmaceutical Sciences* 13(1):38-42

- Rolan P (1994) Plasma protein binding displacement interactions—why are they still regarded as clinically important? *British journal of clinical pharmacology* 37(2):125-128
- Roseman S (2001) Reflections on glycobiology. *Journal of Biological Chemistry* 276(45):41527-41542
- Routledge P, Shand D (1978) Clinical pharmacokinetics of propranolol. *Clinical pharmacokinetics* 4(2):73-90
- Ryu J-M, Chung S-J, Lee M-H, Kim C-K, Shim C-K (1999) Increased bioavailability of propranolol in rats by retaining thermally gelling liquid suppositories in the rectum. *Journal of controlled release* 59(2):163-172
- Saito K, Kobayashi K, Mizuno Y, Fukuchi Y, Furihata T, Chiba K (2010) Peroxisome Proliferator-activated Receptor Alpha (PPAR. ALPHA.) Agonists Induce Constitutive Androstane Receptor (CAR) and Cytochrome P450 2B in Rat Primary Hepatocytes. *Drug metabolism and pharmacokinetics* 25(1):108-111
- Salman SA, Sulaiman SA, Ismail Z, Gan SH (2010) Quantitative determination of propranolol by ultraviolet HPLC in human plasma. *Toxicology mechanisms and methods* 20(3):137-42
- Sastry MS, Satyanarayana N, Diwan P, Krishna D (1993) Formulation, Pharmacokinetic and Pharmacodynamic Evaluation of Fast Releasing Compressed Propranolol. HCL Suppositories. *Drug development and industrial pharmacy* 19(9):1089-1096
- Schmidt M, Schmitz H-J, Baumgart A, *et al.* (2005) Toxicity of green tea extracts and their constituents in rat hepatocytes in primary culture. *Food and Chemical Toxicology* 43(2):307-314
- Setnikar I, Cereda R, Pacini MA, Revel L (1991) Antireactive properties of glucosamine sulfate. *Arzneimittel-Forschung* 41(2):157-61
- Setnikar I, Giachetti C, Zanolo G (1983) Absorption, distribution and excretion of radioactivity after a single intravenous or oral administration of [14C] glucosamine to the rat. *Pharmatherapeutica* 3(8):538-550
- Shabir GA (2003) Validation of high-performance liquid chromatography methods for pharmaceutical analysis: Understanding the differences and similarities between validation requirements of the US Food and Drug Administration, the US Pharmacopeia and the International Conference on Harmonization. *Journal of chromatography A* 987(1):57-66
- Shah VP, Midha KK, Findlay JW, *et al.* (2000) Bioanalytical method validation—a revisit with a decade of progress. *Pharmaceutical research* 17(12):1551-1557
- Shen L, Allix Hillebrand DQ-HW, Liu M (2012) Isolation and primary culture of rat hepatic cells. *Journal of Visualized Experiments*(64)
- Shields KG, Goadsby PJ (2005) Propranolol modulates trigeminovascular responses in thalamic ventroposteromedial nucleus: a role in migraine? *Brain : a journal of neurology* 128(Pt 1):86-97
- Shindo T, Futagami S, Hiratsuka T, *et al.* (2008) Comparison of gastric emptying and plasma ghrelin levels in patients with functional dyspepsia and non-erosive reflux disease. *Digestion* 79(2):65-72
- Smith DA, Allerton C, Kalgutkar AS, Van De Waterbeemd H, Walker DK (2012) *Pharmacokinetics and metabolism in drug design.* John Wiley & Sons

- Snyder BD, Polasek TM, Doogue MP (2012) Drug interactions: principles and practice. *Australian Prescriber* 35(3):85-8
- Song N-N, Zhang S-Y, Liu C-X (2004) Overview of factors affecting oral drug absorption. *Drug Metabolism and Pharmacokinetics* 4(3):167-76
- Tallarida RJ, Cowan A, Raffa RB (2003) Antinociceptive synergy, additivity, and subadditivity with combinations of oral glucosamine plus nonopioid analgesics in mice. *Journal of Pharmacology and Experimental Therapeutics* 307(2):699-704
- Taverniers I, De Loose M, Van Bockstaele E (2004) Trends in quality in the analytical laboratory. I. Traceability and measurement uncertainty of analytical results. *Trends in Analytical Chemistry* 23(7):480-490
- Thakral R, Debnath UK, Dent C (2007) Role of glucosamine in osteoarthritis. *Current Orthopaedics* 21(5):386-389
- Toutain P-L, Bousquet-mélou A (2004) Bioavailability and its assessment. *Journal of veterinary pharmacology and therapeutics* 27(6):455-466
- Uldry M, Ibberson M, Hosokawa M, Thorens B (2002) GLUT2 is a high affinity glucosamine transporter. *FEBS letters* 524(1-3):199-203
- Ungell AL, Nylander S, Bergstrand S, Sjöberg A, Lennernas H (1998) Membrane transport of drugs in different regions of the intestinal tract of the rat. *Journal of Pharmaceutical Sciences* 87(3):360-6
- Varma MV, Kapoor N, Sarkar M, Panchagnula R (2004) Simultaneous determination of digoxin and permeability markers in rat in situ intestinal perfusion samples by RP-HPLC. *Journal of Chromatography B* 813(1):347-352
- Varma MV, Panchagnula R (2005) Prediction of in vivo intestinal absorption enhancement on P-glycoprotein inhibition, from rat in situ permeability. *Journal of pharmaceutical sciences* 94(8):1694-1704
- Walle T, Walle UK, Olanoff LS (1985) Quantitative account of propranolol metabolism in urine of normal man. *Drug Metabolism and Disposition* 13(2):204-9
- Walle T, Webb JG, Bagwell EE, Walle UK, Daniell HB, Gaffney TE (1988) Stereoselective delivery and actions of beta receptor antagonists. *Biochemical pharmacology* 37(1):115-24
- Wang Y, Wang Z, Zuo Z, *et al.* (2013) Clinical pharmacokinetics of buffered propranolol sublingual tablet (Promptol)-application of a new "physiologically based" model to assess absorption and disposition. *Association of Applied Paleontological Sciences* 15(3):787-96
- Watson R, Bastain W, Larkin K, Hayes J, McAinsh J, Shanks R (1987) A comparative pharmacokinetic study of conventional propranolol and long acting preparation of propranolol in patients with cirrhosis and normal controls. *British journal of clinical pharmacology* 24(4):527-535
- WHO (2011) world health organization model list of essential medicines: 17th list, March 2011.
- Xing R, Liu S, Guo Z, *et al.* (2006) The antioxidant activity of glucosamine hydrochloride in vitro. *Bioorganic & medicinal chemistry* 14(6):1706-1709
- Yang JJ, Kim K-J, Lee VH (2000) Role of P-glycoprotein in restricting propranolol transport in cultured rabbit conjunctival epithelial cell layers. *Pharmaceutical research* 17(5):533-538

- Yoshimoto K, Echizen H, Chiba K, Tani M, Ishizaki T (1995) Identification of human CYP isoforms involved in the metabolism of propranolol enantiomers--N-desisopropylation is mediated mainly by CYP1A2. *British journal of clinical pharmacology* 39(4):421-31
- Zakeri-Milani P, Valizadeh H, Tajerzadeh H, *et al.* (2007) Predicting human intestinal permeability using single-pass intestinal perfusion in rat. *Journal of Pharmaceutical Sciences* 10(3):368-379
- Zhou Y, Li W, Chen L, Ma S, Ping L, Yang Z (2010) Enhancement of intestinal absorption of akebia saponin D by borneol and probenecid in situ and in vitro. *Environmental toxicology and pharmacology* 29(3):229-34